Pathophysiology of
Normal Pressure Hydrocephalus

Dr. Brian Kenneth Owler
MB BS BSc(Med)(Hons)

Thesis

Doctor of Philosophy

2004
University of Sydney
Department of Surgery

Table of Contents

Index of Figures V

Index of Tables VI

Statement of Authenticity VII

Acknowledgements VIII

Publications arising from thesis material IX

Abbreviations XIII

SUMMARY 1

INTRODUCTION 3

CHAPTER ONE

LITERATURE REVIEW 7

1.1 Definition 7

1.2 Epidemiology 8

1.3 Clinical Features 9
1.3.1 Gait Disturbance *9*
1.3.2 Dementia *11*
1.3.3 Urinary Incontinence *11*

1.4 Aetiology & Pathology 12
1.4.1 CSF Circulation *12*
1.4.2 Pathology of the Parenchyma *15*

1.5 Treatment of NPH 17

CHAPTER TWO

A CLINICAL STUDY OF LOW PRESSURE HYDROCEPHALUS 23

2.1 Introduction 23

2.2 Summary of Cases 24

2.3 Individual Case Reports 24

2.4 Discussion 33

2.5 Conclusions 35

CHAPTER THREE

CLINICAL FEATURES & CSF INFUSION STUDY REUSULTS IN PATIENTS WITH NPH..... 36

3.1 Introduction 36

3.2 Methods 36
3.2.1 Patients and Clinical Assessment *36*
3.2.2 Patients groups *40*
3.2.3 Computerized Infusion Study Technique *41*
3.2.4 Statistical Comparisons *45*
3.2.5 Ethical Considerations *46*

3.3 Results 46
3.3.1 All Normal Pressure Hydrocephalus Patients *46*
3.3.2 Comparison of Idiopathic to Secondary NPH Patients *51*
3.3.3 Comparison of 'Typical' and 'Atypical' Idiopathic NPH Patients *52*
3.3.4 Comparison of Hypertensive and Non-Hypertensive 'Typical' Idiopathic NPH Patients *53*

3.4 Discussion 53

3.5 Conclusions 58

CHAPTER FOUR

NORMAL PRESSURE HYDROCEPHALUS AND CEREBRAL BLOOD FLOW: A PET STUDY OF BASELINE VALUES. 60

4.1 Introduction 60

4.2 Methods 60
4.2.1 Patients *60*
4.2.2 Controls *62*
4.2.3 PET and MRI Scanning *62*
4.2.4 Analysis *63*

4.3 Results 67
4.3.1 Global CBF Values *67*
4.3.2 Regional CBF Values *68*
4.3.3 Relationship between Clinical Severity and CBF *69*
4.3.4 Response to Shunting *70*

4.4 Discussion 72

4.5 Conclusion 81

CHAPTER FIVE

NORMAL PRESSURE HYDROCEPHALUS AND CEREBRAL BLOOD FLOW: CHANGES DURING CSF PRESSURE MANIPULATION 85

5.1 Introduction 85

5.2 Methods 86
5.2.1 Patients *86*
5.2.2 PET and MRI Scanning *87*
5.2.3 Finite Element Modeling *89*
5.2.4 Analysis *91*

5.3 Results 95
5.3.1 CSF Compensatory Parameters and Change in Intracranial Pressure *95*
5.3.2 Finite Element Analysis *96*
5.3.3 Change in Cerebral Perfusion Pressure *99*
5.3.4 Changes in $PaCO_2$ *100*
5.3.5 Changes in Global CBF *100*
5.3.6 Cerebral Autoregulation *103*
5.3.7 Changes in Anatomical Regional CBF *106*
5.3.8 Changes in Concentric ROI CBF *107*
5.3.9 Response to Shunting *107*

5.4 Discussion 108

5.5 Conclusions 117

CHAPTER SIX

DIFFUSION TENSOR IMAGING OF PATIENTS WITH NORMAL PRESSURE HYDROCEPHALUS 118

6.1 Introduction 118

6.2 Materials and Methodology 119
6.2.1 Patients *119*
6.2.2 Control Group *120*
6.2.3 MR Acquisition *120*
6.2.4 Analysis of the Diffusion Tensor *122*

6.3 Results 123
6.3.1 Regional Analysis *123*
6.3.2 Global Analysis *137*

6.4 Discussion 141

6.5 Conclusions 145

CHAPTER SEVEN

GENERAL DISCUSSION AND CONCLUSIONS 146

7.1 Introduction 146

7.2 Methodological Techniques and Developements 146

7.3 Major findings 148

7.4 Synthesis of Results 150

7.5 Implications for Management of NPH 154

7.6 Future Studies 155

7.7 Conclusions 156

REFERENCES 158

LIST OF APPENDICES 183

APPENDIX A 184

APPENDIX B 189

Index of Figures

Figure 2.1a 26
Figure 2.1b 27
Figure 2.2a 30
Figure 2.2b 30
Figure 2.2c 31
Figure 2.3 31

Figure 3.1 40
Figure 3.2 42
Figure 3.3 45
Figure 3.4 48
Figure 3.5a 49
Figure 3.5b 49
Figure 3.5c 50
Figure 3.5d 50
Figure 3.6 57

Figure 4.1 64
Figure 4.2 66

Figure 5.1 88
Figure 5.2 93
Figure 5.3a 97
Figure 5.3b 99
Figure 5.3c 99
Figure 5.3d 99
Figure 5.4a 101
Figure 5.4b 101
Figure 5.5 104
Figure 5.6 106

Figure 6.1a 124
Figure 6.1b 125
Figure 6.1c 126
Figure 6.2a 127
Figure 6.2b 128
Figure 6.3a 134
Figure 6.3b 135
Figure 6.3c 136
Figure 6.4a 138
Figure 6.4b 139
Figure 6.4c 140

Index of Tables

Table 3.1 38
Table 3.2 39

Table 4.1 67
Table 4.2 68
Table 4.3 69
Table 4.4 71
Table 4.5 71
Table 4.6 72
Table 4.7 76
Table 4.8 83

Table 5.1 95
Table 5.2 99
Table 5.3 100
Table 5.4: 106
Table 5.5:. 106
Table 5.6: 107
Table 5.7: 107
Table 5.8 110

Table 6.1 120
Table 6.2.a 131
Table 6.2.b 132
Table 6.2.c 133

Statement of Authenticity

This thesis contains a record of original research performed by the author at the Academic Neurosurgery Unit, Addenbrooke's Hospital, Cambridge, United Kingdom, the Wolfson Brain Imaging Centre, University of Cambridge, Cambridge, United Kingdom, the Department of Neurosurgery, Royal Prince Alfred Hospital, Sydney Australia and the Department of Surgery, University of Sydney, Sydney, Australia.

In all sections of the thesis, the author was primarily responsible for the conduct and direction of the research, study design and the analysis of results. This work has not been submitted for consideration of an award, diploma or degree at any institution previously.

Research was conducted with approval of the Cambridge Regional Ethics Committee when applicable in accordance with the Declaration of Helsinki as amended in September, 2000.

Acknowledgements

I would like to express my gratitude for the advice, guidance and supervision of Professor John D. Pickard, Associate Professor Michael Besser and Dr. Ian Johnston.

Drs. Zofia and Marek Czosnyka designed and developed the computerised CSF infusion and collaborated in its application to the studies of this thesis. Dr. Alonso Péna designed and performed the finite element modelling during CSF infusion studies. Dr. Shahan Momjian collaborated in performing the cerebral blood flow studies. The staff of Wolfson Brain Imaging Centre assisted in the development and analysis of the experimental data. These researchers include Dr. Neil Harris, Dr Piotr Smielewski, Dr. Tim Fryer, Mr. Tim Donovan and Dr. Adrian Carpenter. I would like to thank my colleagues in Cambridge for their friendship.

I was supported by the Sydney University Medical Foundation Woods Grant and the Madeline Foundation for Neurosurgical Research. I would like to express my appreciation for the support of these two organisations. The work contained in this thesis was also funded by an MRC Programme Grant (No. G42,00005).

My gratitude and appreciation goes to my family and my partner Tara for their understanding and sacrifice that allow me to pursue my career and academic interests.

Publications arising from thesis material

Publications in Peer Reviewed Journals

1. Owler B. K. and Pickard J.D. (2001) Cerebral Blood Flow and Normal Pressure Hydrocephalus. A Review. *Acta Neurologica Scandanavica* 104: 325-342.

2. Owler, B. K., Jacobson, E. E. and Johnston, I. H. (2001) Low Pressure Hydrocephalus Syndrome. Report of 5 cases.. *British Journal of Neurosurgery* 15(4): 353-359.

3. Owler, B. K., Fung, K. Czosnyka, Z. (2001) Importance of ICP monitoring in CSF circulation disorders. *British Journal of Neurosurgery* 15(5): 439-440.

4. Owler, B.K., Momjian, S., Péna, A., Harris, N., Czosnyka, Z., Czosnyka, M., Fryer, T., Smielewski, P., Donovan, T., Coles, J. and Pickard, J.D. (2003) Global & regional CBF in patients with normal pressure hydrocephalus. *Journal of Cerebral Blood Flow and Metabolism* 24: 17-23.

5. Owler, B.K., Péna, A., Momjian, S., Harris, N., Czosnyka, Z., Czosnyka, M., Fryer, T., Smielewski, P., Donovan, T., and Pickard, J.D. (2004) Changes in Cerebral Blood Flow during CSF Pressure Manipulation in Patients with Normal Pressure Hydrocephalus. *Journal of Cerebral Blood Flow and Metabolism* (accepted)

Abstracts in Conference Proceedings

1. Owler, B.K., Péna, A., Momjian, S., Harris, N., Czosnyka, Z., Czosnyka, M., Fryer, T., Smielewski, P., Donovan, T., and Pickard, J.D. (2003). Changes in Cerebral Blood Flow during CSF Pressure Manipulation in Patients with Normal Pressure Hydrocephalus. Proceedings of the Neurosurgical Society of Australasia's Annual Scientific Meeting, Queenstown, New Zealand.

2. Momjian, S., Owler, BK., Czosnyka, Z., Czosnyka, M., Péna, A., Pickard, JD. (2003). Pattern of regional white matter CBF in normal pressure hydrocephalus. Brain 03. Proceedings of the International Society for the Study of Cerebral Blood Flow and Metabolism. Calvary, Canada.

3. Owler, B.K., Pena, A., Harris, N., Czosnyka, Z., Czosnyka, M., Fryer, T., Smielewski, P., Donovan, T., Coles, J. and Pickard, J.D. (2002). Global & regional CBF in patients with normal pressure hydrocephalus. Proceedings of the Neurosurgical Society of Australasia's Annual Scientific Meeting, Broome, Australia.

4. Green, H.A.L., Pena, A., Price, S.P., Owler, B.K., Gillard, J., Pickard, J. D., Carpenter, T. A. Partial Volume effects on Diffusion Tensor Images at 3T. RANZCR. Melbourne, Australia.

5. Owler, B.K., Pena, A., Harris, N., Green, H., Papadakis, N., Martin, K., Donovan, T., Carpenter, A. and Pickard, J.D. (2001). A study of normal

pressure hydrocephalus using diffusion tensor imaging. World Congress of Neurological Surgeons. Sydney, Australia.

6. Owler, B.K., Pena, A., Harris, N., Czosnyka, Z., Czosnyka, M., Fryer, T., Smielewski, P., Donovan, T., Coles, J. and Pickard, J.D. (2001). Global & regional CBF changes in patients with normal pressure hydrocephalus with changes in ICP. Brain 01. Proceedings of the International Society for the Study of Cerebral Blood Flow and Metabolism. Taipei, Taiwan.

7. Pena, A., Harris, N.G., Owler B.K. and Pickard, J.D. (2001) The biomechanics of steady-state ventricular dilatation in normal pressure hydrocephalus. 3rd International Hydrocephalus Workshop, Kos, Greece.

8. Czosnyka, M., Czosnyka, Z.H., Owler B.K., Piechnik, S.K., Smielewski, P. and Pickard, J.D. (2001) Testing of cerebrospinal compensatory reserve in shunted and non-shunted patients (an update). 3rd International Hydrocephalus Workshop, Kos, Greece.

9. Owler, B.K., Pena, A., Harris, N., Czosnyka, Z., Czosnyka, M., Fryer, T., Smielewski, P., Donovan, T., Coles, J. and Pickard, J.D. (2001). Global & regional CBF changes in patients with normal pressure hydrocephalus with changes in ICP. Proceedings of the Royal Society of Medicine, London, UK.

10. Owler, B.K., Pena, A., Harris, N., Czosnyka, Z., Czosnyka, M., and Pickard, J.D. (2000) Response of global CBF to changes in ICP in patients with hydrocephalus – an observational study. ICP 2000, Cambridge, UK.

Abbreviations

AR	Autoregulation
AMP_{beg}	CSF pulse amplitude - baseline
AMP_{end}	CSF pulse amplitude - equilibrium
CBF	Cerebral blood flow
CC	Corpus callosum
CCx	Calcarine cortex
CO_2	Carbon dioxide
CPP	Cerebral perfusion pressure
CSF	Cerebrospinal fluid
CT	Computed tomography
CVR	Cerebrovascular reactivity
D	Mean diffusion
DAT	Dementia of the Alzheimer's type
DTI	Diffusion tensor imaging
DWI	Diffusion weighted imaging
EAM	External acoustic meatus
El	Elastance
EPI	Echo planar imaging
FA	Fractional anisotropy
gCBF	Global cerebral blood flow
GE	Gradient echo
IC	Internal capsule
ICP	Intracranial pressure
ICP_{beg}	Intracranial pressure - baseline

ICP_{end}	Intracranial pressure - equilibrium
i.v.	Intravenous
mmHg	Millimetres of mercury
mmHg/ml/min	Millimetres of mercury per millilitre per minute
MR	Magnetic resonance
MRI	Magnetic resonance imaging
NMR	Nuclear magnetic resonance
NPH	Normal pressure hydrocephalus
OER	Oxygen extraction rate
P	Isotropic component of diffusion tensor
PET	Positron emission tomography
PVI	Pressure-volume index
PVL	Periventricular lucency
Q	Deviatoric component of diffusion tensor
RA	Relative anisotropy
rCBF	Regional cerebral blood flow
R_{csf}	Resistance to CSF absorption
RF	Radiofrequency
sAR	Static Autoregulation parameter
sARi	Static Autoregulation index
SPECT	Single photon emission computed tomography
TE	Echo time
Xe	Xenon

Summary

Normal pressure hydrocephalus (NPH), a CSF circulation disorder, is important as a reversible cause of gait and cognitive disturbance in an aging population. The inconsistent response to CSF shunting is usually attributed to difficulties in differential diagnosis or co-morbidity. Improving outcome depends on an increased understanding of the pathophysiology of NPH. Specifically, this thesis examines the contribution of, and inter-relationship between, the brain parenchyma and CSF circulation in the pathophysiology of NPH.

Of the four core studies of the thesis, the first quantifies the characteristics of the CSF circulation and parenchyma in NPH using CSF infusion studies to measure the resistance to CSF absorption and brain compliance. The second study assesses cerebral blood flow (CBF) was using O^{15}-labelled positron emission tomography (PET) with MR co-registration. By performing CSF infusion studies in the PET scanner, CBF at baseline CSF pressure and at a higher equilibrium pressure is measured. Regional changes and autoregulatory capacity are assessed. The final study examines the microstructural integrity of the parenchyma using MR diffusion tensor imaging.

These studies confirm the importance of the inter-relationship of the brain parenchyma and CSF circulation. NPH symptomatology and its relationship to the observed regional CBF reductions in the basal ganglia and thalamus are discussed. Regional CBF reductions with increased CSF pressure and the implications for autoregulatory capacity in NPH are considered. The reduction in CBF when CSF was increased was most striking in the periventricular regions. In addition, periventricular

structures demonstrated increased diffusivity and decreased anisotropy. The relationship between these changes and mechanisms such as transependymal CSF passage are reviewed.

The findings of this thesis support a role of both the CSF circulation and the brain parenchyma in the pathophysiology of NPH. The results have implications for the approach to the management of patients with NPH.

Introduction

Normal pressure hydrocephalus (NPH), although an established clinical entity for about 40 years, remains contentious with respect to mechanism, diagnosis and treatment. The original description of NPH (Adams *et al.*, 1965; Hakim and Adams, 1965) was of hydrocephalus with normal CSF pressure in patients who were demented and who also exhibited psychomotor deficits. A clinical triad of dementia, gait disturbance and urinary incontinence was proposed as the basis of the clinical definition. It soon became apparent however that cases with only one or two components of the triad were common and responded to CSF diversion, that is, a CSF shunt (Graff-Radford & Godersky, 1986).

The initial enthusiasm for using a CSF shunt to treat patients with dementia, hydrocephalus and normal CSF pressure was replaced by scepticism as several authors reported poor results – probably due to poor patient selection. As a result neurosurgeons became more uncertain about the criteria for selecting patients to undergo CSF shunting for NPH. Although there has been some improvement in clinical, radiological and physiological assessment of patients (Corkill & Cadoux-Hudson, 1999) a number of problems exist in the study of NPH.

The definition of NPH remains an issue of contention. It has been applied to describe the clinical triad even in the absence of CSF pressure measurements. NPH describes a heterogeneous population of patients. By convention, these are divided into idiopathic and secondary NPH on the basis of presumed aetiology. These groups are very different, especially in respect to age as the idiopathic NPH is considered mainly a disease of the elderly. Difficulties of definition and stratification of patient groups

often makes it difficult to draw conclusions from studies where these issues have not been addressed.

Fundamental issues in NPH, which also represent deficiencies in knowledge, are those of pathogenesis and pathophysiology. In general, hydrocephalus, due to obstruction presents with ventricular enlargement and raised CSF pressure. However the apparent paradox of ventricular enlargement with normal CSF pressure is more difficult and a number of mechanisms have been proposed (Hakim, 1971; Hakim *et al.*, 1976; Penar *et al.*, 1995; Levine, 2000; Péna *et al.*, 1999 & 2002a; Stephensen *et al.*, 2002). Investigators have attempted to address these deficiencies by characterizing CSF dynamics, cerebral blood flow and cerebral autoregulation. These studies have met with varying degrees of success and reflect the limitations of the available technologies.

This aim of this thesis is to investigate the pathophysiology of NPH through the application of modern techniques that focus on the role of the brain parenchyma and its interaction with CSF dynamics. These techniques include computerised CSF infusion studies, high-resolution positron emission tomography and diffusion tensor magnetic resonance imaging. The application of such techniques to understanding the pathophysiology of NPH may improve patient selection, treatment and outcome.

The aim of this thesis is addressed by a core of four major human studies. Preceding these chapters a literature review further defines the condition, its management and outstanding problems (Chapter 1). A short clinical study of five patients, diagnosed with NPH where CSF shunting provided no response but in whom CSF drainage at

very low pressures was successful, illustrates the importance of the relationship between CSF dynamics and the brain parenchyma (Chapter 2). The core studies of this thesis are summarized below.

(i) A retrospective study reviewing the clinical features, CSF dynamics and outcome of patients with NPH is presented (Chapter 3). This study utilizes the computerised CSF infusion study technique to examine the interaction between CSF dynamics and brain parenchyma in patients with NPH.

(ii) A study of cerebral blood flow at rest in patients with NPH compared to normal controls is presented (Chapter 4). This study uses ^{15}O-labelled water positron emission tomography (PET) with co-registration of magnetic resonance images (MRI) to investigate the role of the cerebral vasculature in NPH.

(iii) The techniques of the previous two studies are combined in order to study changes in CBF with changes in CSF pressure (Chapter 5). This study therefore characterizes the dynamic properties of the cerebral vasculature in NPH patient and discusses the role cerebral autoregulation.

(iv) Diffusion tensor MR imaging is used to examine the microstructural changes in various regions of brain parenchyma of patients with NPH compared to controls.

Following presentation of the results of these four studies a model of the pathogenesis and pathophysiology of the condition is proposed. Suggestions for further work and the implications for the incorporation of these results into clinical studies are presented.

Chapter One

1. Literature Review

1.1 Definition

Normal pressure hydrocephalus (NPH) may be defined as a disturbance of CSF circulation characterised by normal CSF pressure (<18 mmHg), ventricular enlargement and a clinical triad consisting of a gait disorder with or without dementia and/or urinary incontinence.

There are however problems with this definition. The term is often applied to patients who present with the clinical triad and ventriculomegaly without measurement of the CSF pressure. Likewise, not all elements of the clinical triad may be present. Some would also argue that patients who do not respond favourably to CSF shunting, even in the presence of the clinical, radiological and physiological features of the condition, should not be classified as having NPH.

While for the purposes of research adequate definition of patient groups is important, it is also necessary to recognise that patients who do not satisfy the strictest definitions of NPH may still respond to CSF shunting. This probably reflects the fact that NPH represents a portion of the spectrum of CSF circulation disorders.

1.2 Epidemiology

NPH may be divided into two categories – idiopathic and secondary NPH. Idiopathic NPH is primarily a condition of aging and is rare before the age of 60 years (Fisher, 1982). The true incidence of NPH is unknown but it is probably quite rare. Vanneste (1992) estimated the incidence of shunt responsive NPH to be 2.2/million/year and that it represented about 0.4% cases of all dementias. However these figures are likely to be influenced by factors such as awareness of the condition, referral rates and variation of protocols for the investigation of dementia in the elderly. Indeed the incidence is likely to be underestimated and should increase given improvement in these factors in an ageing population.

Casmiro *et al.* (1989) found that hypertension, ischemic heart disease, high density lipoprotein / cholesterol levels and diabetes were all significant risk factors for the development of idiopathic NPH. A history of transient ischemic attacks, obesity, alcohol use and smoking were not significant risk factors. Krauss *et al.* (1996) found that hypertension, cardiac disease, diabetes, cerebrovascular diseases as well as peripheral vascular diseases were all significantly associated with the development of idiopathic NPH. Moreover there was a relationship between the severity of NPH symptomatology and hypertension. The authors concluded that hypertension has a role in the development and progression of the disease and represents a target for the prevention and slowing of the disease.

Secondary NPH may be a result of intracranial haemorrhage, head injury, meningitis, intracranial tumour, intracranial surgery, aqueduct stenosis and basilar artery ectasia. Thus the epidemiology of the condition in secondary cases is a reflection of the underlying cause.

1.3 Clinical Features

In their initial description of the condition, Hakim & Adams (1965) reported their most striking cases. These cases were much debilitated with dementia predominating their clinical picture. Each had been labelled as exhibiting 'senile dementia' or 'cerebral arteriosclerosis'. They were incontinent of urine and those able to mobilise demonstrated a disturbance of gait. The clinical triad of dementia, gait disturbance and urinary incontinence was thus described. These shall each be considered.

1.3.1 Gait Disturbance

The gait disturbance of NPH is characterised by a broad base and slow shuffling steps. There is a reduced foot-floor clearance. Examination generally reveals an absence of weakness or inco-ordination with an increase in tone and brisk reflexes. The gait is often described as a shuffling or magnetic with difficulty initiating movement (Corkill and Cadoux-Hudson, 1999). A recent study by Stolze *et al.* (2001b) compared patients with Parkinson's disease to those with NPH. As the two diseases can present with similar gait patterns with difficulty in initiating movement, a broad base and foot shuffling, the differential diagnosis can be difficult on the basis of gait alone. However the gait of patients with Parkinson's disease improves with visual and auditory cues whereas patients with NPH do not. Patients with NPH also have a

more pronounced disturbance of equilibrium and have compensatory features evident in their gait such as an increased step width and external rotation of the foot. A common feature of patients with disturbed gait due to NPH is the lack of functional deficit when lying down. Depending on the severity of the disease they may move their legs freely when supine. Likewise patients may not be able to walk but are able to swim using their legs. This finding is typical of a frontal gait apraxia.

Gait disturbance is probably the most important clinical feature of NPH. Shenkin *et al.* (1973) noted that patients with gait disturbance as their presenting symptom responded to CSF shunting more frequently than those in which dementia predominated. Numerous other studies have confirmed such findings (Greenberg *et al.*, 1977; Fisher, 1980, 1982). Casmiro (1989) suggested that the condition be renamed as 'ventricular enlargement with gait apraxia syndrome (VEGAS)'. The Dutch NPH Study (Boon *et al.*, 2000) found that gait disturbance must be present and that the onset of dementia must occur at the same time or after the onset of gait disturbance if patients are to respond to CSF shunting.

Although gait disturbance predominates, there is evidence of more general disorders of posture and motor function. Blomsterwall *et al.* (1995, 2000) demonstrated a postural disturbance in patients with NPH and proposed that this postural disturbance underlies the gait disturbance. Furthermore, patients with NPH had relatively better postural function than controls or patients with Binswanger's disease when their eyes were closed than when open (Blomsterwall *et al.*, 2000). The misinterpretation of afferent visual information might be a mechanism for disturbance of posture and gait (Wikkelso *et al.*, 2003).

1.3.2 Dementia

The dementia of NPH is frontal in nature. It has been characterised by Iddon *et al.* (1999) using neuropsychological tests. Patients typically showed premotor subcortical deficits with spatial recognition and cognitive impairment. Tests of temporal lobe function, known to be impaired in conditions such as Alzheimer's disease, were satisfactory. The marked deficiency in spatial abilities such as spatial perception and spatial memory has been confirmed by others (Gustafson and Hagberg, 1978). Later in the disease process clinical features such as abulia, disorientation and emotional lability may become prominent. Perhaps more significantly, patients who were not in the demented range using the mini mental state examination, demonstrated deficits of executive function, that is, those mental abilities necessary for planning, anticipation, goal establishment and error monitoring. These more sensitive investigations of mental function assist in the differential diagnosis from some of the more common forms of temporal lobe dementia. However similar findings may be seen in the dementias of Parkinson's disease and Huntington's disease as well as subcortical arteriosclerotic disease.

1.3.3 Urinary Incontinence

The urinary incontinence of NPH varies in nature. Early symptoms consist of urge or frequency. At this stage, urge incontinence combined with gait disturbance may exacerbate the problem. Dynamic studies have demonstrated strong bladder contractions in response to increments in bladder of volume as low as 20mL (Fisher, 1982). In addition faecal incontinence may occur late in the course of the disease.

1.4 Aetiology & Pathology

The aetiology and pathophysiology of NPH remain enigmatic. A comprehensive theory to address this issue must be able to describe what the various elements of the disorder are, why they occur and how they interact. In NPH, the elements of the condition may be considered under the headings of CSF circulation and brain parenchyma. Current knowledge in relation to these two topics shall be reviewed.

1.4.1 CSF Circulation

NPH is primarily classified as a disorder of CSF circulation. In analysing CSF circulation disorders, the composition, volume, distribution and pressure of the CSF are considered. The dynamic properties of the CSF circulation require attention as do the anatomy and pathology of the ventricular and subarachnoid space through which the CSF circulates.

The constituents of the CSF are generally normal although routine biochemical, microbiological and cytological analysis may occasionally reveal an unexpected diagnosis. Examination of CSF in NPH patients may reflect the underlying histopathological changes (Tullberg *et al.*, 1998). Sulfatide, an indicator of demyelination, and neurofilament triplet protein, a marker of axonal degeneration, are correlated with the degree of white matter MR hyperintensities (Tullberg *et al.*, 2000, 2002). More recently, the CSF level of TNF alpha, a proinflammatory cytokine, was demonstrated to be higher in patients with NPH and correlated with sulfatide levels

suggesting a possible role for TNF alpha in parenchymal pathology (Tarkowski *et al.*, 2003).

The volume of CSF is of course increased in NPH as it is a requirement for the diagnosis. Apart from some cases of long-standing aqueduct stenosis, NPH is a communicating form of hydrocephalus and the distribution of the increased volume of CSF does have some importance. The relative increase in ventricular volume should be greater than any increase in the subarachnoid space, especially over the convexities. This is may be used a tool to differentiate generalised cerebral atrophy from NPH (Gado *et al.*, 1976; Vanneste *et al.*, 1993; Boon *et al.*, 2000).

The CSF pressure is within the normal range. However, not infrequently, patients with high CSF pressures presenting with identical clinical features to those with normal CSF pressure. Monitoring is performed in patients with NPH in order to determine the baseline CSF pressure and to detect abnormal pressure waves. The presence of B (or vasogenic) waves is common in NPH and is thought to be indicative of a disturbance of CSF dynamics and reduced compliance of the neuroaxis (Hartmann and Alberti, 1977).

CSF dynamics can be investigated using a CSF infusion study involving intrathecal injection, infusion or perfusion of a solution of mock CSF or normal saline at either a constant rate or constant pressure. The flow (ml/min) is then plotted against the ICP. The slope of the regression line is the conductance of CSF outflow and the reciprocal is the resistance of CSF outflow (R_{csf}). R_{csf} represents the CSF pressure that must be applied to the CSF system to produce an absorption rate of 1ml of CSF per minute at

equilibrium. The normal R_{csf} is less than 10 mmHg/ml/min (Ekstedt, 1978; Albeck *et al.*, 1991) but is usually raised in NPH. The Copenhagen Symposium on NPH (1990) concluded that an R_{csf} >11 mmHg/ml/min was suggestive of NPH. It has also been reported to be an important predictor of shunt-response (Borgesen *et al.*, 1979; Borgesen and Gjerris, 1982; Borgesen, 1984; Gjerris *et al.*, 1987; Lundar and Nornes, 1990; Gjerris and Borgesen, 1992).

Anatomically, the subarachnoid space of the convexities may be scarred. This is well known in cases of secondary NPH where subarachnoid or intraventricular haemorrhage induces an inflammatory response resulting in scarring of the leptomeninges with adherence of the arachnoid membrane to the pia and blockage of the arachnoid villi. Infective meningitis may result in similar findings (Penfield & Elvidge, 1932; Russell, 1949). In idiopathic NPH, thickening of chronic meningeal thickening may be seen at autopsy (DeLand *et al.*, 1972; Akai *et al.*, 1987). In support of this, patients with NPH exhibit a convexity block when air, contrast or radiographic tracers are injected into the subarachnoid space (Ojemann *et al.*, 1969; LeMay & New, 1970; Behrman *et al.*, 1971; Greitz & Grepe, 1971; Bannister, 1972; Forslo *et al.*, 1972; Di Chiro, 1973; Shenkin et al., 1973; James *et al.*, 1974a, 1974b; Stein and Langfitt, 1974; Adams, 1975; Drayer *et al.*, 1977; Hindmarsh & Greitz, 1977; Ostertag & Mundinger, 1978).

Chronic disease and involution of the arachnoid granulations may be seen in NPH (Gille Davidson, 1971; Gutierrez *et al.*, 1975; Di Rocco *et al.*, 1977). Akai (1987) noted that the numbers of arachnoid villi were decreased in number in the lateral lacunae of patients with NPH. In addition remaining villi were often compromised by

adhesions. However similar findings are often seen in the brains of patients with no disease at autopsy (Tamura, 1985) and the significance of such findings is unclear. However, such changes may explain the increased R_{csf} seen in some patients.

1.4.2 Pathology of the Parenchyma

There have been relatively few detailed histopathological studies of the brains of patients with NPH. The most commonly described histopathological changes are those of the deep white matter. The periventricular white matter is characterised by demyelination, oedema and spongiosis (Di Rocco et al., 1977; Akai et al., 1987). Axons themselves may be decreased in number with swelling and fragmentation. The peripheral arcuate white matter regions are relatively spared as is the cortex (Akai et al., 1987).

Histopathological findings, after autopsy (Ball, 1976; Del Bigio *et al.*, 1997) or brain biopsy (Stein & Langfitt, 1974; Tedeschi *et al.*, 1995; Del Bigio et al., 1997) consistent with Alzheimer's disease (for example, neurofibrillary tangles and plaques), are also common in patients with NPH. Furthermore, the presence of such findings does not appear to adversely affect the outcome of NPH patients after CSF shunting (Tedeschi et al., 1995; Del Bigio et al., 1997). In addition, the co-existence of Parkinson's disease and NPH is now well documented. It is noteworthy that at least two cases of NPH with co-existing CJD have been diagnosed (Galvez *et al.*, 1980; Galvez and Cartier, 1984).

The histopathological changes of cerebrovascular disease are also frequently found in patients with NPH. Akai *et al.* (1987) found that patients with NPH demonstrated marked sclerosis of the small arteries and arterioles of the subependymal region, deep white matter, thalamus and basal ganglia. Small lacunes were frequent in these regions with focal softening of the tissue. Significant vascular changes have also been reported at autopsy in patients with shunt-responsive NPH who have died of other causes (Lorenzo *et al.*, 1974; Koto *et al.*, 1977; Newton *et al.*, 1989). However, as idiopathic NPH, is primarily a condition of ageing such changes are not surprising.

These histopathological cerebrovascular changes are reflected on MR imaging. MR white matter hyperintensities are thought to represent areas of demyelination due to microvascular changes and not necessarily infarction. Bradley *et al.*, (1991) found a significant association between the presence of deep white matter hyperintensities on MR and the presence of NPH. They are also present in Binswanger's disease and conditions where cerebrovascular disease is a feature.

As noted previously, CSF composition may reflect pathology of the brain parenchyma. Tullberg *et al.*, (2000, 2002) found that sulfatide was increased significantly in those with cerebrovascular disease or deep white matter lesions on MR as well as those with NPH. However patients with subcortical arteriosclerotic encephalopathy primarily had markedly increased sulfatide compared with NPH. The authors suggest that very high sulfatide levels may indicate irreversible demyelination. With the exception of TNF alpha (Tarkowski *et al.*, 2003), other studies of CSF constituents have not yielded any significant results (Wikkelso & Blomstrand, 1982; Wikkelso *et al.*, 1985, 1986, 1991; Poca *et al.*, 2001).

Histologically, the ependyma of the frontal and occipital horn becomes disrupted in hydrocephalus (Del Bigio and Bruni, 1988; Del Bigio, 1993). This is probably due to the fact that this area undergoes maximum strain during ventricular enlargement (Péna *et al.*, 1999 & 2002a). Within the parenchyma adjacent to the frontal and occipital horns periventricular lucencies (PVLs), which are areas of hypodensity on CT scanning, are observed. Their presence was originally thought to represent transependymal seepage of CSF and was thus reversible (Yamada *et al.*, 1978). However the situation is more complex as they may also represent areas of gliosis.

1.5 Treatment of NPH

The mainstay of treatment for NPH is CSF shunting in order to reduce the volume and/or pressure of fluid within the ventricular system and to reduce the effective resistance to CSF absorption. The most common form of CSF shunt used in NPH is a ventriculoperitoneal shunt although ventriculoatrial CSF shunting has also been popular.

The main problem is that the response to CSF shunting is difficult to predict. Vanneste *et al.* (1992) reviewed the literature and found that the response to CSF shunting varied widely between studies (25-80%) with the mean being 50%. In 1,047 patients from the literature, improvement after CSF shunting is notably better in NPH secondary to other conditions (64%) compared to idiopathic NPH (50%). In addition *marked* improvement was noted in 46% of patients with secondary NPH compared to 33% with idiopathic NPH.

The potential for clinical improvement must also be balanced against the potential complications of CSF shunting which are well documented (Illingworth *et al.*, 1971; Vanneste *et al.*, 1992; Hebb and Cusimano, 2001). The most common complications are shunt infection and shunt blockage. Less common complications include subdural haematomas, stroke, shunt disconnection, erosion of the distal catheter through the skin or internal viscus, thrombosis around atrial catheters and shunt nephritis. Gjerris & Borgensson (1992) found that the complication rate in patient with NPH may be particularly high (>50% over 5 year follow-up). This would be expected given the age of the patients and the reduction in general health that comes with reduced mobility and dementia. Others have reported similar findings (Udvarhelyi *et al.*, 1975; Steinbok & Thompson, 1976). Vanneste *et al.* (1992) performed a risk/ benefit study of idiopathic NPH using 1, 047 patients obtained from 19 studies from the literature. The benefit / harm ratio in patients with idiopathic NPH was 1.7 and increased to 6 if high-risk patients with significant co-morbidity were excluded. The potential for unduly compromising patients by subjecting them to CSF shunting procedures must therefore be emphasised.

Given the problems of predicting outcome after CSF shunting and risks associated with such procedures in the elderly, clinicians have sought parameters or investigations which are predictive of a clinical improvement after CSF shunting response. The more common parameters and investigations for this purpose are:

i. Ventricular volume. Various methods to measure ventricular size including the simple Evans's ratio to more complex ventricular indices have not been able to find a correlation between the size of the ventricles

and outcome after CSF shunting. This is true of ventriculograms (Shenkin *et al.*, 1975) or more complex MR techniques (Condon *et al.*, 1986).

ii. Ventricular / Sulcal volume ratio. Ventricular enlargement in the absence of sulcal enlargement was proposed as a method to differentiate simple atrophy from a hydrocephalic process (Gado *et al.*, 1976). Modern CT scanners have improved resolution. The application of a variety of CT criteria which incorporate measures of ventricular dilation and sulcal enlargement by Boon *et al.* (2000) was found to have a predictive value of 65% when combined with clinical data compared to 75% reported by Vanneste *et al.* (1993). Holodny and colleagues (1998) have presented five cases of focal sulcal enlargement which they consider as particular of NPH.

iii. MR white matter intensities. Krauss *et al.* (1996) studied 41 patients with NPH which were well characterised with studies of CSF dynamics. They found that the degree of improvement was negatively correlated with periventricular and deep white matter disease. However, the authors noted that the presence of white matter disease did not preclude improvement but influenced its degree. Godersky *et al.* (1990) found that the degree of periventricular hyperintensity did not predict surgical outcome. More recently Tullberg *et al.* (2001) reported that in 34 patients followed for 3 months post CSF shunting neither the degree nor pattern of deep or periventricular white matter disease influenced outcome after CSF shunting. They concluded that deep white matter hyperintensities on MR

should not be used as a method of predicting shunt response (Tullberg *et al.*, 2001, 2002). Finally, the Rotterdam Scan Study (de Leeuw *et al.*, 2001), reported that deep white matter hyperintensities are frequently found in asymptomatic elderly individuals and their incidence increases with age.

iv. CSF drainage test. This test involves removing an amount of CSF is removed (30-50mL) usually via a lumbar puncture. The logic of the test is that this is akin to CSF shunting. In some cases temporary clinical improvement may be evident but is uncommon. While a CSF drainage test may be positive, that is, indicate improvement after CSF shunting, it should be interpreted with caution as the clinical status of patients with NPH does fluctuate. Likewise, as noted by Adams *et al.* (1966) and Fisher (1978), a negative drainage test does not preclude clinical improvement after CSF shunting. Reasons for failure of the test include failure to remove sufficient fluid and undiagnosed non-communication between the subarachnoid space and the ventricles. More importantly it should be recognised that even after shunt surgery improvement may take several days or weeks for gait and possibly months for cognition. In recognition of this problem Chen *et al.* (1994) proposed a system of temporary, controlled resistance lumbar drainage which appeared to be useful in predicting shunt outcome.

v. CSF dynamics.

   a. B waves. Frequent B waves of >9 mmHg amplitude are thought to be indicative of a successful response to CSF shunting (Crockard *et al.*, 1977; Pickard *et al.*, 1980; Borgesen and Gjerris, 1982; Graff-Radford *et al.*, 1989; Raftopoulos *et al.*, 1994; Reilly, 2001). However their absence does not exclude a diagnosis of NPH or shunt response.

   b. Resistance CSF absorption. Gjerris & Borgensson (Borgesen *et al.*, 1979; Borgesen and Gjerris, 1982; Borgesen, 1984; Gjerris *et al.*, 1987; Gjerris and Borgesen, 1992) using the lumbar-ventricular CSF infusion method found that of 271 patients shunted for NPH, no patient with an R_{csf} < 12 mmHg/ml/min responded to CSF shunting while 80% with R_{csf} >12.5 mmHg/ml/min. Similar findings have been reported by Lundar & Normes (1990). The Copenhagen Symposium on NPH (1990) concluded that an R_{csf} >11 mmHg/ml/min was suggestive of NPH. In a recent study (Boon *et al.*, 2000) involving 95 patients followed for 1 year, it was suggested that the best strategy for management of patients thought to have NPH was to shunt only those patients with a R_{csf} >18 mmHg/ml/min, or if the R_{csf} was lower, only those with objective clinical evidence and CT evidence of NPH.

vi. Other Investigations. These include measurement of CBF and cerebrovascular autoregulation and combinations of these with the CSF drainage test. These have met with limited success and are reviewed in Chapters 4 and 5.

The overall result is that shunt response rates have improved marginally despite these parameters. This may be because in seeking a predictor of shunt response, NPH has been mostly treated as a single entity in the absence of a satisfactory understanding of either the aetiology or pathophysiology of the condition.

In the event that a patient fails to respond to a functioning shunt, failure is usually attributed to a co-existing pathology such as cerebrovascular, Alzheimer's or other disease. However, relatively little attention has been given to the characteristics of the type of shunt and valve used. The majority of patients are shunted using a certain valve type influenced by the individual preference of the neurosurgeon. The only randomised study of shunt valves was that of the Dutch NPH study (Boon *et al.*, 1998a) in which patients were randomised between low and medium pressure Hakim valves. While patients receiving the low pressure valve performed better than those who received the medium pressure valve, the result was not statistically significant. Larsson *et al.* (1992) studied 13 patients NPH who were treated with adjustable Sophy valve. They found that improvement was independent of the adjust valve pressure.

To improve on current knowledge regarding the aetiology and pathophysiology of the condition, this thesis aims to examine the role of the brain parenchyma in NPH and its interplay with the CSF dynamics. Further study of this subject should enhance approaches to predicting the response to CSF shunting in patients with NPH and the design of treatment regimens.

Chapter Two

A Clinical Study of Low Pressure Hydrocephalus

2.1 Introduction

In judging the success or otherwise of the treatment of hydrocephalus of all types greatest reliance is placed on the observed clinical outcome. The degree of change in ventricular size is not a reliable yardstick and there is seldom any detailed post-shunt evaluation or re-evaluation of CSF dynamics and related parameters such as intracranial pressure (ICP). If the patient does not respond satisfactorily to CSF drainage with such systems, and the system is definitely functioning, it is likely to be assumed that either irreversible damage has occurred due to the hydrocephalus itself or related factors, or that the diagnosis was wrong.

The five cases of this study are patients who were deemed to have normal pressure hydrocephalus, were shunted but failed to improve. This group of five patients were re-evaluated after failing to improve clinically. There had been no reduction in ventricular size. Patients therefore underwent periods of increased CSF drainage at low or even negative CSF pressures in order to reduce ventricular size. This reduction resulted in clinical improvement in four patients. Illustrated in this clinical study are the limitations of current knowledge on the interplay between CSF dynamics and the brain parenchyma. Further, it demonstrates the problems of definition and nomenclature.

2.2 Summary of Cases

Over a three year period (January 1996 to January 1999), 7 patients with hydrocephalus were investigated who remained symptomatic and, in 5 instances, had marked neurological disturbance despite a demonstrably functioning internal CSF shunt (4 cases) or external ventricular drain (1 case). The 5 cases with neurological disturbance are those reported below. In the remaining 2 cases, not reported here, there was headache only and this was not clearly postural or activity related. Neither of these 2 patients noted any improvement with a trial of low pressure external ventricular drainage although, of course, the constraints of drainage made the evaluation of a symptom like headache difficult. Both these patients currently have ventriculoatrial shunts with programmable valves at the low setting with some improvement, but not resolution, of their headache. The details of the 5 patients with neurological disturbance are summarised in Table 3.1 and then set out in detail in the individual case reports. There were no complications specifically related to the use of valveless or low pressure shunts. There was 1 shunt revision (due to a blocked ventricular catheter) over an average follow-up period of 2 years in the 4 treated patients.

2.3 Individual Case Reports

Case 1. This 75 year old woman initially presented in 1995 with a para-sellar meningioma which was surgically removed. In the early post-operative period she developed communicating hydrocephalus probably secondary to operative and post-operative haemorrhage. A ventriculoperitoneal shunt was inserted using a medium pressure Hakim valve which was changed after a short period to a high pressure valve due to continuing symptoms attributed to low pressure. Despite this she complained

of persistent headache and was intermittently quite obtunded. At this time, approximately 8 months after the initial surgery, she was complaining of persistent headache, worse on sitting or standing, and was dull and lethargic. In addition to right III, V and VIII nerve palsies from her original problem she had a wide-based ataxic gait. The investigative findings were rather conflicting. A CT scan showed persistent ventriculomegaly with pronounced periventricular oedema yet ICP monitoring, CSF infusion studies and radionuclide shunt studies were all entirely normal. On the basis of the latter, together with the postural component to her headaches, a very tentative diagnosis of low pressure syndrome was made and an anti-siphon device was added to her shunt. Following this procedure she was clearly worse clinically although, again, all the tests for shunt patency were normal. On MR scan the ventricles remained markedly dilated and there was striking peri-ventricular oedema (Figure 2.1a). An external ventricular drain was then inserted in addition to her functioning shunt and free drainage carried out after a 24 hour period of monitoring had shown normal to low pressures. Drainage was carried out first at 5cm above the external acoustic meatus (EAM), then at 0cm, then at –5cm for 24 hours at each level. At 5cm she remained obtunded with a GCS of 10 and very little CSF drainage whereas at the lower levels there was considerable increase in the volume of CSF drained and a sustained clinical improvement. In view of this the shunt was revised with removal of both the valve and the anti-siphon device. She was thus left with a valveless ventriculoperitoneal shunt. Post-operatively her improvement was dramatic and sustained. She became fully mobile and free of headache and, after a period of rehabilitation, returned to an independent existence. Follow-up CT and MR scans showed a marked reduction of ventricular size and complete resolution of her peri-ventricular oedema. (Figure 2.1b) She remained well for a 3 year follow-up period.

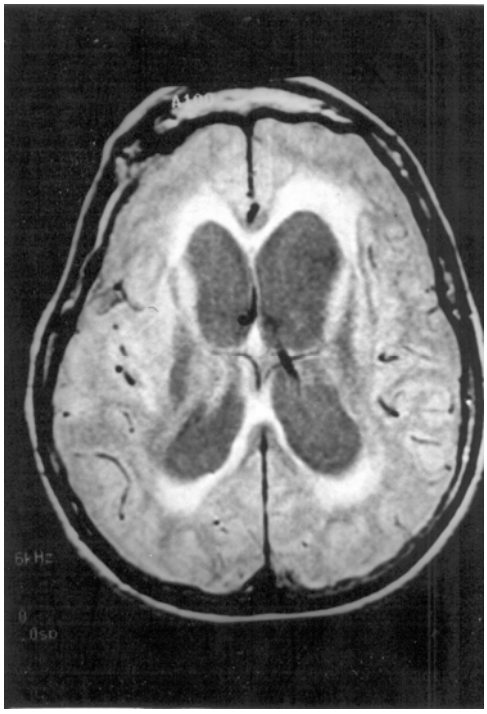

Figure 2.1a. MR scan showing generalised ventricular dilatation with marked peri-ventricular oedema despite functioning ventriculoperitoneal shunt and normal ICP. [Patient 1]

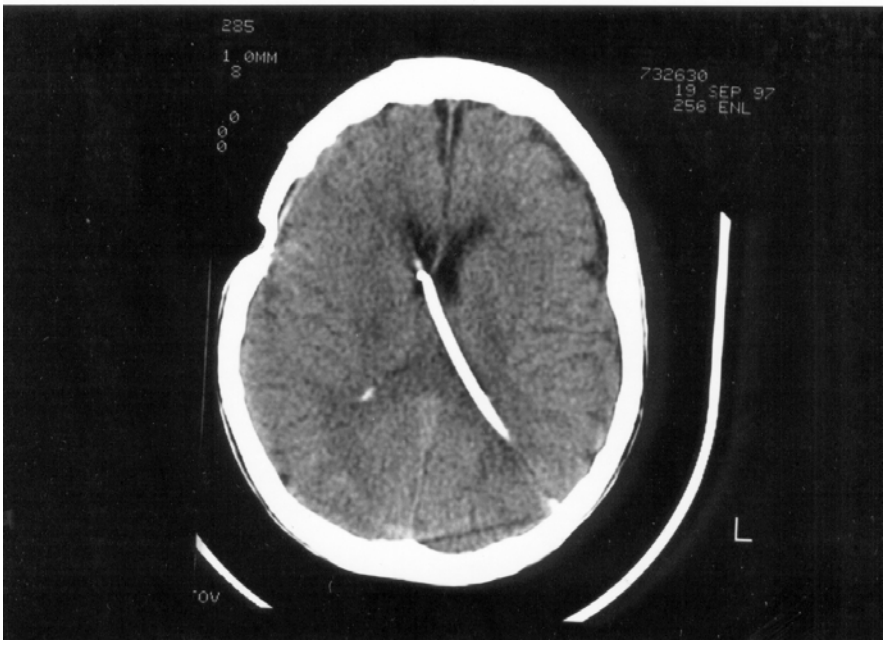

Figure 2.1.b. CT scan of patient 1 twelve months after placement of a valveless VP shunt.

Case 2. This patient, a 53 year old man, had initially presented to a neurologist in 1984 with a vague history of visual disturbance. CT scan revealed marked communicating hydrocephalus which was thought to be arrested so no treatment was initiated. He re-presented 12 years later with the recent onset of gait disturbance and was found to be markedly ataxic. An attempt at third ventriculostomy was unsuccessful and a right ventriculoperitoneal shunt was inserted using a medium-pressure Pudenz valve. His symptoms progressed. A diagnosis of Parkinson's disease was made and he was treated with Sinemet without success. He was then referred to the Department of Neurosurgery at Royal Prince Alfred Hospital. The salient clinical features were slowing of mentation and severe gait ataxia. CT scan showed marked ventricular dilatation. Although demonstrably functioning the shunt was revised by

replacing the medium-pressure Pudenz valve with a Sophy valve at the lowest setting (40 mmH_2O). There was an immediate and sustained improvement in mentation, return of gait to normal and resolution of all apparent Parkinsonian symptoms and signs. A follow-up CT scan, done 5 weeks after shunt revision, showed a slight decrease in lateral ventricular size with a more pronounced decrease in the size of the fourth ventricle. As he became increasingly active he developed apparent low pressure symptoms with postural headache and neck pain. Six months after the revision, the valve setting was changed to medium with amelioration of these symptoms. There was no return of his earlier symptoms over a 2 year follow-up period.

Case 3. This girl initially presented at the age of 2 months with a short history of apparent headache and lethargy. On examination she was relatively inactive and had bilateral VI nerve palsies. A CT scan showed moderately severe ventricular dilatation and a posterior fossa cyst not communicating with the ventricular system. A shunt was inserted with catheters in the right lateral ventricle and the posterior fossa cyst connected via a Y-connector to a single distal tube incorporating a low pressure paediatric Hakim valve. Despite initial problems with shunt infection, necessitating removal of the original shunt and replacement with an identical system on the left side, she progressed well until March 1996 when, aged 2 years, she again presented, this time with intermittent obtundation, abnormal head posturing and vomiting. She was found to have a blocked infected shunt system with marked ventricular enlargement on CT scan (Figure 2.2a). The shunt system was removed, external ventricular drainage instituted and a course of systemic antibiotics given. After 21 days of such treatment, the infection having cleared, the shunt system was reinserted

now using a separate left ventriculoperitoneal shunt (medium pressure paediatric Hakim valve) and a posterior fossa cyst to peritoneal shunt (low pressure paediatric Hakim valve). She did not improve, remaining quite obtunded with abnormal posturing. Both shunts were examined operatively and found to be patent but there was a considerable amount of fluid in the peritoneal cavity. On the assumption that there was poor peritoneal absorption a right atrial shunt was inserted with a low pressure paediatric Hakim valve to the right lateral ventricular and posterior fossa cyst catheters. At this stage she had bilateral lateral ventricular shunts, one atrial and one peritoneal, both with low-pressure valves. Still there was no improvement and the ventricles remained dilated although smaller than before (Figure 2.2b). There were several recordings of low CSF pressure on shunt taps. A period of external ventricular drainage was then instituted at varying levels down to negative values. With the latter she improved markedly. ICP monitoring at this time was unremarkable with levels around 0 to 5 mmHg and no abnormal waves. (Figure 2.3) The left ventriculoperitoneal shunt was revised with removal of the valve. Testing during operation showed the shunt to be patent. She now had the pre-existing, presumably patent, right atrial shunt with a low-pressure valve and the revised left ventriculoperitoneal shunt, now valveless. She improved dramatically after removal of the valve. Apart from one episode of ventricular catheter obstruction necessitating revision in November 1996 she remained well until 1999. CT and MR scans showed marked reduction in ventricular size (Figure 2.2c).

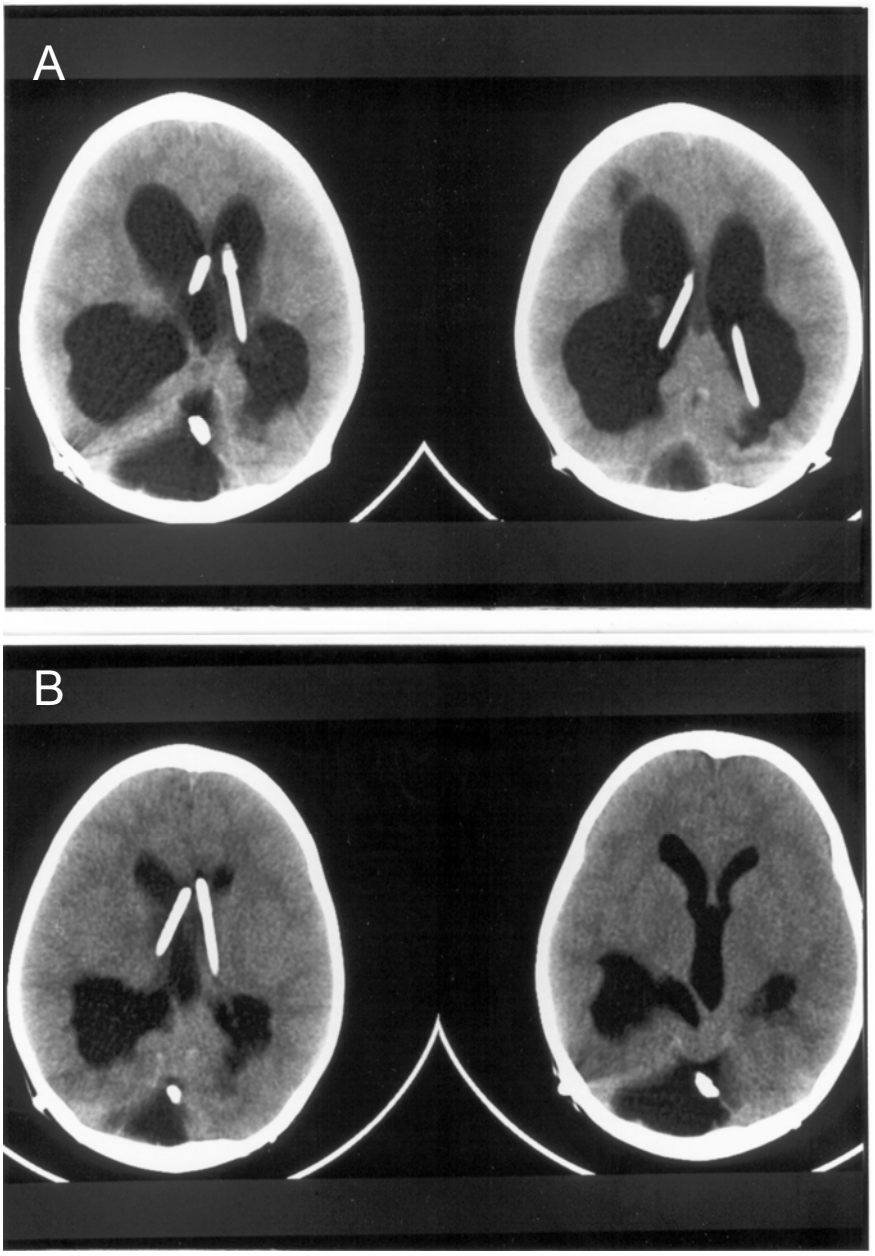

Figure 2.2a. CT scan at time of shunt obstruction in patient

Figure 2.2b. CT scan after shunt revisions with insertion of bilateral ventricular shunts using low-pressure valves.

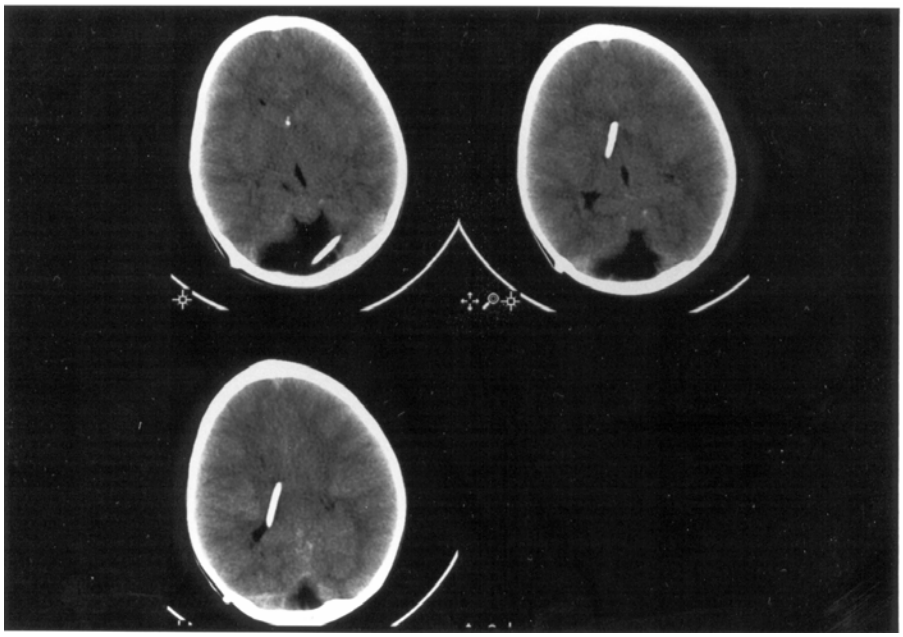

Figure 2.2c. CT scan after further shunt revision and removal of valves.

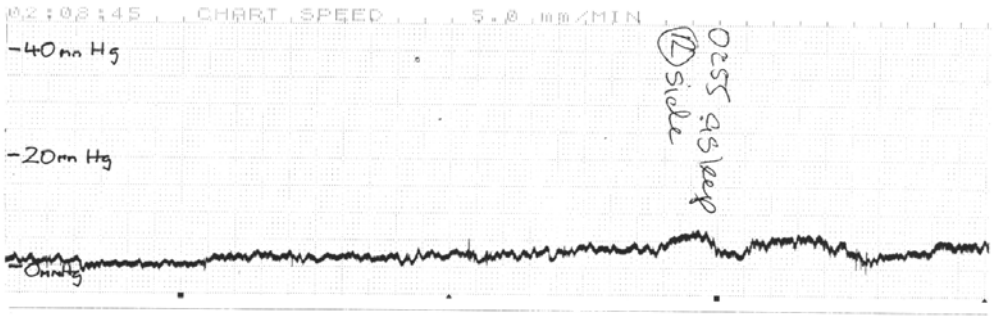

Figure 2.3. Typical section of continuous ICP tracing in patient 3 at time of CT scan shown in Fig 2.2b.

Case 4. This 61 year old Noumean patient presented with a 3 month history of deteriorating consciousness and a progressive left hemiparesis. A diagnosis of cryptococcal meningitis was made and treatment with Fluconazole and steroids initiated. There was some initial improvement but he remained obtunded. CT scans showed increasing ventricular enlargement and he was transferred to Sydney for further treatment. On presentation he was obtunded and had a left hemiparesis. CT scan showed generalised ventricular enlargement particularly involving the fourth ventricle with evidence also of basal meningitis. A frontal ventricular catheter with Rickham reservoir was inserted for CSF sampling and ICP monitoring. His problems were further complicated by the development of Klebsiella meningitis and a persistent chest infection. The Rickham reservoir was removed and replaced with an external ventricular drain. ICP was high initially without free drainage but as the meningitis cleared with appropriate antibiotic treatment it fell to levels around 5 mmHg without drainage. Nevertheless, the patient was clinically unchanged. A period of free CSF drainage at 5 cm above the EAM was instituted without improvement. Only small volumes of CSF were drained (50 mls / 24 hours). His ICP remained low during intermittent periods of monitoring. CT scans continued to show marked ventricular enlargement with some peri-ventricular oedema. A period of external ventricular drainage at –5cm was then instituted with marked clinical improvement. Following this a right ventriculoperitoneal shunt was inserted without a valve. His clinical improvement was sustained. One month later, while undergoing rehabilitation, he again deteriorated and was found to have an isolated left lateral ventricle. A separate left ventriculoperitoneal shunt, also valveless, was inserted with clinical and radiological improvement. Unfortunately, he subsequently developed a recurrence of his chest infection and succumbed.

Case 5. A 70 year old man was referred for continuing management of hydrocephalus. Hydrocephalus was first diagnosed in Lebanon in 1969 and a shunt was inserted in 1970 with one revision in 1972. There were no details as to the cause of the hydrocephalus. In 1994, now living in Australia, he presented to another institution with evidence of brain stem compression. CT and MR scans showed a type II Chiari malformation and persistent ventriculomegaly. He had a posterior fossa decompression and revision of his ventriculoperitoneal shunt using a medium pressure valve. Over the next 18 months he had 2 apparent cerebrovascular episodes resulting in a mild left sided weakness. He presented to the Royal Prince Alfred Hospital in December 1995 with worsening ataxia and bulbar signs. There was moderate ventricular dilatation on CT scan. A right frontal ventricular catheter with Rickham reservoir was inserted. CSF infusion studies and ICP monitoring were carried out on two separate occasions. On both occasions the resistance was low and the ICP normal without waves over a 24 hour period of recording. A period of external ventricular drainage was initiated on the basis of a possible low pressure state but after 24 hours drainage at 0cm and then a further 24 hours at –5cm there was no improvement. No further treatment was undertaken.

2.4 Discussion

The term ‘normal pressure hydrocephalus’ has somewhat clouded the diagnosis and management of hydrocephalus by implying two distinct entities, high pressure and normal pressure hydrocephalus. The physical properties of the brain parenchyma are almost ignored. Studies utilising continuous ICP monitoring have shown that all forms of hydrocephalus can be associated with widely differing pressure patterns

(Hayden *et al.*, 1970; DiRocco *et al.*, 1975) and that this applies to what would be categorised clinically as normal pressure hydrocephalus (Symon *et al.*, 1972). Nonetheless, it is clear that hydrocephalus, as the basis of progressive clinical disturbance, can be associated with essentially normal ICP.

More recently Pang and Altschuler (1994) have attempted to identify a further subgroup which they termed ‘low pressure hydrocephalus’ on the basis of 12 cases, previously shunted, who were symptomatic despite functioning shunts and who required very low pressure CSF drainage for amelioration. These authors also joined the ongoing debate regarding the mechanism of sustained or increasing ventricular enlargement despite the absence of increased ICP, initiated by Hakim and others (Geschwind, 1968; Hakim *et al.*, 1976). Experimental studies also show sustained hydrocephalus despite normal CSF pressures (Hochwald *et al.*, 1972).

The determinants of ventricular dilatation and the causative mechanisms relating pressure levels to physical changes in the brain remain poorly understood. Hakim, in his original proposal invoking Pascal’s Law applied to the ventricles as containers, postulated an initial period of high ICP necessary to establish ventricular dilatation followed by a fall in pressure as the volume of the ventricles increased (Hakim *et al.*, 1976). Pang and Altschuler, and indeed others before them, have taken issue with this concept which is, at the very least, an over-simplification. They have postulated changes in the viscoelastic properties of the brain especially consequent upon loss of brain extracellular fluid as important in maintaining ventricular dilatation in low pressure states (Fried and Shapiro, 1986; Pang and Altschuler, 1994). In support of this is the finding that the reduction in ventricular size after shunt surgery in patients

with NPH is correlated with elastance (Tans and Poorvliet, 1989). More recently, increased elastance has been shown to predict a positive clinical outcome and a reduction in ventricular size in patients with aqueduct stenosis undergoing endoscopic third ventriculostomy (Tisell *et al.*, 2002).

The importance of the first case described above is that the marked degree of periventricular oedema with demonstrated low pressure and a functioning shunt and which resolved with very low pressure CSF drainage would seem to indicate continued transependymal passage of CSF with attendant increase in brain extracellular fluid despite the low pressure.

2.5 Conclusions

What can be concluded from this series of patients is that in hydrocephalic states, CSF dynamics are only one aspect that needs to be considered. The properties of the parenchyma are also important. The apparent paradox of normal or low CSF pressure in the presence of ventricular dilation can only be solved if there is some alteration in the viscoelastic properties of the parenchyma. Thus ventricular dilation can occur without an increase in CSF pressure. This is different from cerebral atrophy where there is loss of cerebral tissue. In addition, the parenchymal changes, at least in some cases, appear to have a dynamic component and may be altered by prolonged CSF drainage.

Chapter Three

Clinical Features and CSF Infusion Study in Patients with NPH

3.1 Introduction

A useful tool for characterizing CSF dynamics and is the CSF infusion study (Boon *et al.*, 1997, 2000; Gjerris and Bech-Azeddine, 2001). Computerized CSF infusion studies (Czosnyka *et al.*, 1996) have been available to patients attending the CSF circulation disorders clinic at Addenbrooke's Hospital, Cambridge during the past six years. Patients referred to the clinic include those cases typical for NPH as well as a significant number who are atypical of NPH. Infusion studies were performed in both typical and atypical cases as this is what clinicians are often faced with.

Apart from providing information regarding the state of CSF dynamics, CSF infusion studies also provide some information regarding the properties of the brain parenchyma. However, this aspect of CSF infusion studies has received very little attention probably because it has not been a predictor of shunt response. A retrospective analysis of the patients' clinical details and infusion study results was undertaken in order to examine the relationship between clinical features, CSF dynamics and the properties of the brain parenchyma.

3.2 Methods

3.2.1 Patients and Clinical Assessment

Between 1996 and 2000, 365 computerized CSF infusion studies were performed in 256 patients for a variety of CSF disturbances including hydrocephalus and

pseudotumor cerebri. The clinical data of these patients was reviewed through a retrospective analysis of the medical records and consultation reports. Where pre-operative clinical information was either insufficient or not available, the patients were excluded from the study. Here the results of CSF infusion studies performed for suspected cases of NPH referred by neurologists or geriatricians are reported. The criteria for inclusion were a prospective clinical and radiological diagnosis of NPH consisting of gait disturbance, with or without cognitive changes or urinary incontinence, dilated ventricles on CT and CSF opening pressure less than 20 mmHg. Objective radiological data was not able to be consistently obtained retrospectively and is thus not reported here.

There were 133 studies performed in 99 patients with idiopathic NPH and 34 with NPH secondary to some cause. These cases included NPH secondary to subarachnoid haemorrhage (11 cases), long-standing congenital aqueduct stenosis (9 cases), head injury (5 cases), meningitis (4 cases), intracerebral haemorrhage (2 cases), intracranial tumour (2 cases), and basilar artery ectasia (1 case).

For each patient, information regarding the presence or absence of an aetiological factor, the clinical features and the presence or absence of vascular hypertension and/or previous cerebrovascular event was obtained. This information was obtained on attending the CSF clinic for their initial assessment. In order to provide a simple method by which to grade the severity of symptoms, an NPH score modified from Larsson (1991) was utilized. This assessed gait, living conditions and urinary incontinence with a score out of 10. It also provided a separate gait score out of 5. (Table 3.1)

Gait	0 – normal
	1- insecure
	2 – insecure (cane)
	3 – bimanual support
	4 – aided
	5 – wheelchair
Living condition	0 – Independent
	1 – at home with assistance
	2 – retirement home
	3 – nursing home
	4 – hospital
Urinary symptoms	0 – nil
	1 – present

Table 3.1: Basis of clinical NPH score

This resulted in a NPH score out of 10 points as well as a gait score. A separate urinary incontinence score was obtained (0 – nil; 1 – frequency; 2 – occasional incontinence and 3 - daily incontinence). In addition, as a measure of overall function, a modified Stein-Langfitt score was recorded (Table 3.2).

Modified Stein-Langfitt Score
0 – no neurological deficit and able to work
1 – minimal deficit and able to function independently at home
2 – some supervision required at home
3 – custodial care required despite considerable independent function
4 – no capacity for independent function

Table 3.2: Modified Stein-Langfitt Score

Of the 133 patients, there was clinical data available for 46 patients who underwent CSF diversion; 36 idiopathic and 10 secondary NPH patients. Patients were shunted if R_{csf} was raised (>13 mmHg/ml/min) and the clinical picture was consistent with NPH. Some patients with lower R_{csf} were also shunted if the clinical picture was convincing, that is, prominent gait disorder and judged fit to undergo surgery. The 46 shunted patients reported represent a subset of the shunted patients, that is those with clinical notes available and whose treatment was completed at this institution. The majority of patients were treated with programmable Codman valves initially set at 140 mmH_2O or Medtronic Strata valves. After post-operative CT scans excluded the presence of asymptomatic subdural collections, the opening pressure of the valve was decreased. Outcome was assessed on the basis of a change as well as the amount of change in each of the clinical scores. The mean follow-up time for shunted patients was 13.5 months (range 1-106 months). Shunt function of patients who did not improve was checked by a computerised CSF infusion study.

3.2.2 Patient groups

On the basis of clinical features, patients were subdivided into different groups (Figure 3.1). First, idiopathic (n=99) and secondary NPH (n=34) patients were compared. Next, patients with idiopathic NPH were classified into two groups – clinically 'typical' and 'atypical' idiopathic NPH. 'Typical' idiopathic NPH patients (n=72) were those who demonstrated no focal neurological signs and reported gait disorder as the first manifestation of their NPH. Atypical patients (n=26) had either cognitive disturbance as their first symptom of NPH or a focal neurological deficit, for example mild hemiparesis. Patients with 'typical' idiopathic NPH symptoms were further separated into patients with a history of hypertension or cerebrovascular event (n=36) and those without (n=28).

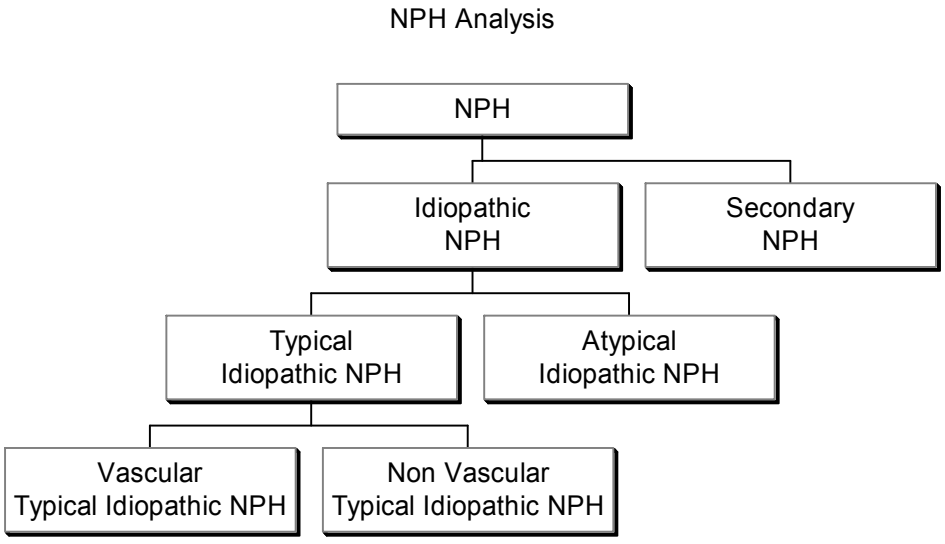

Figure 3.1

3.2.3 Computerized Infusion Study Technique

All patients underwent computerized CSF infusion studies as described by Czosnyka. (1990 &1996) The computerised CSF infusion study was designed to examine the state of a patient's CSF circulation and its ability to compensate. It is performed via a pre-implanted ventricular access device or the lumbar CSF space. In either case two needles are inserted (22g spinal needles for lumbar tests; 25g butterfly needles for ventricular studies). One needle is connected to a pressure transducer via a stiff saline-filled tube and the other to an infusion pump mounted on a purpose-built trolley containing a pressure amplifier (Simonsen & Will, Sidcup, U.K.) and an IBM-compatible Personal Computer running software written in-house (Czosnyka *et al.*, 1996) (Figure 3.2). Occasionally a single needle is used if access is difficult with a three-way tap to periodically switch between CSF infusion and pressure monitoring. The routes used for patients in this report were lumbar (2 needles) in 65 patients, Ommaya reservoir (2 needles) in 61, lumbar puncture (single needle) in 7 and an external ventricular drain in one patients.

Set-up of CSF infusion Study Equipment

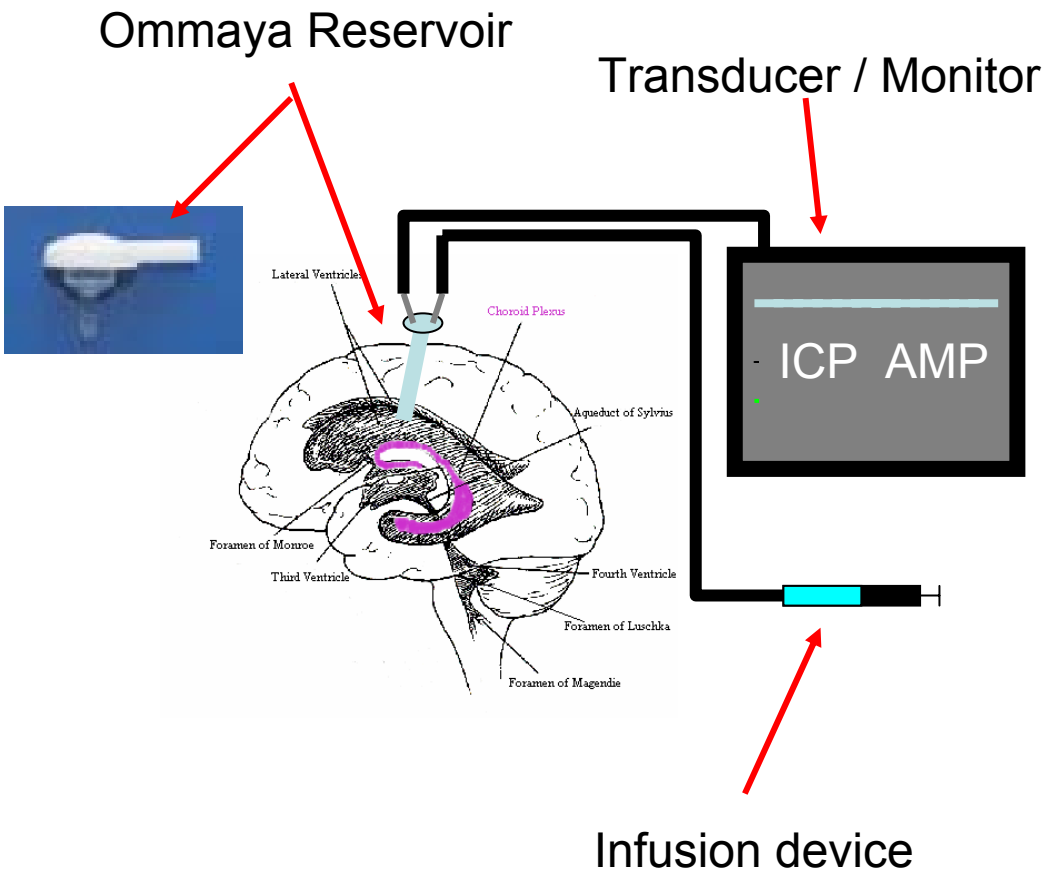

Figure 3.2: Computerised CSF infusion Study Setup.

After 10 minutes of baseline measurement, normal saline was infused at a constant rate (0.5 ml/min to 1 ml/min) until a steady state ICP plateau was achieved. If the ICP reached 45 mmHg, the infusion was stopped. Following cessation of the infusion, ICP was recorded until it decreased to steady baseline levels. All compensatory parameters were calculated using computer-supported methods based on physiological models of CSF circulation (Ekstedt, 1978; Marmarou *et al.*, 1978; Avezaat and Eijndhoven, 1984).

During the test both mean ICP and its pulse amplitude increase in time from values ICP_{beg} and AMP_{beg} to ICP_{end} and AMP_{end} respectively (Figure 3.3). Baseline ICP (ICP_{beg}) and the resistance to CSF outflow R_{csf} characterise static conditions of CSF circulation, whilst the cerebrospinal elasticity coefficient (E1) and pulse amplitude of ICP waveform (AMP) express dynamic components of CSF pressure volume compensation.

The R_{csf} represents the CSF pressure that must be applied to the CSF system to produce an absorption rate of 1ml of CSF per minute at equilibrium. R_{csf} is therefore calculated by the dividing the difference in ICP_{end} and ICP_{beg} by the infusion rate. It assumes a constant CSF production rate and constant superior sagittal sinus venous pressure. A particular advantage of the computerized CSF infusion test is that if a steady state is not obtained or the infusion rate is changed during the test, the program can compute R_{csf} based on non-linear ICP regression analysis.

In addition to the R_{csf}, information regarding the compliance of the neuroaxis may be obtained from the CSF infusion study. The compliance of a distensible elastic chamber is given by the ratio of the change in volume to the change in pressure. Due to the presence of the skull and the different components of the brain (including blood) the pressure-volume relationship for the brain is non-linear. The curve is hyperbolic with compliance decreasing as pressure increases. A linear approximation of the P-V curve is the volume – log pressure curve. The slope of this curve is the pressure volume index (PVI). Thus the PVI may be defined as the amount of CSF that needs to be added to the ventricular compartment to raise the pressure by a factor of 10 (Marmarou *et al.,* 1978). The P-V curve represents all the point of equilibrium

where there is no CSF absorption. In order to measure the PVI the rate of volume addition needs to be much greater than the rate of CSF absorption. If the PVI is considered to be a fundamental property of the CSF system then a single rapid bolus injection may be used.

$$PVI = \Delta V/Log_{10}P_i/P_0$$

However it may also be theoretically calculated using the computerised infusion study method from the Elastance co-efficient (El) (Czosnyka *et al.*, 1996). The relationship between El and PVI is given by:

$$PVI = 1/(0.43 \times El)$$

E1 describes the compliance of the CSF compartment according to the formula: Compliance of CSF space= $C_i = 1/ \{E1*(ICP-p_0)\}$ where p_0 is the unknown reference pressure level, representing hydrostatic difference between the site of ICP measurement and pressure at different points of cerebrospinal axis (Raabe *et al.*, 1999). Cerebrospinal compliance is inversely proportional to ICP, therefore comparison between different subjects can be made only at the same level of the difference: ICP- p_0. The elastance coefficient E1 is independent of ICP, thus this coefficient is a much more convenient parameter when comparing individual patients. A low value of E1 is specific for a compliant system, whilst a high value indicates decreased pressure-volume compensatory reserve.

Time-constant Tau is calculated as a product of brain compliance (C) and R_{csf}. It describes the time needed by the volume of CSF compartment during the test to reach new stable value.

Figure 3.3: CSF infusion study. The upper graph contains shows a time-trend of pulse amplitude of ICP and the lower graphs show the mean values of ICP. X-axis: time in minutes counted from the beginning of the recording. A constant rate infusion (1.5 ml/min) was started 8 minutes after the start of the recording and finished 15 minutes later. AMPbeg, ICPbeg, AMPend and ICPend demonstrate baseline and end-equilibrium values of the recorded parameters.

3.2.4 Statistical Comparisons

A comparison of parameters measured by CSF infusion study and clinical features of patients on presentation was made using the Mann Whitney U test. The clinical parameters for comparison included the gait score, urinary incontinence score, NPH scale and modified Stein and Langfitt scores. Correlation between these parameters was performed using the Spearman Rank Order Correlation test. This series of comparisons was utilized for each group of patients analyzed, that is, the group as a

whole, idiopathic and secondary NPH, 'typical' and atypical idiopathic NPH, and hypertensive and non-hypertensive 'typical' idiopathic NPH groups.

3.2.5 Ethical Considerations

The data in this paper was collected for purely clinical purposes so ethical approval was not sought. All data had been anonymised to protect patient confidentiality.

3.3 Results

3.3.1 All Normal Pressure Hydrocephalus Patients

Pre-Treatment

The mean R_{csf} for the 133 patients was 15.3 ± 6.0 mmHg/ml/min with an opening pressure of 9.6 ± 5.0 mmHg. The distribution of the R_{csf} among the patients studied is shown in Figure 3.4. It demonstrates a large number of patients in the 10-15 mmHg/ml/min range. In comparing the clinical and CSF compensatory parameters of all NPH patients, R_{csf} was significantly correlated with all scores (Figure 3.5 a-d). However, although the correlation was significant ($p<0.05$), it was weak ($R = 0.174$-0.247).

Post-Treatment

Of the 46 patients who were shunted, 65% demonstrated improvement in the NPH score, 50% in modified Stein-Langfitt score and 64% in gait score. Of the 29 shunted patients with pre-operative urinary incontinence, 58% experienced improvement. The mean R_{csf} of the shunted patients overall was 17.4 ± 6.0 mmHg/ml/min with only 7

patients with an R_{csf} < 13 mmHg/ml/min reflecting the use of R_{csf} to decide whether to shunt. Hence, it is not surprising that there was no significant difference between shunt responders and non-responders in terms of their CSF infusion study results. Likewise, there was no correlation between clinical improvement *per se*, or the degree of clinical improvement, compared to the CSF infusion study results.

Several patients experienced complications related to CSF diversion with a shunt. Eight shunt revisions were performed in 7 patients for a combination of blockage and infection. Three patients developed small chronic subdural haematomas and one developed an acute subdural haematoma requiring treatment. One patient developed a left hemiparesis in the perioperative period. There was one peri-operative death due to an acute myocardial infarction on day four post-operatively. Despite these complications only 5 of the 46 patients were noted to be worse after treatment with the majority of shunt non-responders remaining unchanged.

Histogram of R_{csf} of NPH patients

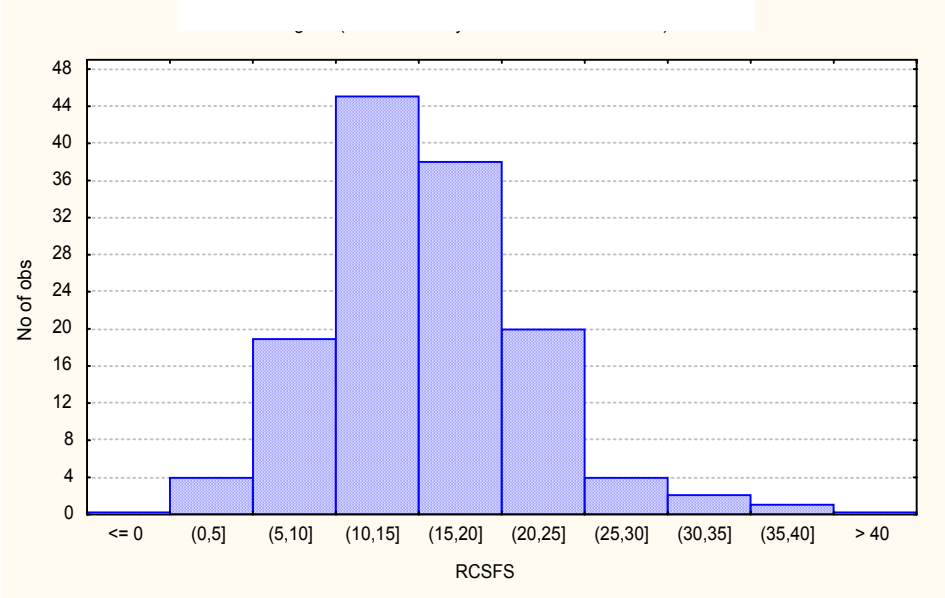

Figure 3.4: Histogram of Rcsf of all patients

Scatter Diagrams of
Clinical Parameters v. CSF Infusion Data
All NPH Patients

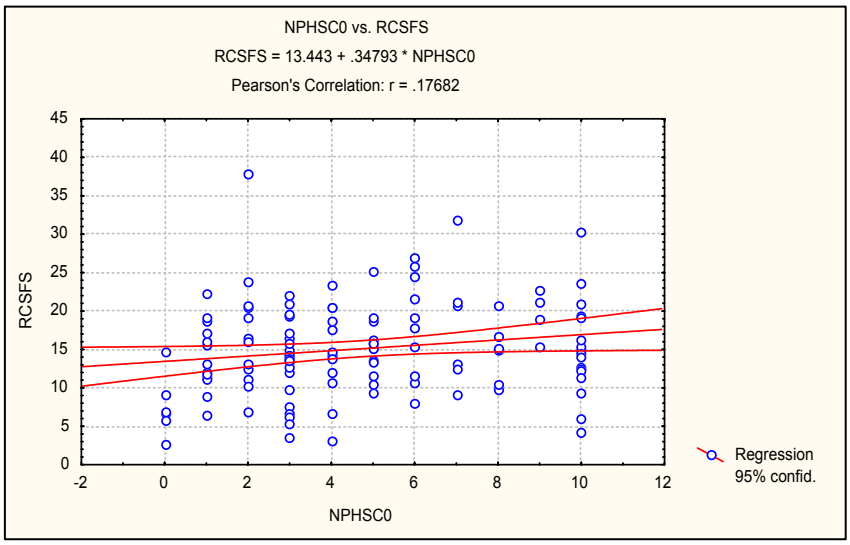

Figure 3.5a: NPH v. Rcsf: (R =0.193; p<0.05)

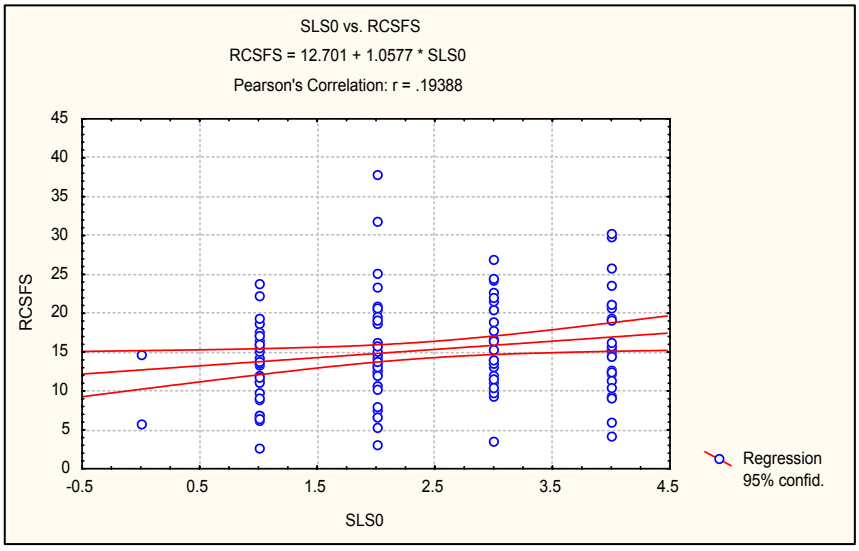

Figure3.5b: Modified Stein Langfitt Score v. Rcsf (R=0.187, p<0.05)

Scatter Diagrams of
Clinical Parameters v. CSF Infusion Data
All NPH Patients

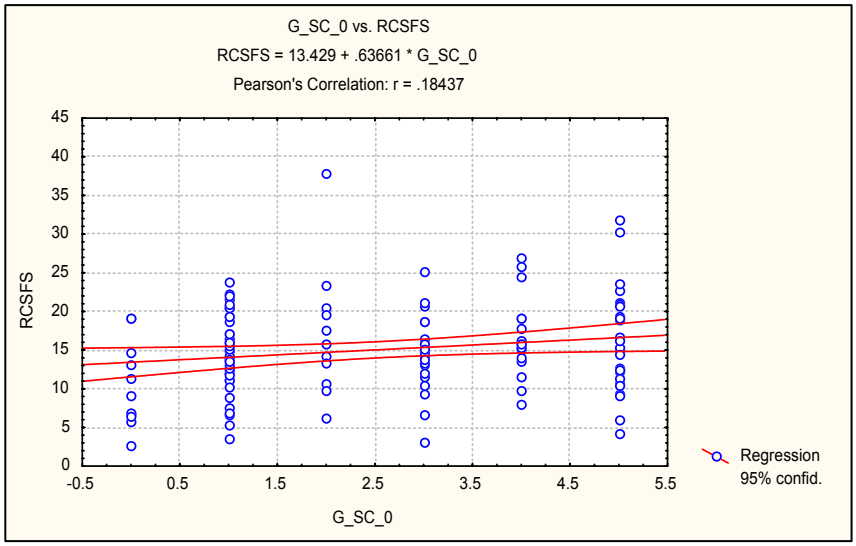

Figure 3.5c Gait Score v. Rcsf (R=0.174, p=0.05)

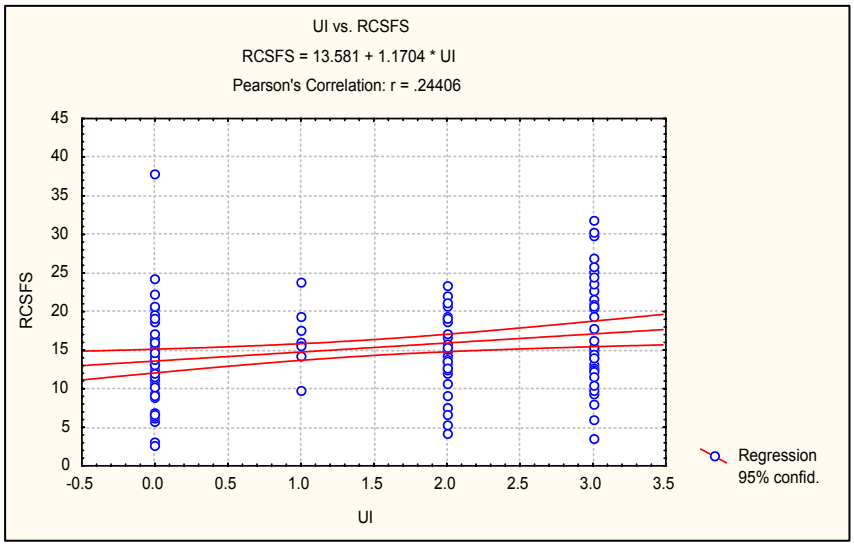

Figure 3.5d: Urinary Incontinence Score v. Rcsf (R=0.247, p<0.005)

3.3.2 Comparison of Idiopathic to Secondary NPH Patients

Pre-treatment

There were significant differences in measured CSF parameters between patients with idiopathic (n=99) and secondary NPH (n=34). Although baseline CSF pressures were almost identical, $R_{csf,}$ and associated parameters such as ICP_{end} and AMP_{end}, were slightly higher in the patients with idiopathic NPH (Table 3.3). When the idiopathic or secondary NPH patients were analyzed as separate groups, the numbers became small and the correlation between R_{csf} and clinical parameters was lost with the exception of that with the urinary incontinence score in patients with secondary NPH ($p<0.05$; $R=0.218$).

Parameter	Idiopathic	Secondary	p
ICP_{beg} mmHg	9.8	9.0	0.623
ICP_{end}	31.4	27.6	0.026
AMP_{beg}	2.2	1.8	0.120
AMP_{end}	8.8	6.0	0.001
PVI	14.4	15.9	0.415
El	0.23	0.22	0.848
R_{csf} mmHg/ml/min	15.8	13.9	0.049

Table 3.3

Post-treatment

Of the 37 patients with idiopathic NPH who were shunted, 24 improved while of the 9 patients with secondary NPH, 5 demonstrated clinical improvement. There were no

significant differences between CSF infusion study parameters for either the idiopathic or secondary groups with one exception. In the idiopathic group, AMP_{beg} was significantly ($p<0.05$) higher in patients whose gait improved after receiving a shunt (2.77 mmHg) compared to those in whom it did not (1.89 mmHg). Furthermore, the AMP_{beg} was positively correlated with gait improvement after placement of a shunt ($p<0.05$; $R=0.367$). There were no other such correlations.

3.3.3 Comparison of 'Typical' and 'Atypical' Idiopathic NPH Patients

Pre-treatment

Patients with clinically 'typical' idiopathic NPH had a higher mean R_{csf} ($p<0.05$; 16.5 vs. 13.7 mmHg/ml/min) compared to atypical patients. Regarding correlations between NPH symptoms and CSF infusion study results for that group, the only correlations ($p<0.05$) were that between the NPH score ($R=0.269$), the modified Stein-Langfitt score ($R=0.315$) and the urinary incontinence score ($R=0.299$) with tau.

Post-treatment

Twenty of 30 patients with 'typical' idiopathic NPH responded to a CSF shunt. There was no significant correlation between R_{csf} and clinical outcome. However, parameters closely related to R_{csf} did demonstrate significant correlations. There was a correlation ($p<0.05$) between improvement in the modified Stein-Langfitt score and ICP_{end} ($R=0.425$) and AMP_{end} ($R=0.379$). The degree of clinical improvement in the NPH score was also positively correlated with the ICP_{end} ($p<0.05$; $R=0.396$).

Only 4 of the 26 patients with atypical NPH were shunted therefore it is not possible to make any statistical comparisons between the two groups and their relation to outcome but 2 of the 4 patients did demonstrate clinical improvement.

3.3.4 Comparison of Hypertensive and Non-Hypertensive 'Typical' Idiopathic NPH Patients

Pre-treatment

There was no statistical significance between the groups for either the CSF infusion study results or the degree of pre-operative disability. However, for patients with 'typical' idiopathic NPH without hypertension or a previous cerebrovascular event there was a significant correlation between the modified Stein-Langfitt score and R_{csf} ($p<0.05$; $R = 0.444$) as well as between the NPH score and R_{csf} ($p<0.05$; $R = 0.407$). The modified Stein-Langfitt score was also positively correlated with the ICP_{end} value ($p<0.05$; $R=-0.377$). No such correlations were observed for the patients with cerebrovascular disease.

Post-treatment

There was no significant difference in outcome between the vasculopathic 'typical' idiopathic NPH group (11 of 14 improved) compared to the non-vasculopathic group (8 of 17 improved). Neither group demonstrated a correlation between improvement and R_{csf}.

3.4 Discussion

The majority of patients reported in this study represent a group of patients referred to the CSF circulation disorder clinic for further assessment. These patients referred to

the centre were a very mixed group and symptoms were not always typical of NPH. The threshold for referring patients for CSF infusion study was relatively low. The preferred route of infusion was the Ommaya reservoir as the lumbar route may yield erroneously normal results. This may occur either due to a leak around the lumbar spinal needle or an occult CSF pathway obstruction. There was a wide range of R_{csf} with a mean of 15.3 ± 6.0 mmHg/ml/min. A large number fell into the range between 10 and 15 mmHg/ml/min; a range where characterization is difficult. In this study, 46 of the 133 patients had a value for R_{csf} of < 13 mmHg/ml/min.

In considering the correlation between the R_{csf} and the four clinical parameters, inspection of the scatter diagrams (Figure 3.5 a-d) demonstrates the difficulties in predicting whether patients will have a high R_{csf} or not, based on the severity of their clinical scores. For example, even with regard to gait disorder some patients with a low gait score had a very high R_{csf} while in a number of others the reverse was true. It is this result that demonstrates the value of the CSF infusion study and, in particular, the R_{csf} value in management. The loss of correlation between the clinical and CSF infusion study parameters when idiopathic and secondary NPH patients were analyzed separately probably reflects the weakness of the correlation and the high number of patients needed for statistical significance – a further demonstration of the difficulty of predicting CSF dynamics from clinical features alone.

There were distinct differences between the CSF infusion study results in patients with idiopathic compared to secondary NPH. R_{csf} and associated parameters, ICP_{end} and AMP_{end}, were all significantly higher in those with idiopathic NPH. To some extent, the results of CSF infusion in such patients reflect the underlying pathology of their

conditions. Patients with congenital aqueduct stenosis may have some degree of CSF dynamic compensation. In addition, patients with idiopathic NPH tend to be older compared to those with secondary NPH due to the epidemiological characteristics of their underlying aetiology. R_{csf} is known to increase with age (Albeck *et al.*, 1998; Czosnyka *et al.*, 2001).

As mentioned previously the idiopathic NPH cohort was very heterogeneous, with many patients presenting with atypical features such as prominence of cognitive over gait disturbances; hence the decision to categorise the patients as 'typical' or atypical NPH patients. The R_{csf} and ICP_{end} were both significantly higher in the 'typical' compared to atypical NPH group although there was no correlation between the R_{csf} and clinical parameters for either of the two groups. As only 4 of the 26 patients with atypical idiopathic NPH were shunted it was not possible to make a statistical comparison of the results of CSF shunting between the 'typical' and atypical groups. However, as the mean R_{csf} for atypical patients was only marginally above the level considered to be predictive of a successful response to CSF shunting, the results are consistent with other investigators who have emphasized the importance of gait disorder over cognitive disturbances in predicting a successful outcome.

The degree of clinical symptoms in patients with 'typical' idiopathic NPH did not correlate with the R_{csf} or other parameters with the exception of tau. Tau was significantly correlated with NPH, Stein-Langfitt and urinary incontinence scores. Tau reflects a combination of R_{csf} and compliance and thus indicates that, in patients with 'typical' NPH, the time taken during CSF infusion to reach equilibrium (ICP_{end}) in patients with 'typical' NPH is longer in patients with more severe symptoms. Given

that there was no correlation between R_{csf} or El with clinical parameters, a possible interpretation of this data is that patients with 'typical' idiopathic NPH include a heterogeneous group of patients with different combinations of increased R_{csf} and compliance – that is NPH reflects a combination of CSF circulation disturbance and a parenchymal pathology.

Although closely related to AMP_{end} and ICP_{end}, R_{csf} was not correlated with parameters of clinical improvement after CSF shunting. These results may reflect bias in the selection of patients for CSF shunting (R_{csf} >13 mmHg/ml/min). It may also reflect the association between tau and clinical parameters in these patients. Compliance is probably increased by factors such as vascular disease and degenerative cerebral processes (Earnest *et al.*, 1974). If the clinical expression of the illness is positively correlated with tau but not R_{csf}, it may be that symptoms in some patients, even with 'typical' NPH, are related to other processes apart from a CSF circulation disorder. These processes may allow ventricular dilation in the presence of a normal CSF pressure. If this is so, response to CSF diversion in such cases will depend both on processes that increase compliance and those that increase R_{csf}. For instance, a patient with clinically severe NPH may have a very raised R_{csf} and a slightly raised compliance whereas another may have high compliance and a moderately raised R_{csf}. If an increase in compliance is due to some degenerative process, the former patient is more likely to respond to CSF shunting, which lowers R_{csf}, than is the latter patient in whom the underlying problem is more closely related to the parenchyma than to CSF circulation (Figure 3.6).

Relationship between CSF circulation disorders, parenchymal disease and response to CSF shunting

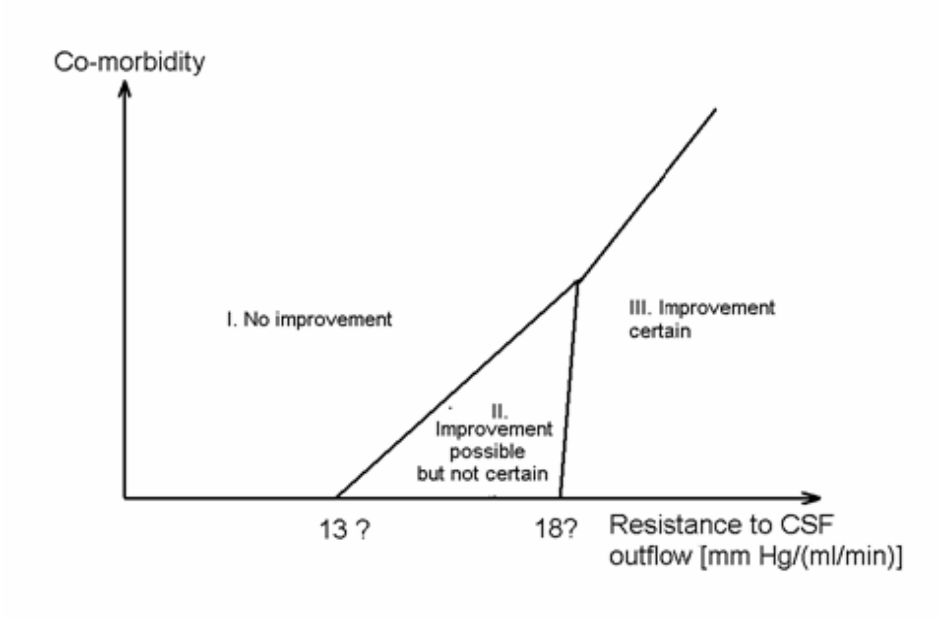

Figure 3.6: Schematic representing the combination of CSF circulation disorder and other co-morbid processes in patients with NPH. Improvement after CSF shunting will occur if processes affecting the parenchyma have not reached a certain point in development. In section I., if Rcsf is sufficiently low, a shunt will not improve CSF circulation. In areas II., and III., Rcsf is high and improvement is more likely after shunting but will depend on the extent of co-morbidity.

Factors that may be involved in increasing the compliance of the brain (thus decreasing the likelihood of a successful outcome after CSF shunting) are those of hypertension and cerebrovascular disease (Boon *et al.*, 1999). Both are known risk factors for the development of NPH (Casmiro *et al.*, 1989). Therefore, patients with 'typical' idiopathic NPH were divided on the basis of presence or absence of a history of hypertension or a cerebrovascular event. There was no difference either in the degree of clinical severity or in CSF infusion study parameters. However, the R_{csf} was correlated with both the NPH and modified Stein-Langfitt scores while there was no

such correlation in the group with hypertension or previous cerebrovascular event. This is consistent with the view outlined above, that is, patients with 'typical' idiopathic NPH, consist of patients whose condition is prominently a reflection of a circulation disorder and others in whom the condition is associated with another factor which affects the parenchyma.

In terms of differences in response to CSF shunting between these two groups, over half of both groups responded positively although there was no statistical difference. However, the number of patients under consideration was relatively small and will require further assessment

3.5 Conclusions

The experience from this institution demonstrates that there is an important role for CSF infusion studies in the management of patients with suspected NPH. It must be stressed that the role of this study was not to validate the use of R_{csf} in the management of patients with NPH as this has been addressed previously. Indeed, as noted, it is not possible to determine the CSF dynamics on the basis of clinical examination alone although patients with a typical presentation are more likely to have a raised R_{csf}. CSF infusion studies are not able to assure the clinician that a patient will respond to CSF shunting. They do however allow confirmation of raised R_{csf} in patients with typical symptoms as well as identification of those patients with raised R_{csf} who present with atypical features. In short, if R_{csf} is normal then a shunt is less likely to assist in the management of the patient.

Our results also demonstrate that in some patients with NPH, including those with a raised R_{csf}, it is likely that there may be a separate process affecting the parenchyma which plays a role in some patients. Improvement in the ability to determine and detect an associated process is likely to be key in developing additional parameters that can be applied at the bedside in order to increase the likelihood of a successful outcome.

.

Chapter Four

Normal Pressure Hydrocephalus and Cerebral Blood Flow:

A PET study of baseline values.

4.1 Introduction

The previous two chapters of this thesis have demonstrated that alterations in the properties of the brain parenchyma are associated with NPH. A key component of the parenchyma is the cerebral vasculature. By analogy with experimental hydrocephalus, it has been proposed that cerebral blood flow (CBF) in general and periventricular white matter CBF in particular may be reduced in NPH; changes which are reversed in patients who respond to CSF shunting. The cerebral vasculature has therefore been studied by several investigators and these studies, which include some 631 cases, have been reviewed (Appendix A) (Owler and Pickard, 2001). Although a variety of techniques have been utilized including ^{131}Xenon clearance, stable xenon CT, SPECT and PET, very little consensus exists, possibly because the technology had insufficient resolution and the patients were poorly characterised clinically. In order to overcome these limitations, global and regional CBF was measured in NPH patients using O^{15}-labelled water PET with anatomical region-of-interest (ROI) definition on co-registered MR.

4.2 Methods

4.2.1 Patients

Seventeen patients (age 69.6 ± 9.8 years; 8 males and 9 females) with NPH who were referred to the CSF Clinic at Addenbrooke's Hospital are reported. Twelve patients

presented with idiopathic NPH and 5 with NPH secondary to meningitis following a head injury, intracerebral haemorrhage, meningitis, surgery for removal of meningioma and basilar artery ectasia. In addition one of the idiopathic NPH patients also had Steel-Richardson syndrome.

The criteria for inclusion were gait disturbance, with or without cognitive changes or urinary incontinence, dilated ventricles on CT and normal CSF pressure measured via an Ommaya reservoir. All patients were assessed clinically using an NPH scale modified from Larsson *et al.*, (1991) a gait score and a modified Stein-Langfitt score calculated in the same manner as in chapter 3.

The degree of periventricular white matter hyperintensities were determined from T2-weighted MR images and a score from 0-4 points was assigned to each patient (0 – no white matter hyperintensities; 1 – minimal white matter intensities; 2- capping of frontal and/or occipital horns of the lateral ventricles; 3 – almost continuous white matter hyperintensities from frontal to occipital horns and 4 – continuous white matter hyperintensities from frontal to occipital horns).

Patients with a provisional diagnosis of NPH who were suitable for further treatment underwent insertion of a frontal Ommaya reservoir. After a post-operative period of at least two days, a computerised CSF infusion study (Czosnyka *et al.*, 1996) was performed in order to characterise the CSF dynamics including the resistance to CSF absorption (R_{csf}). Patients with an increased R_{csf} who were medically suitable underwent CSF ventriculoperitoneal CSF shunting incorporating either a Codman Medos programmable valve or Medtronic Strata valve. At the time of analysis, ten

patients had been shunted and followed up in the CSF clinic. A clinical score was assigned as per pre-operatively. Patients were considered to have responded to CSF shunting if the NPH score decreased by 2 or more points.

4.2.2 Controls

The control group consisted of 12 volunteers (mean age: 42.8 ±9.8 years) who underwent both MRI and PET scanning in the same manner as the patient group. All volunteers were healthy with no history of either cardiovascular or neurological abnormalities or disease.

4.2.3 PET and MRI Scanning

PET scanning was performed on a GE Advance scanner at the Wolfson Brain Imaging Centre. A radial arterial line and peripheral venous line were inserted. The patient's Ommaya reservoir was accessed in order to monitor CSF pressure throughout the procedure. The patient was positioned supine on the scanner table and encouraged to lie quietly in a darkened room. A 10 minute transmission scan was performed using two rotating $^{68}Ge/^{68}Ga$ rod sources (~600MBq in total) in order to correct for photon attenuation. An intravenous infusion of 800 MBq of O^{15}-labelled water was then delivered to the patient over 20 minutes; after a ten minute build-up period to achieve tracer steady state, PET data was acquired in 3D mode in two contiguous 5 minute frames. Arterial blood samples were taken at 10, 15 and 20 minutes into the infusion to monitor blood gases (including $PaCO_2$) and to determine the radioactivity concentration in blood during the PET acquisition, as required by the CBF kinetic model. The PET images were reconstructed using the 3D PROMIS filtered back-projection algorithm (Kinahan and Rodgers, 1989) implemented on the

scanner, with corrections applied for randoms, dead time, normalisation, attenuation and scatter.

In addition, a volumetric 3 Tesla SPGR MRI scan (voxel size: 1x1x1mm) of the brain was obtained on the same day as the PET scan in all of the control subjects and 14 of the 17 patients; three patients were unable to tolerate the MR scanner due to claustrophobia. The PET and MR images were co-registered using SPM-99 and CBF maps (voxel size 2.34 x 2.34 x 4.25 mm) were calculated using standard kinetic models (Frackowiak *et al.*, 1981) (PETAN2001, Dr. Piotr Smielewski, Cambridge). The spatial resolution of the CBF maps is approximately 6 mm.

4.2.4 Analysis

For those subjects who had undertaken an MR scan, global CBF was assessed by drawing regions-of-interest (ROIs) on the co-registered MR images. For the cerebrum and the cerebellum these regions were outlined with AnalyzeAVW using a combination of computer threshold drawing and manual correction. CSF spaces and large vessels were excluded from the ROIs. The process was repeated for each slice. For each ROI a mean CBF was calculated based on the entire ROI volume. In this way a true mean CBF for the ROI was obtained and the overall mean not artificially affected by the size of the ROI. For the three patients without an MR scan, global ROIs for the cerebrum and cerebellum were drawn using AnalyzeAVW directly on the CBF maps (Figure 4.1).

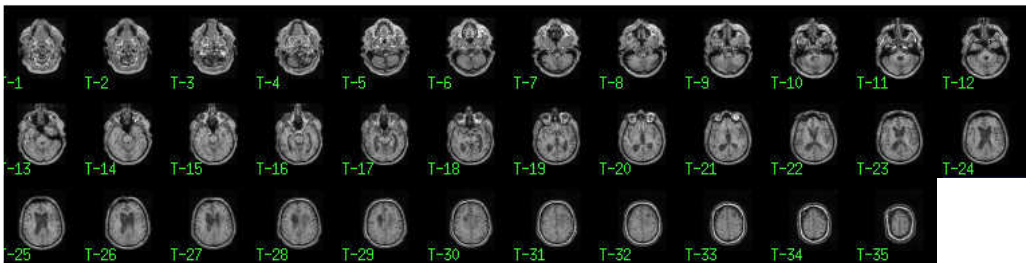

MRI

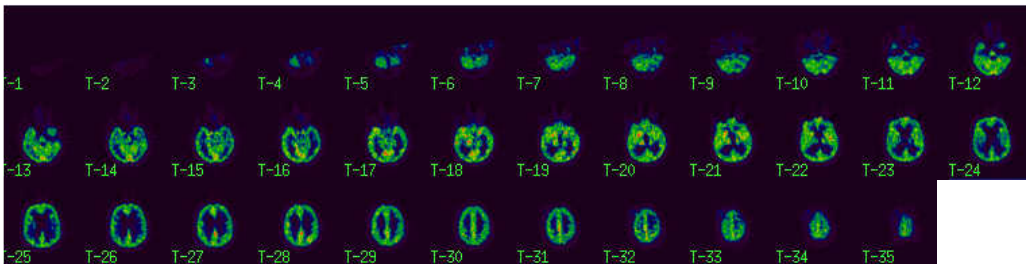

Co-registered PET CBF maps

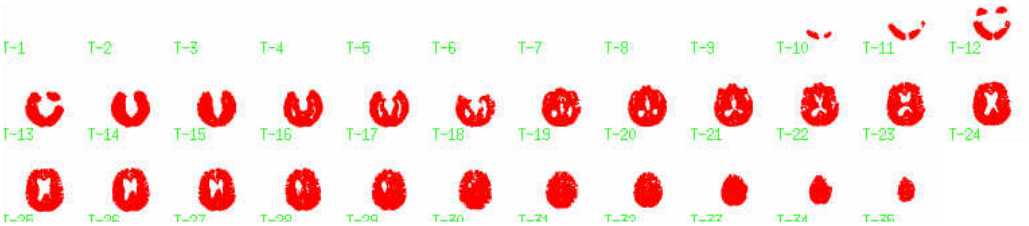

ROIs: Cerebrum

ROIs: Cerebellum

Figure 4.1: Co-registered MR images, PET CBF maps and global ROIs for the cerebrum and cerebellum of a patient with NPH.

The regional CBF results were obtained by manually placing small circular ROIs (each 15 voxels in size) bilaterally within anatomical regions on the slices of the MR scan where that structure was visible. This was performed for the frontal, occipital, temporal and parietal white matter regions, as well as the thalamus, head of caudate and the putamen (Figure 4.2). Care was taken to place ROIs away from anatomical

boundaries so as to minimize partial volume contamination of the ROI by other structures with different CBF. A regional CBF analysis could not be accurately performed in the three patients for whom there were no MR images. Therefore results for the regional CBF analysis are based on 11 patients with idiopathic NPH and three patients with secondary NPH.

The mean CBF values for global and anatomical regions were compared between patient groups and the control group using the Mann-Whitney U test. The pre-operative NPH, gait and modified Stein-Langfitt scores were compared to the mean for each region using Spearman rank order correlation.

All patients, relatives and control subjects involved in the study gave informed consent. The study was performed with the approval of the Cambridge Local Region Ethics Committee (LREC # 96/172, 96/209) and the UK Administration of Radioactive Substances Committee (ARSAC # 083-2050(14649), 083-2050(10170)).

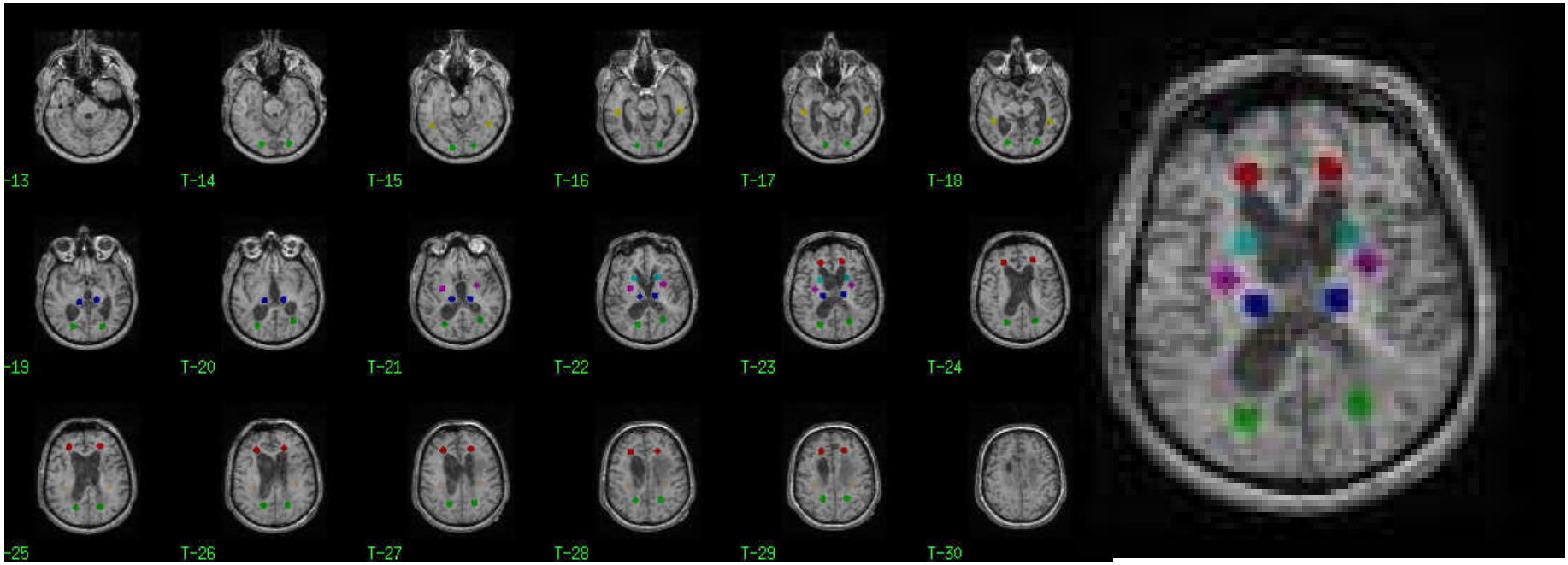

A B

Figure 4.2: A. Anatomical ROIs for the white matter and deep gray matter regions drawn directly onto co-registered MR images of a patient with NPH. **B.** Illustrative MR image with multiple regional ROIs.

4.3 Results

4.3.1 Global CBF Values

There was a significant ($p<0.0005$) difference between the mean CBF for the cerebrum of the NPH group (24.8 ± 4.3ml/100g/min) and that of controls (30.5 ± 5.2 ml/100g/min) (Table 4.1). When the idiopathic NPH subjects were analyzed separately to the secondary NPH group the difference remained with the mean CBF being significantly lower ($p<0.0001$) in the idiopathic NPH group (24.0 ± 2.9ml/100g/min) compared to the controls. The mean CBF for the cerebrum of the secondary NPH group (26.7 ± 6.7 ml/100g/min) was also lower than controls but the difference was not significant.

The mean CBF for the cerebellum was 35.4 ± 7.4 ml/100g/min for the NPH group compared to 40.6 ± 6.0 ml/100g/min in the control group. This difference was significant and remained so when the idiopathic group (35.1 ± 4.0 ml/100g/min; $p<0.05$) was analyzed separately.

Region of Interest	**Controls**	**NPH All** (n = 17)	**NPH Idiopathic** (n = 12)	**NPH Secondary** (n = 5)
Cerebrum	30.5 ± 5.2	24.8 ± 4.3, p<0.0005	24.0 ± 2.9 p<0.0001	26.7 ± 6.7, NS
Cerebellum	40.6 ± 6.0	35.4 ± 7.4, p<0.01	35.1 ± 4.0 p<0.05	35.5 ± 13.3, NS

Table 4.1: Analysis of mean CBF (ml/100g/min ± SD) in global regions of interest.

The mean arterial $PaCO_2$ values measured during PET data were compared between the control and patient groups. The mean $PaCO_2$ of the control group was 42.6 ± 4.3 mmHg compared to 40.0 ± 2.6 mmHg ($p<0.05$) for the NPH patients. The $PaCO_2$ of the idiopathic patients (39.2 ± 2.0 mmHg) was also significantly lower compared to the control group ($p<0.05$). However, all of these values were within the physiological range.

4.3.2 Regional CBF Values

In the white matter regions, that is, frontal, temporal, parietal and occipital regions, there was no difference between the whole patient group and controls. Furthermore, no significant difference became apparent when the idiopathic and secondary NPH groups were analyzed separately (Table 4.2)

White matter ROI	**Controls** (n = 12)	**NPH All** (n = 14)	**NPH Idiopathic** (n = 11)	**NPH Secondary** (n = 3)
Frontal	15.2 ± 2.1	16.1 ± 4.2 NS	17.2 ± 4.0 NS	12.0 ± 2.5
Parietal	15.7 ± 2.7	17.8 ± 4.7 NS	17.3 ± 3.4 NS	19.7 ± 8.9
Temporal	18.9 ± 2.7	20.4 ± 4.1 NS	20.2 ± 2.6 NS	21.1 ± 8.5
Occipital	18.1 ± 2.6	18.1 ±6.2 NS	16.7 ± 2.3 NS	23.4 ± 13.4

Table 4.2: Analysis of mean CBF (ml/100g/min±SD) in white matter anatomical regions (NS = not significant).

Unlike the regional analysis of CBF in the white matter, marked differences in mean CBF between controls and NPH patients were demonstrated in the deep gray matter. In the thalamus, the mean CBF of controls was 44.7 ± 5.7 ml/100g/min compared to 36.0 ± 7.5 ml/100g/min in the NPH patients ($p<0.005$). The difference remained

significant ($p<0.005$) when the idiopathic NPH patients (35.6 ± 6.5 ml/100g/min) were analyzed separately. For mean CBF in the head of the caudate nucleus, the mean control CBF was 38.5 ± 7.0 ml/100g/min which was significantly different to the NPH group as a whole (24.8 ± 6.5 ml/100g/min; $p<0.00005$) and the idiopathic NPH group (23.6 ± 5.6 ml/100g/min; $p<0.00005$). Mean CBF in the putamen of NPH patients (35.6 ± 8.3 ml/100g/min) was significantly ($p<0.05$) lower than for controls (42.6 ± 7.1 ml/100g/min). Again, when the idiopathic NPH group (34.9 ± 8.3 ml/100g/min) was analyzed separately, the difference remained significant ($p<0.05$)

Region of Interest	**Controls** (n = 12)	**NPH All** (n = 14)	**NPH Idiopathic** (n = 11)	**NPH Secondary** (n = 3)
Thalamus	44.7 ± 5.7	36.0 ± 7.5 p<0.005	35.6 ± 6.5 p<0.005	37.3 ± 12.2
Head of Caudate	38.5 ± 7.0	24.8 ± 6.5 p<0.00005	23.6 ± 5.6 p<0.00005	29.0 ± 8.9
Putamen	42.6 ± 7.1	35.6 ± 8.3 p<0.05	34.9 ± 7.7 p<0.05	38.0 ± 11.9

Table 4.3: Analysis of mean CBF (ml/100g/min±SD) in deep gray matter anatomical regions.

4.3.3 Relationship between Clinical Severity and CBF

Correlation analysis was used to assess any relationship between mean CBF for the various regions and clinical severity of NPH as assessed using the NPH, modified Stein-Langfitt and gait scores. As the clinical scoring of patients with secondary NPH reflected not only their NPH but also their primary pathology and its consequences patients with secondary NPH were excluded from the analysis. No significant correlation between the CBF of individual patients and their NPH, gait or modified Stein-Langfitt scores could be demonstrated when the all idiopathic NPH patients

were analysed. This was true of both the global and anatomical regions examined. However, the patient with co-existing Steel-Richardson syndrome had a relatively high mean CBF but clinically was in poor condition. When this patient was excluded from the analysis to obtain a group with purely idiopathic NPH the following correlations became apparent. There was an inverse correlation between mean thalamic CBF and NPH score ($R = -0.70$; $p<0.05$). In addition, the modified Stein-Langfitt score was inversely correlated with mean CBF in the putamen ($R = -0.72$; $p<0.05$).

There were no significant correlations between the severity of periventricular white matter hyperintensities and CBF for any ROI, including white matter CBF.

4.3.4 Response to CSF shunting

Of the 17 patients, 10 underwent CSF shunting. Of these patients, 7 improved as defined by a decrease in the NPH score of 2 or more points using the clinical assessment outlined above. The follow-up period for these patients ranged from 6-26 months (mean 11.6 ± 8.8 months). There was one shunt revision required for shunt malfunction. One patient had a stroke several months post-shunt insertion. There was no other associated morbidity or mortality. Both the shunt-responders and non-responders consisted of a mixture of patients with idiopathic and secondary NPH.

The relatively small number of patients did not allow for statistical comparison but it is noteworthy that the overall pattern of CBF described above was clearly seen in those patients who responded to CSF shunting and hence unequivocally had NPH. There was a tendency for the white matter CBF to be lower in non-responders. It was

not possible to define in this small number of patients whether resting CBF distinguished between responders and non-responders.

Parameter	Shunt Responders (n = 7)	Shunt Non-responders (n=3)
Age	69.6 ± 4.5 years	69.3 ± 4.7
ICP_{beg}	10.7± 4.2 mmHg	11.4 ± 4.6
R_{csf}	21.5 ± 7.5 mmHg/ml/min	16.6 ± 8.1
PVI	20.5 ± 10.3	27.1 ± 9.1
WM Hyperintensities	2.3 ± 1.7	3.0 ± 1.7

Table 4.4: Age and CSF compensatory parameters of patients with NPH and relationship to clinical outcome after CSF shunting.

Region of Interest	Shunt Responders (n = 7)	Shunt Non-responders (n=3)
Cerebrum	24.7 ± 1.7	24.0 ± 5.0
Cerebellum	35.2 ± 3.5	31.5 ± 6.0

Table 4.5: Mean CBF (ml/100g/min) of global regions of interest in patients with NPH prior to CSF shunting and relationship to clinical outcome after CSF shunting.

Region of Interest	Shunt Responders (n = 5)	Shunt Non-responders (n = 3)
Frontal White Matter	18.5 ± 1.5	11.3 ± 3.7
Parietal White Matter	19.0 ± 2.5	13.3 ± 2.3
Temporal White Matter	20.8 ± 2.5	16.1 ± 3.2
Occipital White Matter	17.8 ± 2.4	15.1 ± 1.7
Thalamus	36.2 ± 6.8	34.3 ± 9.0
Head of Caudate	25.3 ± 4.6	26.7 ± 7.6
Putamen	33.1 ± 6.8	33.9 ± 8.3

Table 4.6: Mean CBF (ml/100g/min) of anatomical regions of interest in patients with NPH prior to CSF shunting and relationship to clinical outcome after CSF shunting.

4.4 Discussion

The combination of PET scanning with anatomic ROI definition on coregistered MR for the study of CBF in patients with NPH has several advantages over other available technologies. The partition coefficient of ^{131}Xenon may be affected by pathology, and study of its clearance is non-tomographic and hence unable to study deep tissues accurately. Xenon CT is limited to measurement of CBF in only a few selected slices, and there are problems with quantification. SPECT CBF studies are limited by poor spatial resolution and difficulties in obtaining quantitative images. In addition, some SPECT tracers are metabolically active, and the results therefore reflect tissue metabolism as well as CBF. PET is a more accurate method of measuring CBF as the tracer (^{15}O-water) is not metabolized, the spatial resolution is superior, and image quantification is more easily achieved. In addition, CBF can be measured for the whole brain, not just in a few slices. Finally, coregistration with MR images allows measurement of CBF in specific anatomic locations.

Despite the advantages of PET, significant methodological problems needed to be overcome in this study. One major methodological issue is the definition of the regions of interest. One option is to spatially normalise (warp) the PET images to a template defined in a standard space, such as Taliarach space, and calculate mean CBF values using standard ROIs. Spatial normalisation programs, such as the one embedded in SPM99, are unable to successfully warp hydrocephalic brains, where the ventricles are enlarged by definition and other distortions such as sulcal dilation may be present, to a 'normal' template brain. In addition, an attempt at such a warping ignores the underlying pathological morphology of the hydrocephalic brain itself. Hence, ROIs were defined on the MR image of each subject, or directly on PET if MR was unavailable, using techniques aimed at making the ROIs as consistent as possible for all the subjects.

The methods of global and regional analysis used in this study are therefore aimed at overcoming these problems. For the global analysis the combination of seeding and threshold drawing functions on a slice-by-slice basis allowed reproducible ROIs to be drawn. Accuracy was checked and necessary corrections of the ROIs were then made to the ROIs of each slice to ensure anatomical integrity. Partial volume contamination, particularly bordering the ventricle is a potential source of error. However, the effects of such partial volume contamination of the CBF values are probably minimal due to the methods used, the relatively high resolution of the PET images and the number of voxels involved compared to the total number each slice. The regional analysis is less prone to such partial-volume error as ROIs were placed away from tissue boundaries.

The major disadvantage of these methods is that they are time consuming and to some degree operator dependent.

Significant reductions in mean CBF of both the whole cerebrum and the cerebellum were found in NPH patients compared to controls. Furthermore, regional analysis revealed that the deep gray matter regions of the thalamus, putamen and head of caudate had significantly lower mean CBF compared to controls. There was no significant difference in mean CBF of white matter ROIs. When the secondary NPH group were excluded from the comparison with controls, the difference in mean CBF for the cerebrum, cerebellum, thalamus, putamen and caudate nucleus remained significant, whilst the mean CBF for the white matter regions remained similar to the controls.

The age of the control group was significantly younger compared to the patient groups; specific controls were not recruited for this project as controls from the acute head injury program (Coles *et al.*, 2002) were used to minimise radiation exposure. The relationship between age and CBF is somewhat controversial although Meltzer *et al.* (2000) using PET with MR co-registration and partial volume correction found that there was no decrease in CBF with healthy ageing. In addition, the regional nature of the findings suggests that age is not the major factor influencing these results. The mean $PaCO_2$ of both NPH patients as a whole and the subset with idiopathic NPH were lower compared to controls. However, this is unlikely to have been responsible for the degree of CBF reduction in the patient groups as $PaCO_2$ was well within the normal range. In addition, mean CBF was not correlated with $PaCO_2$ in any ROI for the NPH patients.

In a previously published review of CBF studies in NPH patients, there was little consistency between investigators except that overall CBF was reduced (Owler and Pickard, 2001). Significant differences between NPH patients and controls were found in all but one study (Waldemar *et al.*, 1993), although a reduction in cerebellar CBF was not reported in any study. In fact, some investigators using SPECT utilised the cerebellum as a reference region as it was not thought to be involved in NPH. The findings suggest that such an assumption should not be made and that the process affecting the parenchyma of the cerebrum may also involve the cerebellum. With regards to regional analysis, there was no consensus on which regions of the brain were affected. Some authors suggested that the reduction in CBF may predominately involve the frontal region (Mathew *et al.*, 1977; Meyer *et al.*, 1985a; Graff-Radford *et al.*, 1987; Moretti *et al.*, 1988; Graff-Radford *et al.*, 1989; Granado *et al.*, 1991; Larsson *et al.*, 1994; Maeder and de Tribolet, 1995; Kristensen *et al.*, 1996; Nakano *et al.*, 1996). There was only one study in which CBF in the thalamus was found to be reduced (Meyer *et al.*, 1985b). The basal ganglia have not been previously examined as distinct structures. The studies that examine CBF in patients with NPH are summarised in Table 4.7.

Table 4.7: Studies of CBF in NPH: Methods and Baseline CBF findings

Reference	Class	Method	NPH	Aetiology	Baseline CBF	Control Group	Other Findings
Greitz *et al.*, 1969	B	^{133}Xe IC 2-comp	21	Mixed 4 Idiopathic	Reduced	Cerebral atrophy & Age-matched controls	In cases without a vascular component, correlation between ventricular dilation and ↓CBF
Greitz *et al.*, 1969	B		7	Mixed 1 Idiopathic	Reduced	Normal contols & Other various conditions	
Salmon & Timperman *et al.*, 1971a	C	^{133}Xe IC 2-comp	5	Trauma	Reduced	Normal controls	Unclear in diagnosis whether truly NPH but Gp2 have clinical triad. CBFg and CBFw both reduced in the 5 patients of Gp2
Salmon & Timperman *et al.*, 1971b	C	^{133}Xe IC 2-comp	7	Mixed 3 Idiopathic	Reduced	Other controls	-
Mathew *et al.*, 1975	B	^{133}Xe IC 2-comp + stochastic	15	Mixed 5 Idiopathic	Reduced	Cerebral atrophy & Age-matched controls	Not possible to distinguish between atrophy and NPH on basis of CBF. No correlation between CBF and ventricular size but dilation of frontal horn correlated with decrease in CBF of ACA territory. ↓CBF mostly in frontal lobe / anterior cerebral artery territory
Mathew *et al.*, 1977	B		4	Not reported	Reduced		
Hartmann *et al.*, 1977	C	^{133}Xe IC stochastic	11	Not reported		Acute SAH HC & High pressure HC	-
Grubb *et al.*, 1977	B	H_2O^{15} PET IC ISI/1-comp	11	10 Idiopathic	Reduced	Cerebral atrophy & Age-matched controls	Not possible to distinguish between atrophy and NPH on basis of CBF. No definite pattern of CBF could be identified in NPH patients.
Lying-Tunnell *et al.*, 1977 & 1981	B	AV-Difference NO_2	7	Mixed	Reduced	Age-matched controls & SDAT patients	CBF reduced especially in the most demented patients.
Tamaki *et al.*, 1984	C	^{133}Xe inhal ISI	24	Not reported	NA	Nil	No correlation between CBF and incidence of B-waves or between CBF and pattern seen on CT metrizamide cisternography.
Hayashi *et al.*, 1984	B	^{133}Xe IC ISI/2-comp	16	All SAH	Reduced	Normal controls & Other HC groups	↓CBF correlated with ↑ventricular size. ↓CBF less in acute stage of HC
Kushner *et al.*, 1984	A	^{133}Xe IC 2-comp/ISI	19	Mixed 11 Idiopathic	Reduced	Other dementias & Age-matched controls	No difference in CBF between NPH and non-NPH dementia patients.
Meyer *et al.*, 1984	B	^{133}Xe inhal 2-comp	11	Mixed 6 Idiopathic	Reduced	Cases of SDAT & Age-matched controls	-
Meyer *et al.*, 1985a	B	^{133}Xe inhal 2-comp & Xe contrast CT	8	Not reported ?Idiopathic	Reduced	Cases of SDAT & Age-matched controls	CBF and partition-coefficients decreased CBF most reduced in frontal, parietal and temporal cortex, thalamus and fronto-temporal white matter. Partition co-efficients most reduced in frontal white matter
Meyer *et al.*, 1985b	B	Xe contrast CT	10	Mixed 6 Idiopathic	Reduced	Nil	
Brooks *et al.*, 1986	B	$C^{15}O_2$ PET inhal	3	Idiopathic	Reduced	Normal controls & other types of HC	-
Mamo *et al.*, 1987	B	^{133}Xe IV 2-comp	25	Mixed 18 Idiopathic	Reduced	Cases of SDAT or presenile dementia	↓CBF compared to controls No correlation between ventricular size and CBF reduction

Vorstrup *et al.*, 1987	A	^{133}Xe inhal 1-comp SPECT	17	Mixed 14 Idiopathic	Reduced	Atherosclerotic & Age-matched controls	NPH patients had abnormal CBF maps. In 14/17 cases there was correlation between ↓CBF and ↑ventricular size. No correlation between symptoms and CBF.
Graff-Radford *et al.*, 87 & 89	C	^{133}Xe inhal 2-comp SPECT	26 +35	Mostly Idiopathic	Reduced	Cases of SDAT & Age-matched controls	No difference between CBF in SDAT and NPH patients. ↓CBF more severe in frontal region in NPH patients
Morretti *et al.*, 88	A	^{123B}AMP IV SPECT	23	Mixed 15 Idiopathic	NA	Nil	Frontal hypoactivity seen in 19/23 NPH cases No correlation between CBF and ventricular size.
Meixenberger *et al.*, 89	C	^{133}Xe inhal 2-comp	31	Not reported	Reduced	Normal controls	No sig difference in CBF between NPH pts with & without ICP abnormalities NPH patients with neuro deficits had lower CBF NPH patients with neuro deficits and ICP abnormalities had lowest CBF
Matsada *et al.*, 90	A	^{133}Xe inhal ISI	13	Mixed 1 Idiopathic	Reduced	Normal controls	↓CBF correlated with ↑ventricular size. No inter-regional differences compared to controls.
Granado *et al.*, 91	B	^{99m} Tc-HMPAO SPECT	14	Idiopathic	NA	Nil	↓CBF in frontal region correlated with severity of dementia
Kimura *et al.*, 92	B	Xe contrast CT	7	All SAH	Reduced	Age-matched controls	Generally ↓CBF in NPH
Waldemar *et al.*, 92	A	^{99m} Tc-HMPAO SPECT & ^{133}Xe inhal 2-comp SPECT	14	Mixed 9/14 Idiopathic	Not reduced	Age-matched controls	No difference in global CBF using Xe CT or ^{99m} Tc-HMPAO SPECT. Slightly lower CBF in central white matter in NPH patients. Enlargement of area of low subcortical CBF in 19/14 NPH patients. NPH patients had lower frontal/parietal ratio CBF. No difference in frontal/temporal CBF ratio.
Shimoda *et al.*, 94	B	Xe contrast CT	22	Mostly SAH No Idiopathic	NA	Nil	No comments on pre-operative CBF pattern.
Maeder *et al.*, 95	C	Xe contrast CT	4	Mixed 2/4 Idiopathic	Reduced	Age-matched controls	↓CBF frontal cortex and white matter
Shih *et al.*, 95	C	^{99m} Tc-HMPAO SPECT	1	Idiopathic	Reduced	Nil	Perfusion deficits noted in posterior temporoparietal and occipital cortices.
Kristensen *et al.*, 96	B	^{99m} Tc-HMPAO SPECT	31	Idiopathic	Reduced	Age-matched controls	↓CBF in Inferior frontal and temporal cortex. ↓CBF in Frontal and parietal white matter .
Nakano *et al.*, 96	B	Xe contrast CT	14	Mixed	NA	Nil	↓CBF in region of frontal periventricular lucencies. Other regions not examined
Tanaka *et al.*, 97	A	Xe contrast CT	21	Mixed 6 Idiopathic	Reduced	Age-matched controls	-
Klinge *et al.*, 98	B	H_2O^{15} bolus PET	21	Not reported	Reduced	Normal controls	Generally ↓CBF
Klinge *et al.*, 99	B	H_2O^{15} bolus PET	10	Idiopathic	Reduced	Normal controls	Generally ↓CBF
Matsuda *et al.*, 99	B	Xe contrast CT	16	Not reported	NA	Nil	Combined with NAA/Cr MR Spectroscopy.

Abbreviations: CBF: Cerebral blood flow, 1-comp/2-comp: single or bi-compartmental curve analysis, HC: hydrocephalus, IC: intra-carotid, inhal: inhalation, ISI: Initial slope index curve analysis, IV: intravenous, NA: not applicable, NPH: Normal pressure hydrocephalus, pt: patient, SDAT: Senile dementia of the Alzheimer's type, sig: statistical significance

Note to Table 4.7 and 4.8: Several difficulties arise in attempting to apply a strict a definition of levels of evidence to these studies (Ball *et al.*, 1999). When considering the utility of CBF measurements as a diagnostic or prognostic tool, there are no reference or gold standard tests by which patients can be assessed. In addition, the patient groups were almost always mixed, that is, consisted of heterogeneous groups of patients with idiopathic and secondary NPH analysed together. There were often mixed radiological and CSF study results. Few studies could be regarded as providing level II evidence. Rather, most of the literature mostly consists of level III, IV and V evidence. The lack of studies with high levels of evidence is not a direct criticism of the studies themselves but is a reflection of the nature of the subject. In order to circumvent some of these problems, and assist the comparison of studies an alternate method of classification was formulated. Class A evidence consisted of case-control studies in which the full details of the patient and control groups were available. Patients included in these studies needed to satisfy the following definition: all patients had to demonstrate: 1) the complete clinical triad or primarily a disorder of gait; 2) ventricular dilatation on CT scan without significant cerebral atrophy; 3) absence of focal neurological deficit or focal pathology on CT; 4) normal CSF pressure (<15 mmHg) with either ICP monitoring or CSF infusion study data; and 5) objective, well documented follow-up. Class B evidence included case-control studies in which patient details did not necessarily satisfy the strict criteria above but the authors had diagnosed the syndrome of NPH. Class C studies included case-series and case reports of patients diagnosed with NPH whether or not the definition of NPH was satisfied. Tables replicated from Owler & Pickard (2001) (see appendix one).

As discussed in chapter 1, NPH is primarily a CSF circulation disorder (Czosnyka *et al.*, 1996; Boon *et al.*, 1998b, 2000). However, it is likely that a disorder of CSF circulation *per se* is probably not the only pathological process rather some process affecting the viscoelastic properties of the brain parenchyma itself may play a role (Pang and Altschuler, 1994; Owler *et al.*, 2001). Such a process may be related to the cerebral vasculature (Bradley *et al.*, 1991). An association between hypertension and idiopathic NPH has been described by several authors (Haidri and Modi, 1977; Koto *et al.*, 1977; Shukla *et al.*, 1980; Casmiro *et al.*, 1989; Krauss *et al.*, 1996). Histopathological findings of intimal thickening and hyalinisation of arterial walls in the white matter, basal ganglia and thalamus (Akai *et al.*, 1987) have been discussed. The vessels most at risk of such changes are the lenticulostriate vessels as these are end arteries with a prolonged course through the brain parenchyma. As the lenticulostriate vessels and similar vessels are the main arterial supply to the regions of the thalamus, caudate and putamen, the reduction of CBF seen in patients with idiopathic NPH compared to controls supports the role for cerebrovascular disease in the pathophysiology of idiopathic NPH. Although white matter hyperintensities were common in NPH patients, there was no significant correlation between the degree of white matter hyperintensities and mean CBF for any ROI. Of course, this does not exclude the possibility that such white matter changes are small infarcts but simply that the CBF of the remaining white matter is not reduced.

The most important clinical feature of NPH is that of gait disturbance (Shenkin *et al.*, 1973; Greenberg *et al.*, 1977; Fisher, 1982; Casmiro *et al.*, 1989; Boon *et al.*, 2000) although its mechanism is not fully understood. The gait has characteristics such as poor balance, hypokinesia and freezing which are consistent with a frontal gait

apraxia (Fisher, 1982). Stolze *et al.* (2000 & 2001a) noted the lack of balance regulation and motor programming in the gait of patients with NPH. They suggest that the lack of response to external cues in patients with NPH indicates that the role of the basal ganglia and supplementary motor cortex is limited. However some of the features of the gait disorder may also be related to pathology within the basal ganglia. The findings of this study suggest that mean CBF in the white matter, including that of the frontal region, of patients with idiopathic NPH is no different to controls. However, the mean CBF for the thalamus, putamen and head of caudate were all significantly reduced. It was demonstrated that a lower CBF in patients with purely idiopathic NPH correlated with an increased NPH score. In addition, CBF in the putamen of these patients was correlated with a poorer level of functioning as assessed using the modified Stein-Langfitt score. Thus it appears likely that the role of the basal ganglia in the gait disorder of NPH may be underestimated at the present time.

Whether the reduction in CBF in the basal ganglia and thalamus is a primary phenomenon or whether it occurs secondary to de-afferentation in other areas remains to be elucidated. In Huntington's disease, CBF in the caudate nucleus, an area of primary pathology, is reduced. The reduction in CBF in the caudate nucleus correlates with disease progression (Hasselbalch *et al.*, 1992; Deckel *et al.*, 2000; Reynolds *et al.*, 2002). In Parkinson's disease CBF is decreased throughout the basal ganglia (Wolfson *et al.*, 1985) and changes in CBF, presumably secondarily to the primary pathology, are seen in distant regions such as the supplementary motor cortex (Kikuchi *et al.*, 2001).

Moreover, the reduction in CBF in the basal ganglia and thalamus may also contribute to the cognitive deficits of NPH. The striatum receives widespread cortical input and, via other basal ganglia and the thalamus, projects to frontal cortex. Interruption of frontostriatal pathways is a possible explanation for the cognitive deficits of Parkinson's disease (Owen *et al.*, 1998) and may explain the frontal lobe cognitive deficits seen in NPH.

The relationship between mean CBF and outcome after CSF shunting is not clear. Previous studies (Table 4.8) that have examined this issue have not examined CBF in anatomical ROIs. Klinge *et al.* (1998 & 1999) reported that a lower global CBF indicated a favourable outcome after CSF shunting. In contrast, several other authors have found that a lower CBF indicates that improvement after CSF shunting is less likely (Mathew *et al.*, 1975; Mathew *et al.*, 1977; Hayashi *et al.*, 1984). A relatively low frontal CBF (Graff-Radford *et al.*, 1987; Moretti *et al.*, 1988; Larsson *et al.*, 1994) or a large subcortical low flow region (Waldemar *et al.*, 1993) have also been suggested as indicators of a successful shunt procedure. In this study non-responders appeared to have a lower mean CBF in the white matter regions, especially in the frontal region. There appeared to be no difference in mean CBF in the gray matter global ROIs. Although interesting, the results in terms of outcome must be treated as a preliminary observation until a larger number of patients are studied.

4.5 Conclusion

In summary, using ^{15}O-water PET combined with anatomical ROI definition on co-registered MR, it was demonstrated that mean CBF was decreased in the cerebrum and cerebellum of patients with idiopathic NPH compared to normal healthy controls.

Most importantly, the regions most likely to be related to this decrease in CBF were the deep gray regions of the thalamus, putamen and caudate nucleus. In comparison, white matter (including periventricular) mean CBF was not reduced in NPH compared to normal controls. This study supports the concept that, apart from being a disorder of CSF circulation, there are cerebrovascular factors involved in the pathophysiology of NPH and that these factors may be related to the gait disorder of NPH.

Table 4.8: Studies of CBF in NPH: Results of CSF shunting

Reference	Class	Response	Predictive Value of Baseline CBF	FU	Change in CBF
Greitz *et al.*, 1969	B	6/7	-	3w-2mo	↑CBF most marked in those with greatest clinical improvement; ↑CBF variable but relate to outcome. In 6/7 patients ↑CBF correlated to decrease in ventricular size.
Salmon & Timperman *et al.*, 1971a	C	4/5	-	3-8mo	-
Salmon & Timperman *et al.*, 1971b	C	6/7	-	2-4mo	↑CBFg 62%, the change in CBFw was more variable. States that decease in ICP is responsible for increase in CBF.
Mathew *et al.*, 1975	B	11/17	Higher CBF related to better clinical outcome.	2w-6mo	-
Mathew *et al.*, 1977	B	3/4	Higher CBF related to better clinical outcome.	-	-
Grubb *et al.*, 1977	B	2/5	No pattern	-	-
Lying-Tunnell *et al.*, 1977 & 1981	B	4/7	No pattern	5w & 5mo	↑CBF but only temporary in some.
Hayashi *et al.*, 1984	B	11/16	Shunt only effective if CBF <25ml/100g/min	>3mo	
Kushner *et al.*, 1984	A	12/19	No pattern to identify shunt-responders	10d-12w	↑CBF post-op not correlated with degree of clinical improvement
Meyer *et al.*, 1984	B	7/10	No pattern to identify shunt-responders	-	Post-operative CBF reported in 3 patients and ↑CBF was reported in each. However only 2/3 patients clinically improved. Therefore no conclusions drawn.
Meyer *et al.*, 1985a	B	7/7	NA	6w & 6mo	↑CBF in frontal and temporal cortex and basal ganglia; but mostly ↑ in frontal white matter. Partition co-efficients: No change in cortex but significantly ↑ in white matter especially in frontal lobe.
Meyer *et al.*, 1985b	B	6/8	No pattern	Up to 8mo	Similar findings to previous study. ↑CBF correlated with improvement in ADLs, gait, incontinence and MMSE. No correlation between ↑CBF and ↓ventricular size.
Brooks *et al.*, 1986	B	0/3	NA	6w & 6mo	No ↑CBF post-shunt in NPH patients.
Mamo *et al.*, 1987	B	22/25	No pattern re: frontal or global CBF	1w-4mo	No correlation between ↑CBF and clinical improvement. Those with excellent outcome had more sustained ↑CBF compared to patients with good/fair outcome.
Vorstrup *et al.*, 1987	A	8/17	No pattern	4mo	No significant change in CBF in either responders or non-responders. Positive correlation between ↑CBF and ↓Evan's ratio.
Graff-Radford *et al.*, 1987	C	23/30	Pre-op CBF significant predictor of outcome, especially Anterior/Posterior ratio	6mo	No correlation between post-shunt CBF and clinical improvement.
Morretti *et al.*, 1988	A	8/12	Degree of frontal hypoactivity not predictive of outcome	-	-

Graff-Radford *et al.*, 1989	C	16/26	Only Anterior/Posterior ratio CBF a significant predictor of outcome.	6mo-12mo	-
Meixensberger *et al.*, 1989	C	-	No predictive value	-	No significant change in post-operative CBF. Some patients did have increase in frontal CBF.
Matsada *et al.*, 1990	A	13/13	NA	4-25d	No significant change in CBF.
Granado *et al.*, 91	B	10/14	Non-DAT pattern CBF predictor of improvement and DAT pattern predicts non-improvement (see text)	<7d	No significant change in CBF.
Kimura *et al.*, 92	B	7/7	NA	-	Restoration of CBF greatest in frontal, temporoparietal white matter and also improved in cortex and thalamus. Clinical improvement closely correlated with restoration of CBF in white matter.
Waldemar *et al.*, 92	A	11/13	Enlargement of subcortical low flow region related to good outcome.	3mo-6mo	Post-operative clinical improvement did not parallel CBF changes. Some patients had (9/10) had reduction in subcortical low flow region. Also normalised some cortical defects.
Shimoda *et al.*, 94	B	14/22	No pattern	2-3w	In responders there were significant ↑CBF in all ROIs, except in basal ganglia. In non-responders, there were no ↑CBF in any ROI.
Maeder *et al.*, 95	C	2/2	NA	<1mo	↑CBF in frontal cortex and white matter.
Shih *et al.*, 95	C	1/1	NA	5.5mo	Improvement in cerebrum/cerebellar ratio from 1.3 to 1.6. Improvement in posterior temporoparietal and occipital cortex perfusion defects.
Nakano *et al.*, 96	B	10/14	-	4-6w	Only concerned with CBF frontal peri-ventricular lucencies.
Tanaka *et al.*, 97	A	9/21	Patients only responded if CBF >20ml/100g/min	2-3w	In responders, CBF increased by 65% in white matter and 25% in cortex. In non-responders, CBF marginally decreased. No patients with idiopathic NPH responded.
Klinge *et al.*, 98	B	12/21	Responders had lower pre-op CBF compared to non-responders.	1w-7mo	No significant change in post-operative CBF.
Klinge *et al.*, 99	B	5/10	Responders had lower pre-op CBF compared to non-responders.	1w-7mo	No significant change in post-operative CBF.
Matsuda *et al.*, 99	B	11/16	No pattern	3-4w	In responders mean CBF increased while there was no increase non-responders.

Abbreviations: CBF: Cerebral blood flow, mo: month, NA: not applicable, NPH: Normal pressure hydrocephalus, pt: patient, ROI: region of interest, SDAT: Senile dementia of the Alzheimer's type, sig: statistical significance, w: week

Chapter Five

Normal Pressure Hydrocephalus and Cerebral Blood Flow: Changes during CSF pressure manipulation

5.1 Introduction

In the previous chapters, it has been demonstrated that the brain parenchyma is an important component in the pathophysiology of NPH. Within the brain parenchyma, the cerebral vasculature may also play a role. Global and regional CBF in NPH patients was measured and found to be reduced compared to controls, especially in the deep gray matter nuclei. However, these baseline CBF measurements provide information about the cerebral vasculature at rest. It does not describe the dynamic qualities of the circulation and how it might respond to various challenges. In health, CBF is protected against moderate fluctuations in arterial blood pressure and CSF pressure by cerebrovascular autoregulation.

The aim of this study was to define the effect of CSF pressure on regional CBF (rCBF) in patients with possible NPH particularly in light of the findings in the previous chapter that periventricular white matter CBF was not greatly reduced in patients with NPH at rest. However global CBF was reduced with regional reductions in the thalamus and basal ganglia. These findings were not predicted by experimental studies of hydrocephalus. The logistical problems of studying patients during CSF infusion studies, performed as part of their clinical work-up, within the PET scanner followed by MR co-registration, have been resolved. The topography of the changes in CBF with CSF pressure rises during the infusion study were defined.

5.2 Methods

5.2.1 Patients

This study reports 15 patients (age 69.5 ± 5.2 years; 7 males and 8 females) with NPH who were referred to the CSF Clinic at Addenbrooke's Hospital. Twelve patients presented with idiopathic NPH and 3 with NPH secondary to either meningitis (2 cases, one of which followed a head injury) or an intracerebral haemorrhage. In addition, one of the idiopathic NPH patients also had progressive supranuclear palsy. This patient initially improved after CSF shunting but then deteriorated.

Full details of the clinical features and assessment including the definition of the NPH scale (Larsson *et al.*, 1991) have been described in chapter 3. Patients suspected of having NPH and who were suitable for further treatment underwent insertion of a frontal Ommaya reservoir. After a post-operative period of at least 2 days, a computerized CSF infusion study (Czosnyka *et al.*, 1996) was performed in order to characterize the CSF dynamics including R_{csf}. The infusion study was performed in the PET scanner during acquisition of CBF PET data as described below. Patients with an increased R_{csf}, and who were medically suitable, underwent CSF ventriculoperitoneal CSF shunting incorporating either a Codman Medos programmable valve or Medtronic Strata valve. Nine patients were shunted and were followed up in the CSF clinic and a score assigned as per pre-operatively. Patients were considered to have responded to CSF shunting if the NPH score decreased by 2 or more points.

5.2.2 PET and MRI Scanning

The patient was positioned supine on the PET scanner table and encouraged to lie quietly. The patient's Ommaya reservoir was accessed using two 25G-butterfly needles. The first needle was connected to a fluid pressure transducer and CSF pressure monitor. The second needle was connected to a CSF infusion pump containing 60mls of normal saline. The CSF pressure was monitored continuously until after all PET scanning had ceased. Mean arterial blood pressure (MAP) was also recorded continuously in 10 patients thus allowing continuous monitoring of the CPP. PET scanning was performed using the same system as outlined in the previous chapter.

A single 10 minute transmission scan was acquired. Two PET scans to measure CBF were then performed using the following protocol. The first PET scan was performed in order to measure the baseline CBF during which time the patients resting ICP and MAP were recorded. At the end of this scan the computerized CSF infusion study was commenced. A constant rate (0.5-1.0 ml/min) of normal saline was infused into the Ommaya reservoir during which time the ICP and MAP continued to be monitored. The ICP was thus elevated until a new higher equilibrium ICP was established. The time to equilibrium was generally 5-15 minutes. Once the equilibrium had been established for 5 minutes a second PET scan, using the same method as the first, was performed in order to measure the CBF at the higher ICP. At the end of the PET scanning the ICP was allowed to return the baseline ICP. Arterial CO_2 tension (PCO_2) was measured during baseline and equilibrium PET scans. The details of the transmission scan and ^{15}O-water PET data acquisition are described in Chapter 4. The experimental setup is illustrated in Figure 5.1.

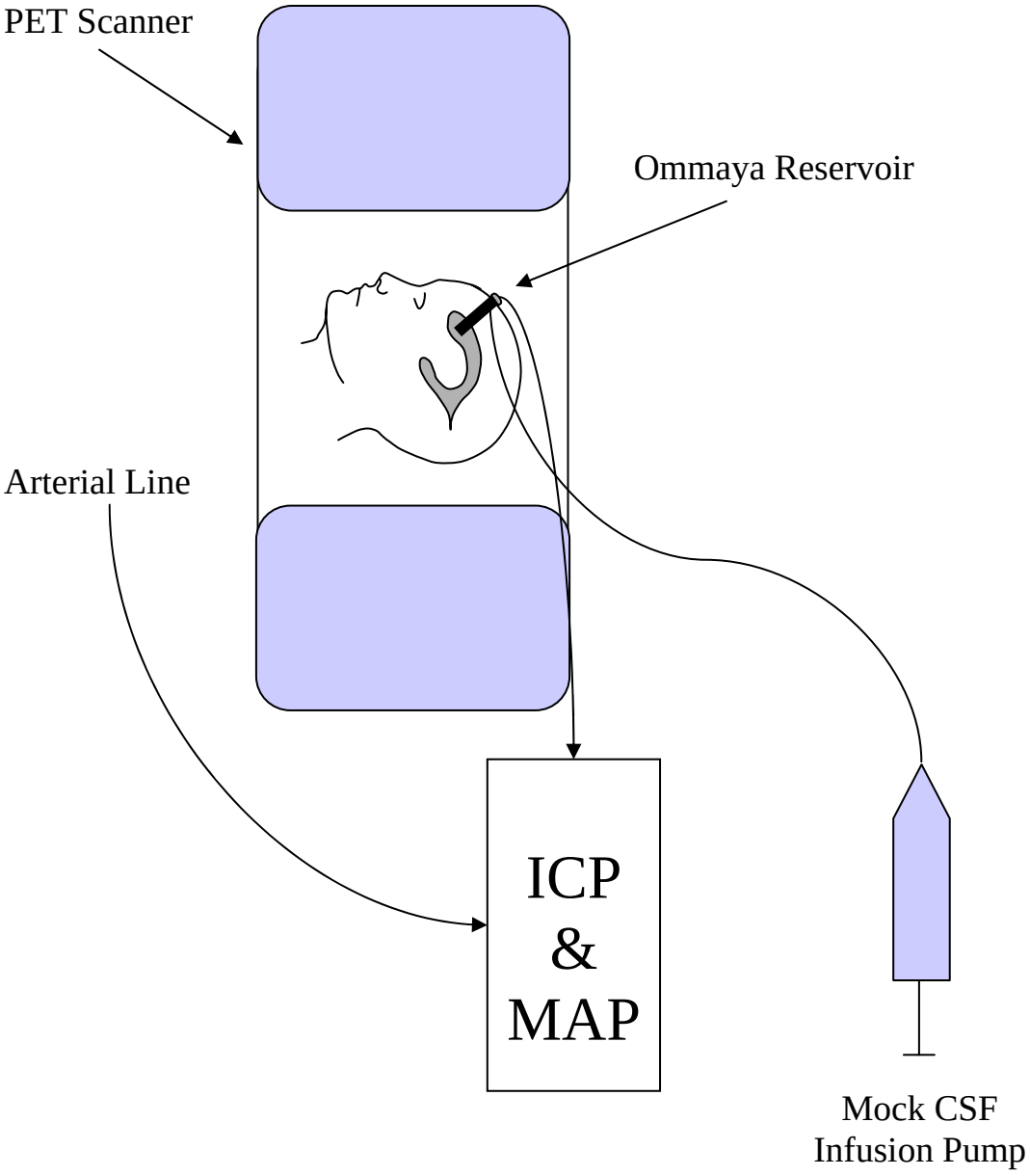

Figure 5.1: Experimental set-up. Patients were positioned in the PET scanner with an intravenous line to deliver the O15-labelled water and a radial arterial line for arterial blood sampling and arterial blood pressure monitoring. The previously implanted Ommaya reservoir was accessed and set-up for a CSF infusion study and ICP monitoring.

A volumetric 3 Tesla SPGR MRI scan (voxel size: 1x1x1mm) of the brain was obtained on the same day as the PET scan in 14 of the 15 patients. One patient was unable to tolerate the MR scanner due to claustrophobia. The PET and MR images were co-registered using SPM-99 and CBF maps (voxel size: 2.34 x 2.34 x 4.25 mm) were calculated using standard kinetic models (Frackowiak *et al.*, 1981) (PETAN2001, Dr. Piotr Smielewski, Cambridge). The spatial resolution of the PET data was approximately 6 mm.

5.2.3 Finite Element Modelling

Finite element (FE) analysis is a common engineering technique used to study the behaviour of a complex medium when various loads are applied and has found some utility in neurosurgery (Kyriacou *et al.*, 2002; Miga *et al.*, 2000; Péna *et al.*, 1999 & 2002b). As an adjunct to this study a FE modelling analysis of the distribution of mean stress, shear stress and displacement of the brain during a CSF infusion study was performed. There were two purposes of this modelling were: 1) to compare the baseline and equilibrium CBF maps for significant enlargement of the ventricular system during CSF infusion, and 2) to compare the regional changes in CBF with the distribution of physical stress and strain throughout the brain during CSF infusion.

FE simulation was implemented using the software ABAQUS/Standard 6.3 (HKS Ltd.,Pawtucket, USA). A FE simulation requires the following input data: the geometry of the object to model, a definition for the type of material being deformed, and the specification of boundary values. The brain and skull geometry were taken from MRI scans. A FE mesh composed of 2318 nodes and 2154 elements was constructed using an automatic mesh generator. As, brain tissue is composed of 80%

water and 20% solids, where the fluids correspond to the intra and extra-cellular fluids and the solids to the neurones, neuroglia and interstitium, it is a valid assumption to regard tissue as a porous elastic material, composed of a solid linear elastic matrix saturated by interstitial fluid. In this model, the volume occupied by the 'solids' corresponds to the neurons and neuroglia, while the 'voids' correspond to the extracellular space of the tissue. A poroelastic material is defined by three material parameters: E (Young's elastic modulus), K (hydraulic permeability) and v (Poisson's ratio). Values of E=30 kPa, v = 0.3 and K=1e8 m/s were used. The boundary conditions specified were: zero displacement at the cortical regions and a fluid pressure based on the reading from the infusion study.

For a two-phase material, that is, a mixture of solids and fluids, the stress tensor has the form

$$\sigma_{ij} = \sigma_{ij}^{solid} + u\,\delta_{ij}$$

or

$$\sigma_{ij} = \begin{bmatrix} \sigma_{xx} & \sigma_{xy} & \sigma_{xz} \\ \sigma_{yx} & \sigma_{yy} & \sigma_{yz} \\ \sigma_{zx} & \sigma_{zy} & \sigma_{zz} \end{bmatrix} + \begin{bmatrix} u & 0 & 0 \\ 0 & u & 0 \\ 0 & 0 & u \end{bmatrix} \quad .$$

Displacement in tissue was characterised in terms of its magnitude (d). Stress concentrations in tissue were characterised in terms of compression (mean stress, p), shear (Von Mises shear stress, q) and interstitial fluid pressure (u). In terms of the principal stresses,

$$p = \frac{\sigma_1 + \sigma_2 + \sigma_3}{3}$$

and

$$q = \sqrt{\frac{3}{2}}\sqrt{(\sigma_1 - p)^2 + (\sigma_2 - p)^2 + (\sigma_3 - p)^2}\ .$$

5.2.4 Analysis

For each individual patient, global CBF was assessed by drawing regions-of-interest (ROIs) on the co-registered MR scans. The method for defining global and anatomical ROIs has been previously described (Chapter 4). Global regions (cerebrum and cerebellum) regions were outlined with AnalyzeAVW using a combination of thresh-holding and manual inspection. CSF spaces and large vessels were excluded from the ROIs. The process was repeated for each slice. A mean CBF for the whole ROI was obtained using the method described previously. For the patient in whom co-registration was not possible due to lack of a suitable MR scan, global ROIs for the cerebrum and cerebellum were drawn using AnalyzeAVW directly onto the CBF maps.

The regional CBF results were obtained by manually placing small circular ROIs (15 voxels in size each) bilaterally within anatomical regions on all slices of the MR scan where that structure was visible. This was performed for the frontal, occipital, temporal and parietal white matter, as well as thalamus, head of caudate and putamen. Care was taken to place ROIs away from the boundaries of anatomical regions so as to minimize partial volume contamination of the ROI by other structures with different CBFs. A regional CBF analysis could not be accurately performed in the patient for whom there were no co-registered MR images.

A third type of analysis, based on the distance from the lateral ventricles, was performed. Three ROIs were described using the co-registered MR images (Figure 5.2). Only MR slices in which the lateral ventricles were visible and which were above the level of the thalamus were included. All cerebral tissue at a maximum distance of 15 mm from the wall of the lateral ventricle was included in the first ROI. The second ROI contained tissue within 15-30 mm of the walls of the lateral ventricle. The remainder of the tissue to the cortical surface made a third ROI. Thus, all of these ROIs contained a mixture of gray and white matter. The type of tissue contained within these ROIs will vary between patients depending on the size of the ventricles and the morphology of the brain. However, the aim was to study change in CBF with distance from the lateral ventricle when CSF pressure is increased rather than absolute values.

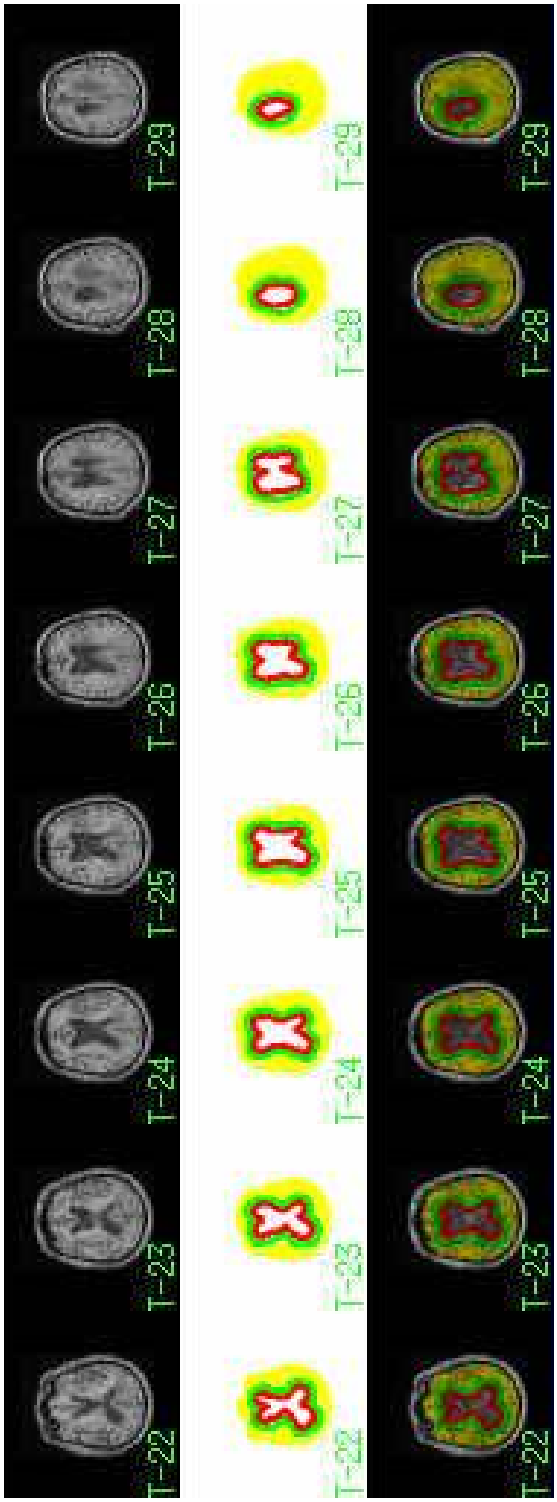

Figure 5.2: Concentric ROIs based on distance from lateral ventricles.

Two measures of static pressure autoregulation were performed. For all patients a static autoregulation parameter (sAR) was calculated on the basis of the percentage change in mean CBF for the cerebrum divided by the increase in CSF pressure during CSF infusion. This measure of static autoregulation is based on CSF pressure only and not the CPP. The threshold proposed for impaired sAR is between 0.5 and 3-4%/mmHg (Panerai, 1998).

In 10 patients, the CPP was continuously measured throughout the study thus allowing for simultaneous changes in MAP during changes in CSF pressure. The CPP also allowed calculation of the cerebrovascular resistance (CVR = CPP/CBF) and therefore the calculation of the static autoregulation index (sARi) using the standard formula (sARi = %Δcerebrovascular resistance / %Δcerebral perfusion pressure). When pressure autoregulation is intact a change in CPP should be matched by a change in CVR and sARi should equal one. With disrupted autoregulation CVR does not change in relation to CPP and sARi would be zero. In practice values between 0.85 and 0.95 would be represent intact pressure autoregulation given that the slope of the autoregulatory 'plateau' is not zero (Panerai, 1998).

The mean CBF values for global and anatomical regions were compared between CBF values at baseline CSF pressure and equilibrium CSF pressure during CSF infusion using the Wilcoxon matched pairs test. Changes in CSF pressure, R_{csf}, sAR and sARi were compared to changes in CBF and examined for correlations using the Spearman Rank Order Correlation Test.

All patients and control subjects involved in the study gave informed consent. The study was performed with the approval of the Cambridge Local Region Ethics Committee (96/172) and the Administration of Radioactive Substances Advisory Committee (083-2050(14649).

5.3 Results

5.3.1 CSF Compensatory Parameters and Change in Intracranial Pressure

All patients were studied using the computerised CSF infusion technique. Mean ICP during the acquisition of the baseline PET scan was 11.0 ± 3.5 mmHg [mean ± SD]. The average increase in ICP during CSF infusion to equilibrium ICP was 22.1 ± 7.8 mmHg providing a mean equilibrium ICP of 33.1 ± 9.9 mmHg and R_{csf} of 20.1± 7.3 mmHg/ml/min (Table 5.1). In one patient, in whom CSF infusion precipitated large plateau waves to 60 mmHg, the infusion was immediately terminated. Calculation of R_{csf} was estimated to be approximately 24 mmHg/ml/min in this patient given the mean ICP of 35 mmHg during the time of data acquisition of the second PET.

	Mean	**Min - Max**	**Std.Dev.**
Age	64.0 years	59 - 76	11.3
Rcsf	20.1 mmHg/ml/min	10.4 - 31.8	7.3
Baseline ICP	11.0 mmHg	6.0 - 16.4	3.5
Equilibrium ICP	33.1 mmHg	18.2 - 48.5	9.9
Change in ICP	22.1 mmHg	10.7 – 33.0	7.8
PVI	23.4	7.6 – 49.9	12.6

Table 5.1: Age and CSF compensatory parameters obtained from CSF infusion studies. R_{csf} and ICP results do not include the patient with large plateau waves.

5.3.2 Finite Element Analysis

The results of the three-dimensional FE modelling of the brain during CSF infusion with an increase in CSF pressure of 30 mmHg are illustrated in Figure 5.3a-d. With regards to displacement, the results suggest that small changes in the size and shape of the lateral ventricles do occur. These changes are <2 mm and are located in the regions of the body of the lateral ventricles and around the corpus callosum. The magnitude of displacement is well within the abilities of the MR/PET co-registration process.

Figures 5.3 a-d: Illustrates the results of the finite element analysis modelling of changes that occur during CSF infusion. **A.** The 3-dimensional finite element mesh. **B.** Pressure exerted in the brain is maximal in the corpus callosum and region of the basal ganglia but low or even negative at the region of the frontal horns. **C.** Shear (von Mises) stress is maximal at the frontal and occipital horns. **D.** Interstitial fluid pressure is shown to be maximal in the regions of around the lateral ventricles and corpus callosum.

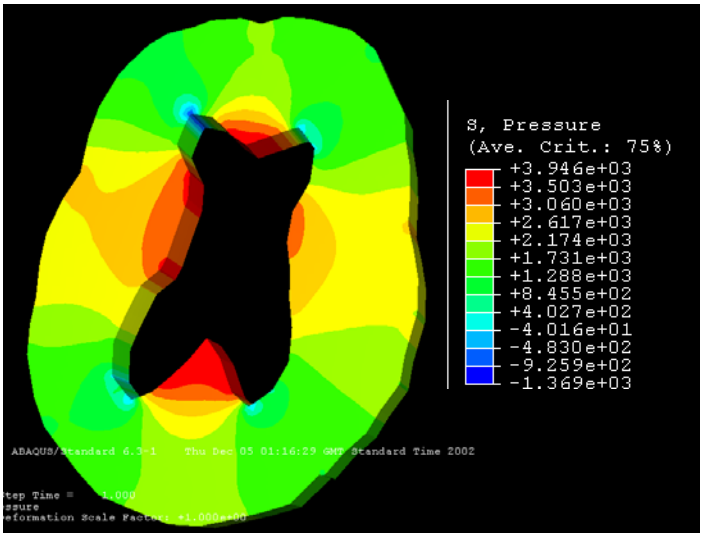

Figure 5.3b

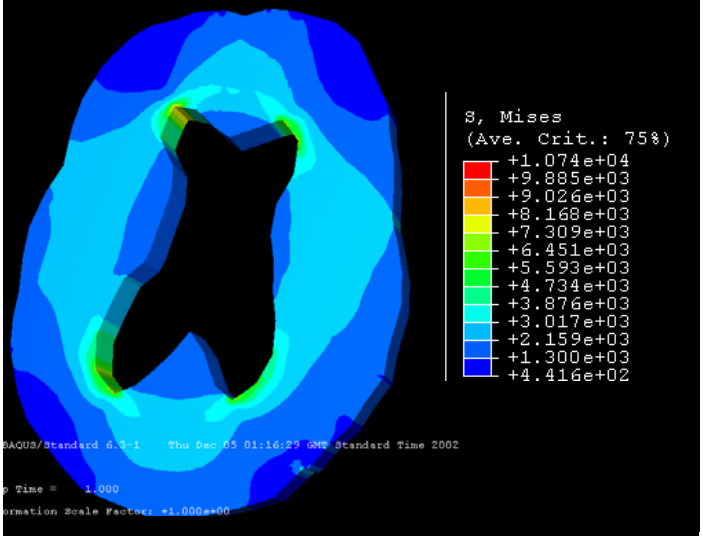

Figure 5.3c

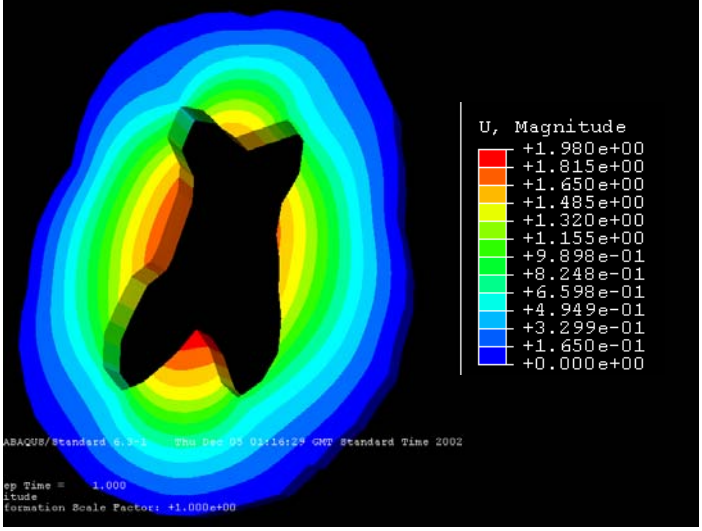

Figure 5.3d

Mean stress was distributed throughout the brain during CSF infusion. The location in which the mean stress (p), indicating compression, was maximal was the region of the thalamus and corpus callosum (≈ 2.5 kPa) with a smaller increase in the cortical regions (≈1 kPa). The smallest increase occurred in the regions of the ventricular horns (≈ 0.5kPa). White matter surrounding the ventricular horns was the site of maximal Von Mises shear stress (≈ 3kPa). The smallest shear stresses were in the cortical regions (≈ 0.7 kPa).

5.3.3 Change in Cerebral Perfusion Pressure

Mean arterial blood pressure was measured in 10 patients throughout scanning. There was a small but significant (p=0.005) increase in MAP of 8.2 ± 3.6 mmHg from baseline to equilibrium ICP. However, as the increase in ICP was higher than the increase in MAP, the CPP was however still significantly decreased during CSF infusion by 14.0 ± 8.8 mmHg (Table 5.2).

Parameter (mmHg)	n	Baseline	Equilibrium	Difference	P value
ICP	15	11.0 ± 3.5	33.1 ± 9.9	+ 22.1 ± 7.8	P<0.001
MAP	10	90.4 ± 19.3	98.6 ± 19.2	+ 8.2 ± 3.6	P=0.005
CPP	10	79.1 ± 18.4	65.1 + 19.4	- 14.0 ± 8.8	P<0.01
$PaCO_2$	15	39.5 ± 1.9	38.3 ± 3.6	- 1.2 ± 2.3	NS

Table 5.2: Changes in ICP, MAP and CPP, as well as $PaCO_2$ during CSF infusion.

There was a strong correlation between change in ICP and change in CPP (R=-0.95; $p<0.00005$) as well as R_{csf} and change in CPP (R=-0.83; $p<0.01$). There was no correlation between the change in MAP and the change in CPP.

5.3.4 Changes in $PaCO_2$

Mean $PaCO_2$ was not significantly different comparing baseline and equilibrium values (39.5 ± 1.9 mmHg versus 38.3 ±3.6 mmHg) (Table 5.2).

5.3.5 Changes in Global CBF

Significant changes in global CBF were demonstrated in the cerebrum and the cerebellum (Table 5.3). For the cerebrum, 12 of 15 patients showed a decrease in CBF of >5%, one patient had no change, whilst 2 patients had a small increase. The difference in CBF between baseline and equilibrium ICP was significant ($p<0.01$) and correlated with the measured R_{csf} (R=-0.82; $p<0.0005$) (Figure 5.4).

In the cerebellum, mean CBF was significantly decreased ($p<0.05$) during CSF infusion. However, regarding individual patients, 2 patients changed by <5% and two had increases of >5%. The change in CBF correlated with the measured R_{csf} (R=-0.64; $p<0.05$).

ROI	n	Baseline	Equilibrium	P value
Cerebrum	15	24.9 ± 4.6	23.1 ± 4.8	P<0.01
Cerebellum	15	35.8 ± 7.8	33.6 ± 9.2	P<0.05

Table 5.3: Changes in CBF for the cerebrum and cerebellum.

While change in ICP was correlated with change in CBF for both global ROIs, the change in MAP or CPP was not. However, the percentage change in CPP correlated with the percentage change in CBF in both regions (cerebrum: $R= 0.65$; $p<0.05$ and cerebellum: $R=0.71$; $p<0.05$),

The patients who had an increase rather than decrease in CBF during CSF infusion were those with high-normal R_{csf}.

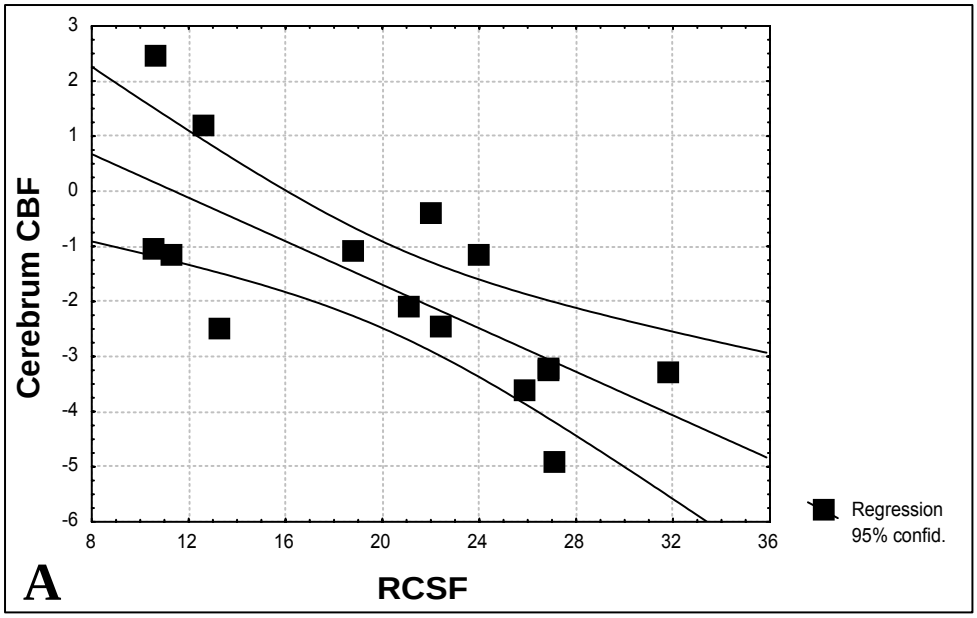

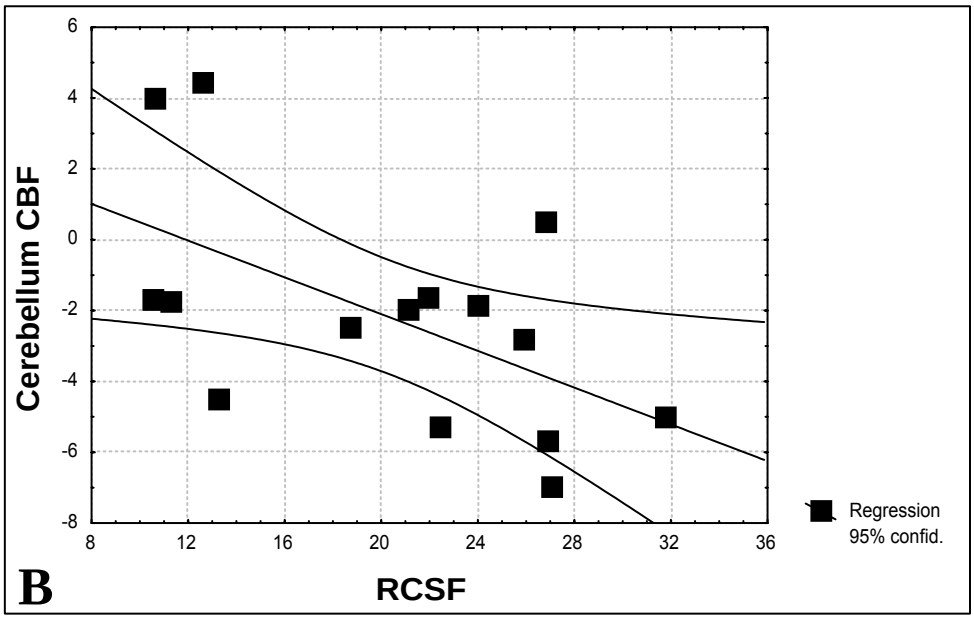

Figure 5.4: A. Correlation between Rcsf and decrease in CBF of the cerebrum. **B.** Correlation between Rcsf and the decrease in CBF of the cerebellum.

5.3.6 Cerebral Autoregulation

The sAR was calculated in 15 patients. It ranged from -0.74 to 1.01 %/mmHg with a mean of -0.28 %/mmHg (Figure 5.5). The patients with a positive sAR were those with relatively small increases in CSF pressure but without true CPP measurement the meaning of the increase in CBF is questionable. The threshold for intact static autoregulation is considered to be in the range of -0.5 – -3.0 %/mmHg. The majority of patients were > -0.5 %/mmHg and all were >-0.74 %/mmHg indicating that cerebral autoregulation was probably intact.

With the additional information provided by monitoring the MAP, the sARi was calculated as described above. In two patients the change in CPP was < 9 mmHg and therefore the calculation of sARi was considered invalid. The sARi of the remaining 8 patients is illustrated in (Figure 5.6). Two patients had very low sARi values (<0.2) indicating that CBF passively followed the change in CPP, that is, failure of autoregulation. The remaining 6 patients had values of 0.48 – 0.94, four of which were above 0.65 indicating that some of these patients had intact cerebral autoregulation.

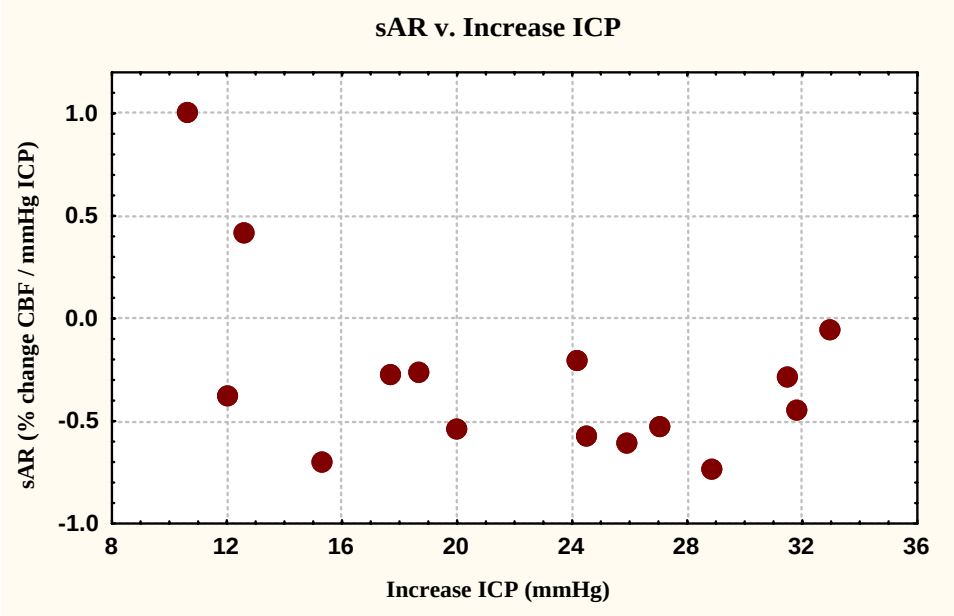

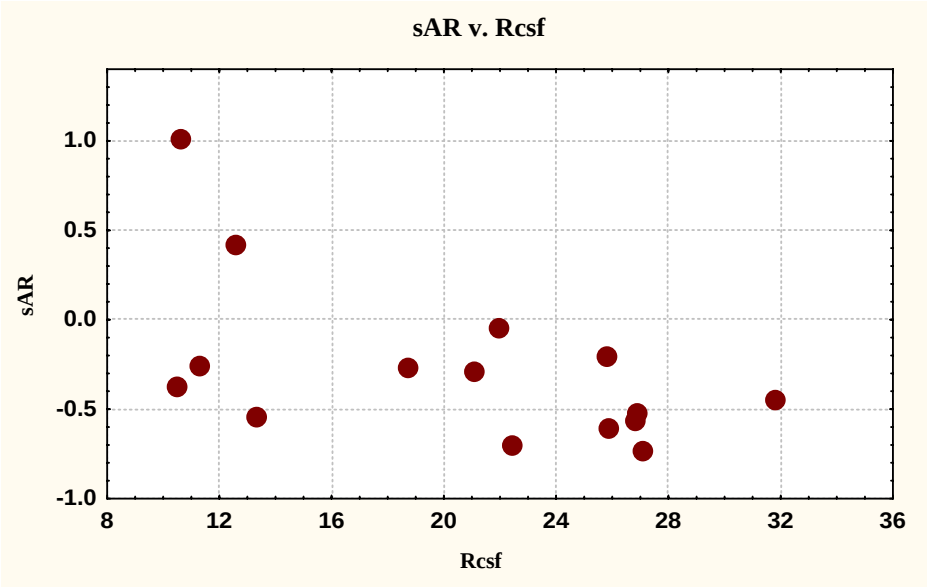

Figure 5.5: Cerebral autoregulation as measured using sAR versus the increase in CSF pressure during CSF infusion (top) and Rcsf (bottom).

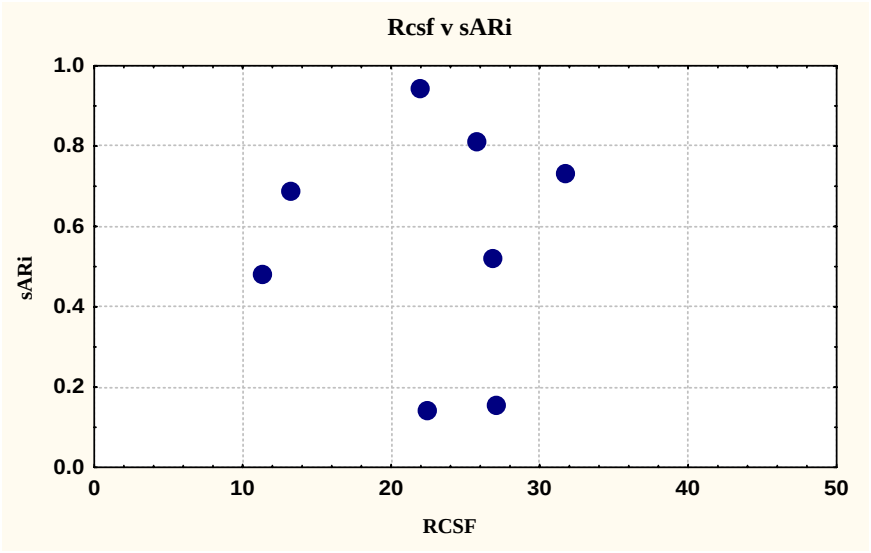

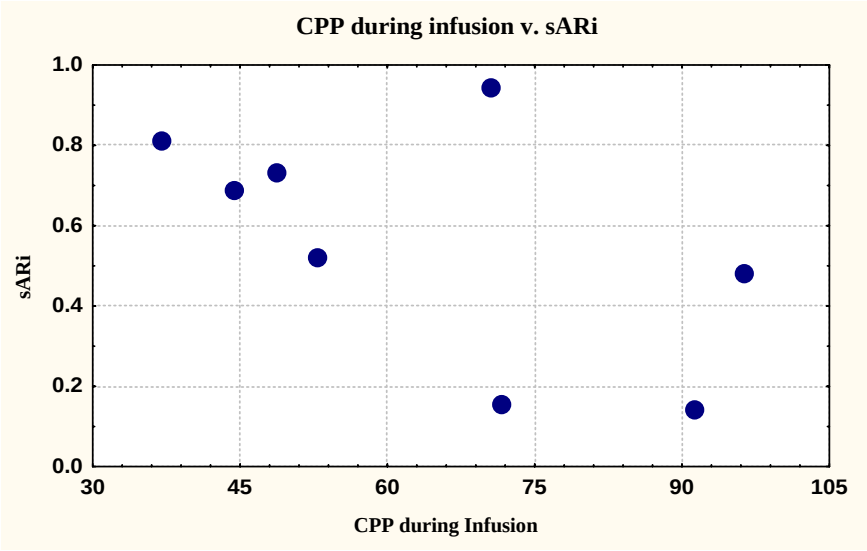

Figure 5.6: Cerebral autoregulation as measured using sARi versus Rcsf (top) and CPP during CSF infusion (bottom).

5.3.7 Changes in Anatomical Regional CBF

For the white matter anatomical ROIs there were significant decreases in mean CBF for all four regions (Table 5.4). These regions all demonstrated significant correlation between R_{csf} and the decrease in CBF ($p<0.05$; $-0.68>R>-0.56$). There was no correlation between change in MAP or CPP and CBF. However, the percentage change in frontal white matter CBF correlated significantly with the percentage change in CPP ($R=0.68$; $p<0.05$). There was no correlation between the degree of white matter hyperintensities and the change in CBF.

ROI	n	Baseline	Equilibrium	P value
Frontal	14	16.1 ± 4.3	15.0 ± 3.6	P<0.05
Parietal	14	17.8 ± 4.7	16.2 ± 4.7	P<0.001
Temporal	14	20.4 ± 4.1	18.7 + 4.6	P<0.005
Occipital	14	18.1 ± 6.2	16.4 ± 6.2	P<0.05

Table 5.4: Changes in CBF for white matter ROIs during CSF infusion.

Mean CBF in the thalamus and the head of the caudate were both significantly lower during CSF infusion. However there was no significant difference in CBF found in the putamen (Table 5.5). The falls in CBF for the thalamus were significantly correlated with R_{csf} ($R=-0.59$; $p<0.05$). There were no correlations between changes in CBF and change in ICP or CPP.

ROI	n	Baseline	Equilibrium	P value
Thalamus	14	36.0 ± 7.5	32.3 ± 7.0	P<0.05
Caudate	14	24.8 ± 6.5	22.6 ± 6.0	P<0.05
Putamen	14	35.6 ± 8.3	34.1 + 7.5	NS

Table 5.5: Changes in CBF for deep gray matter ROIs during CSF infusion.

5.3.8 Changes in Concentric ROI CBF

There were significant decreases in mean CBF for each of the three concentric type ROIs during CSF infusion (Table 5.6).

ROI	n	Baseline	Equilibrium	P value
Inner	14	15.5 ± 3.1	14.1 ± 3.1	P<0.001
Middle	14	26.6 ± 5.8	24.7 ± 5.9	P=0.005
Outer	14	25.8 ± 7.2	24.4 + 7.6	P<0.01

Table 5.6: Changes in CBF of concentric ROIs during CSF infusion

These changes correlated with R_{csf} and ICP_{end} for all three ROIs. These correlations were closest for the inner ROI and decreased towards the outer ROI. Changes in CPP and ICP were also correlated with change in CBF for the inner and middle ROIs but not the outer. Change in MAP was not correlated with change in CBF for any ROI (Table 5.7).

ROI	Rcsf		ICPend		ICPdiff		CPP	
	R	P value	R	P value	R	P value	R	P value
Inner	-0.90	<0.00005	-0.73	<0.005	-0.70	<0.01	0.77	<0.01
Middle	-0.87	<0.0005	-0.67	<0.01	-0.68	<0.01	0.69	<0.05
Outer	-0.77	<0.005	-0.54	<0.05	-0.49	0.07	0.59	0.07

Table 5.7: Correlations between changes in CBF of concentric ROIs and R_{csf}, ICP and CPP during CSF infusion

5.3.9 Response to CSF shunting

Nine of the 15 patients were treated using a ventriculoperitoneal shunt. Six patients responded to CSF shunting while three did not. The CSF compensatory parameters,

changes in MAP and CPP as well as changes in CBF during CSF infusion studies were compared between the shunt responders and non-responders. The mean R_{csf} was higher in patients who responded to CSF shunting (22.7 ± 7.5 versus 16.6 ± 8.1 mmHg/ml/min) but there were no statistically significant differences between the two groups of patients given the small numbers.

5.4 Discussion

This study is unique in its approach to studying the dynamic characteristics of the cerebral vasculature in patients with NPH. Most studies aimed at investigating the state of the cerebral vasculature of patients with NPH measured CBF at rest. These studies have been reviewed (Owler and Pickard, 2001; Appendix A). Baseline CBF was measured using ^{15}O-water PET and MR co-registration in Chapter 4.

The combination of the computerised CSF infusion study and measurement of CBF using ^{15}O-water PET scan has allowed us to manipulate CSF pressure in order to assess the response of the cerebrovascular system to changes in ICP. Cerebral pressure autoregulation may be defined as the ability of the cerebrovascular system to maintain a constant CBF during changes in CPP. Previous studies of autoregulation in a population of patients with ventriculomegaly presenting to a multidisciplinary CSF clinic revealed that hemispheric autoregulation, as assessed by transcranial Doppler ultrasonography, was more likely to be relatively intact when R_{csf} was raised (Czosnyka *et al.*, 1999 & 2000). Global autoregulation was more likely to be impaired when CSF outflow resistance was not raised, that is, in patients where the predominant pathology was ‘cerebrovascular’ rather than a primary disturbance of

CSF circulation. Most investigators have not been able to assess pressure autoregulation directly but have studied cerebrovascular reactivity, that is, metabolic autoregulation. Klinge *et al.* (1999) and Chang *et al.* (2000) have both studied cerebrovascular reactivity using the administration of i.v. acetazolamide. Klinge utilised PET without MR coregistration while Chang utilised ^{99m}Tc-HMPAO SPECT before and after administration of acetazolamide and found that the response to acetazolamide was decreased in patients with NPH. Lee *et al.*, (1998) using transcranial Doppler of the middle and anterior cerebral arteries to measure cerebrovascular reactivity after inhalation of 5%CO_2, found that cerebrovascular reactivity was also decreased in patients with NPH. The previous studies of cerebral autoregulation in patients with NPH are summarised in Table 5.8.

Table 5.8: Studies of Cerebrovascular Reactivity and Autoregulation in NPH: Predictive Value

Reference	Methods	Cases	Baseline results	Comments
Mathew *et al.*, 75	CSF drainage 30-40mL / CSFP: ↓50% / T: Nil	15pts	↑CBF and ↑CBV	Appears to be relationship between ↑CBF and response to CSF shunting.
Mathew *et al.*, 77	CSF drainage 30-40mL / CSFP: ↓50% / T: Nil	3pts	↑CBF	Appears to be relationship between ↑CBF and response to CSF shunting.
Grubb *et al.*, 77	CSF drainage 30-40mL / CSFP: NA / T: Nil	7pts	↑CBF small but significant.	Also small but significant ↑ in patients with cortical atrophy.
Hartmann *et al.*, 77	CSF drainage NAmL / CSFP:14mmHg / T:NA	11pts	Small ↑CBF and ↑CBV: Not significant Also an increase in CO_2 reactivity.	-
Stump *et al.*, 83	CO_2 reactivity ^{133}Xe inhalation	1pt	CVR pre-op 20% ie reduced. CVR post-op 47%.	Improvement in CVR appeared to correlate with clinical improvement.
Kushner *et al.*, 84	CSF drainage 25-40mL / CSFP: ↓50% / T: 1hr	19pts	No change in mean CBF. ↑CBF just as likely as ↓CBF.	Not useful.
Meyer *et al.*, 84	CSF drainage 25-35mL / CSFP: ↓50% / T: Nil & 100% O_2 response	7pts	↑CBF post LP in 6/7 (other pt had SDH) ↑CBF frontal region the greatest.	CVR to 100% O_2 restored to normal range after CSF removal.
Mamo *et al.*, 87	CSF drainage 20-35mL / CSFP: ↓50% / T: 30min	25pts	No overall ↑CBF, some cases ↓CBF; ↑CBF related to ↑ on one side in cases of asymmetry.	No correlation between ↑CBF and response to CSF shunting.
Morretti *et al.*, 88	CSF drainage 10-60mL / CSFP: ↓50% / T: 30min	23pts	↑CBF 7/10 & ↓CBF 3/10	100% predictive value; all with ↑CBF responded & no cases with ↓CBF responded.
Schmidt *et al.*, 90a	Autoregulation: Vacuum lower limbs and CO_2 reactivity	14pts	Autoregulation maintained in 13/14 pts.	After Captopril autoregulation remained intact and CO_2 reactivity unchanged.
Schmidt *et al.*, 90b	Response to Nimodipine iv A-V O_2 difference	8pts	-	4/8 pts had ↓CPP of 20mmHg. All of these patients experienced ↓CBF. Other pts experienced no change.
Shimoda *et al.*, 94	CVR: 10% Glycerol iv Xe CT	22pts	More widespread increases in CBF post glycerol in shunt responders.	Authors suggest glycerol is a predictor of tissue salvagability.
Kristensen *et al.*, 96	CSF drainage 30-40mL/ CSFP: 0/ T: 3-4hr	31pts	No change in CBF overall.	No significant correlations between change in CBF and clinical changes. Gait often improved after LP.
Lee *et al.*, 98	TCD: ACA/MCA CO_2 Reactivity	11pts	↓CVR and ↑PI in ACA and MCA. Not predictive of outcome.	CVR↑ post-operatively; ↑CVR in ACA and MCA appeared related to improvements in gait and that of MCA related to mental impairment.
Klinge *et al.*, 99	CVR: Acetazolamide 1g iv PET: H_2O^{15}	10pts	CVR not different between responders and non-responders pre-operatively.	In responders, CVR increased post-operatively. In non-responders, CVR decreased and then returned to baseline levels.
Chang *et al.*, 00	CVR: Acetazolamide 500mg iv ^{99m}Tc-HMPAO	41pts	↓CVR pre-operatively: Complete triad significantly lower CVR compared to incomplete triad.	Post-operatively ↑CVR in both groups.

Abbreviations: CSF: cerebrospinal fluid, CSFP: CSF pressure, CVR: cerebrovascular reactivity, 1-comp/2-comp: single or bi-compartmental curve analysis, HC: hydrocephalus, IC: intra-carotid, inhal: inhalation, ISI: initial slope index curve analysis, IV: intravenous, LP: lumbar puncture, NPH: normal pressure hydrocephalus, pt: patient, PI: pulsatility index.

CBF was measured using ^{15}O-water PET because it provides whole brain coverage, allows accurate measurement of CBF in deep as well as superficial structures and the measurement is obtained during a steady-state period. In addition, maps of CBF could be co-registered to MR images allowing accurate identification of anatomical structures and therefore anatomical analysis. The method of defining the ROIs has been explained in the previous chapter but certain points unique to this study need to be addressed. However, regarding the potential for error due to partial voluming and other issues related to the definition of ROIs, these errors are likely to be minimal due to the fact that each subject forms his/her own control and the issue in this study is not the absolute CBF value but the change.

An obvious concern with this study is whether baseline and infusion CBF maps of individual patients are comparable. During the CSF infusion, the increase in CSF pressure may change the size and shape of the ventricles. Therefore a three-dimensional FE analysis was performed and the morphological changes that may occur during CSF infusion studied. The results suggest that small changes in the size and shape of the lateral ventricles do occur but they are small (<2 mm) and are located in the region of the body of the lateral ventricles and around the corpus callosum. Changes in the geometry of the brain of this magnitude during CSF infusion are accounted for by the co-registration process as the CBF maps are co-registered to the same MR volume for each patient. In addition, most ROIs are located well away from the ventricular system and therefore not affected. Finally, manual inspection of the CBF maps demonstrates that there are no gross differences in the morphology

between the images that may account for the measured differences in CBF between the baseline and infusion CBF measurements.

Using the CSF infusion study CSF pressure was raised in a controlled fashion and maintained CSF pressure at a higher equilibrium pressure. The changes in CSF pressure were such that the new equilibrium pressure was significantly different to the baseline CSF pressures. In utilising the CSF infusion study to alter ICP, the patients with high R_{csf} will demonstrate the largest change in ICP and therefore generally CPP. This is demonstrated by the correlation between R_{csf} and the change in CPP. Therefore patients with normal or high-normal R_{csf} will exhibit a relatively small change in ICP and therefore CPP. Thus autoregulatory capacity of those patients with a normal R_{csf} is not tested using such a study. This would explain the reason for the lack of change in global in the patients with normal R_{csf}.

The mean CPP during CSF infusion was 65.1 mmHg which should be within the normal range for cerebral autoregulation of the healthy brain. Three of the 10 patients in who MAP were monitored had a CPP of 45-50 mmHg during CSF infusion while one patient had a CPP of 37 mmHg. Thus these patients may well be below the lower limit for cerebral autoregulation. However, there was no correlation between CPP during infusion and the change in CBF for the cerebrum. Figure 5.5 demonstrates that the patients with low CPP during infusion had intact autoregulation and the patients exhibiting failure of autoregulation were well within the range physiological range for pressure autoregulation.

Small but significant decreases in mean for the cerebrum, cerebellum and all anatomical ROIs, with the exception of the putamen, have been demonstrated. This would suggest that a disturbance of pressure autoregulation in patients with NPH. However, scrutiny of both the sAR parameter and sARi indicate that autoregulation is intact in the majority of these patients. This disparity results because the slope of the pressure autoregulatory plateau is not zero. With respect to sAR, the threshold for normal autoregulation is approximately a decrease in mean CBF of 0.5-3 %/mmHg. The majority of the patients in this study demonstrated a decrease in CBF of <0.5 %/mmHg with the largest decrease being 0.74 %/mmHg which would indicate that pressure autoregulation is intact.

The sARi value is a more accurate measure of pressure autoregulation as CPP is incorporated in the calculation. This is important as MAP usually increased during a CSF infusion thus the change in CPP was usually less than the change in CSF pressure. The sARi was calculated for the eight patients in whom CPP could be calculated and who demonstrated a change in CPP of >9 mmHg. A value of 1 indicates perfect autoregulation while 0 indicates passive changes in CBF with changes in CPP, that is, no autoregulation. Again, as the slope of the autoregulatory plateau is no zero and normally sARi would be expected to be <1. There is no standard value to denote intact autoregulation with thresholds of 0.5-0.85 being used in different studies. In this study, the majority of patients had values of >0.6. Only 2 patients had values of <0.2 indicating almost complete failure autoregulation in these two patients who also demonstrated the largest decrease in sAR. From the results it can be concluded that while pressure autoregulation was deficient in some patients, in the majority of patients with NPH, it was intact.

These findings are in agreement with the study by Czosnyka *et al.* (2000) who examined the relationship between R_{csf} and cerebral autoregulation using a correlation between the middle cerebral artery flow velocity on transcranial Doppler and the CPP. A finger-cuff was used to monitor ABP during CSF infusion studies and thus enable calculation of the CPP. A correlation between flow velocity and CPP (Mx) indicated poor autoregulation while a negative correlation was indicative of intact cerebral autoregulation. It was reported that patients with a higher R_{csf} had better autoregulation than those with lower R_{csf}. While the relationship was weak and Mx was a poor predictor of R_{csf}, the results suggest that abnormalities of pressure autoregulation are not the predominant factor in the pathophysiology of NPH. However, it should be noted that current notions of cerebral autoregulation are in some ways probably naïve given the findings of this study. Clearly the brain is not a fluid but a semi-solid. Therefore, as demonstrated by the FE analysis stresses and strains are distributed to different regions of the brain. The regional nature of these forces and changes in CBF demonstrate that global concepts of cerebral autoregulation, especially in disease states may not be correct.

The mechanism responsible for the observed reduction in mean CBF during CSF infusion was examined. The ‘concentric ROI’ analysis was performed in order to assess whether, the reduction in CBF during CSF infusion was related solely to the proximity from the lateral ventricle. As these ROIs were drawn above the level of the thalamus, the majority of the inner ROI consists of periventricular white matter. The middle and outer ROIs contain a mixture of white matter and cerebral cortex. A significant decrease in mean CBF was observed for all three ROIs. This correlated

with the R_{csf} and the ICP_{end}. The strength of the correlation was greatest for the inner ROI and decreased to the outer ROI. In addition the change in CPP and ICP was correlated to the fall in CBF for the inner and middle ROIs but not for the outer ROI. This suggests that there is a relationship between the proximity to the ventricles and the fall in CBF. This is consistent with the results of the FE analysis which demonstrates that the mean stress as well as shear stress are maximal in regions closest to the ventricle and are lowest in the cortical regions. These findings suggest that increases in CSF pressure cause a reduction in CBF by direct compression of the cerebral tissues. An alternative explanation may be that infusion of mock CSF into the ventricular system of patients with NPH may cause an increase in the transependymal seepage of CSF into the parenchyma. The ependyma of the lateral ventricles is often disrupted in patients with hydrocephalus and transependymal CSF absorption is a likely alternative pathway for CSF absorption in patients with NPH. Increased intraparenchymal fluid may result in compromise of CBF. This would also be consistent with the direct relationship between R_{csf} and the reduction in CBF.

The baseline CBF values in NPH patients were compared to normal controls in the previous chapter and were shown to be significantly reduced. The relatively small reduction in CBF in response to the increase in CSF pressure during CSF infusion may be significant. Such increases in CSF pressure during B-wave activity, for example, due to an increase in cerebral blood volume. Changes in CBF secondary to changes in CSF pressure may result in ischemic stress on tissues in an already precarious state. In those patients with disturbed autoregulation this may be even more so as CBF changes passively with CPP.

With regard to outcome, there are as yet insufficient numbers of patients to answer this satisfactorily. The only difference between shunt-responders and non-responders was the R_{csf} that was higher in the former group. Patients who responded to CSF shunting did include one patient with failure of pressure autoregulation as assessed using sARi. The non-responder group also included patients with intact autoregulation.

5.5 Conclusions

Cerebral pressure autoregulation has been measured directly in patients with NPH using a combination of a computerized CSF infusion study and ^{15}O-water PET scanning with anatomical ROI definition on co-registered MR. Although changes in mean CBF were demonstrated for both global and anatomical ROIs, most but not all patients with NPH in this study had intact pressure autoregulation. In patients in whom CBF changed, a relationship between CBF change and proximity to the lateral ventricles has been demonstrated. This is consistent with the location of mean and shear stress within the brain as shown using FE analysis. The importance of changes in CBF with changes in ICP, and the implications for shunt outcome, will be made clearer with further studies and correlation with clinical outcomes.

Chapter Six

Diffusion Tensor Imaging of Patients with Normal Pressure Hydrocephalus

6.1 Introduction

Application of diffusion sensitive gradients during MR imaging allows the self-diffusion of water, a normal biological process, to be quantified. Diffusion in three-dimensions may be described by the diffusion tensor; a mathematical matrix. In biological tissues diffusion is restricted in both quantity and direction by cell membranes and other structures. If diffusion is equal in all directions it is termed isotropic and the diffusion tensor describes a sphere. If diffusion is greater in a particular direction, for example, parallel to white matter tracts, it is termed anisotropic and the diffusion tensor usually describes an ellipsoid.

In order to compare the diffusion properties of different materials a number of 'scalar invariants' are used. Scalar invariants are a single number (as opposed to a matrix) that is independent of rotation or translation of the tensor relative to an arbitrary frame of reference. The three most commonly used scalar invariants are the trace, relative anisotropy (RA) and fractional anisotropy (FA). The 'trace' is defined as the sum of the eigenvalues. The eigenvalues quantify the amount of diffusion along the principal axes of the diffusion ellipsoid, that is, the eigenvectors. The trace therefore represents the overall quantity of diffusion. Relative anisotropy (RA) is defined as the ratio of anisotropic diffusion to isotropic diffusion. Fractional anisotropy (FA) is defined as the ratio of anisotropic diffusion to total diffusion.

Diffusion tensor MR imaging is known to be sensitive to microstructural cerebral pathology, especially white matter changes. DTI was therefore applied to the study of cerebral pathology of NPH patients. The aim of the study was to determine whether pathological changes were demonstrable in patients with NPH using DTI and to define the characteristics of such changes in terms of the trace, RA and FA.

6.2 Materials and Methodology

6.2.1 Patients

Nine patients, 68.9 ± 10.5 years of age [mean ± SD] with a clinical diagnosis of NPH underwent diffusion tensor MR imaging as part of their clinical assessment. All patients underwent a clinical assessment through the CSF clinic at Addenbrooke's Hospital as well as routine static MR imaging (SPGR, proton density and T2-weighted imaging). Appropriate patients underwent CSF infusion studies via a previously implanted Ommaya reservoir. Five patients underwent placement of a CSF shunt. The clinical details of these patients including the outcome of CSF shunting are summarised in Table 6.1.

	Age	Diagnosis	Symptoms	CSF P (mmHg)	R_{csf} (mmHg/ ml/min)	Shunt	Outcome
1	85	Idiopathic	Gait / dementia / UI	10.5	19.0	Yes	Slight
2	64	ICH	Gait	15.7	25.9	Yes	Nil
3	75	CVD	Gait	-	-	No	Spontaneous
4	70	Idiopathic	Gait	-	-	No	-
5	69	Idiopathic	Gait / dementia / UI	6.3	14.8	Yes	Good
6	73	Idiopathic	Gait	-	-	-	-
7	47	Idiopathic	Gait / memory	-	-	-	-
8	63	Idiopathic	Gait / UI	6.1	12.1	Yes	Good
9	74	Idiopathic	Gait / UI	13.1	26.9	Yes	Good

Table 6.1: Clinical details of patients. Patient 4 spontaneously improved prior to implantation of an Ommaya reservoir for a CSF infusion study. Patient 4 refused further investigation or treatment and is being followed conservatively. Patients 6 and 7 are currently awaiting further investigation. (Abbreviations: ICH = intracerebral haemorrhage, CVD = cerebrovascular disease, UI = urinary incontinence)

6.2.2 Control Group

Six healthy volunteers, 35.5 ± 8.1 years of age, also underwent MR imaging. Volunteers were screened to exclude neurological disease, vascular disease or hypertension. Imaging of normal volunteers was approved by the Cambridge Local Research Ethics Committee.

6.2.3 MR Acquisition

Imaging was performed on a 3T whole-body system consisting of a Bruker Medspec 30/100 spectrometer (*Bruker Medical*, Etlingen, Germany) attached to an Oxford 3 Tesla 910 mm bore whole body actively shielded magnet (*Oxford Magnet Technology*, Oxford, UK). The whole body gradient coil had an internal diameter of 63 cm (Bruker BG 630), was actively shielded and had a maximum strength per axis of 35 mT/m, using 22.5 μs ramps. The manufacturer supplied DW-EPI sequences were modified so that the DW gradient could be applied along any user defined

direction, with maximal separation of the two DW gradient pulses (maximising the efficiency of the pulse sequence). A single shot Spin Echo (SE) Echo Planar Imaging (EPI) with Stejskal-Tanner diffusion sensitising pulses (Stejskal and Tanner, 1965) was used with imaging parameters of TR = 5070 ms, TE = 107 ms, α =90°, δ = 21ms and Δ = 66 ms. Images were performed using a 25x25cm field-of-view yielding a 128 x 128 acquisition matrix.

For each subject, 8-10 inter-leaved transverse 5 mm thick contiguous slices were acquired with a phase template in the near axial plane. For each slice images were collected from 12 non-collinear gradient directions. For each gradient direction a T2(b0) image and five diffusion weighted images were collected at equally spaced b-values between b_{min} = 318 s/mm^2 to b_{max} = 1541 s/mm^2. In order to remove residual Nyquist ghost artefacts, a non-phase-encoded EPI reference (template) scan was performed. After Fourier transformation of the image and template data along the read direction, a non-linear point-by-point phase correction of the image relative to the template data was performed. The images were finally reconstructed by Fourier-transforming the corrected image data along the phase-encoded direction. The reconstructed image was symmetrically zero-padded to a 256x256 matrix.

The diffusion tensor was computed on a voxel by voxel basis with an in-house program implemented in MATLAB (*The MathWorks Inc*., Natick, MA, USA), which used a singular value decomposition fitting (Golub and Van Loan, 1996) of the signal intensities to the Stejskal-Tanner equation (Stejskal and Tanner, 1965), following the method proposed by Basser (1995). From the diagonalised tensor, maps for the trace (Tr), fractional anisotropy (FA) and relative anisotropy (RA) were calculated for each

subject. Colour maps illustrating directional anisotropy were also constructed for patients and controls.

6.2.4 Analysis of the Diffusion Tensor

A regional analysis of the scalar invariants was conducted by identifying 25 anatomical regions of interest (ROIs). In the frontal lobe, ROIs were placed in the cortex/subcortex, deep white matter and periventricular white matter, the latter region being that where periventricular lucencies are frequently observed in patients with NPH. In the occipital lobe, ROIs were placed in the cortex/subcortex, deep white matter and periventricular white matter in a similar manner to the placement of ROIs in the frontal lobe. In the parietal and temporal lobes, ROIs were placed in the parietal cortex, parietal white matter, temporo-parietal cortex, temporal white matter stem, temporo-parietal white matter. The insular cortex and parieto-opercular white matter were also examined. ROIs were positioned in various regions of the corpus callosum including the splenium, genu, fronto-lateral region (forceps minor) and the occipito-lateral region (forceps major). For the deep gray nuclei, ROIs were positioned in the putamen, head of the caudate nucleus and the thalamus. The thalamus was divided into three regions, the medial thalamus, lateral thalamus and pulvinar, with ROIs in each. ROIs were also placed in various regions corresponding to the CSF of the lateral ventricles.

ROIs were 20 voxels each in size on the T2 b(0) of each patient image using Analyze AVW. Where an ROI was visible in multiple slices of the scalar invariant maps, the relevant ROI was drawn on all appropriate slices and the average value was calculated. Care was taken to exclude CSF spaces in order to avoid partial volume

contamination by CSF in ROIs close to the ventricles and cortical surface. The scalar invariants of each ROI were compared between controls and NPH patients using the Mann-Whitney U test.

In order to obtain an indication of the global distribution of each of the scalar invariants a single slice at the level of the lateral ventricles just above the basal ganglia was chosen for each subject. The region of the brain was carefully outlined and the CSF spaces excluded (Analyze AVW). Histograms depicting the distribution of each invariant within that slice were constructed. An average histogram for each invariant for controls and for NPH patients was then constructed.

6.3 Results

6.3.1 Regional Analysis

The results of the regional analysis are depicted in Table 6.2a-c and Figures 6.3a-c.

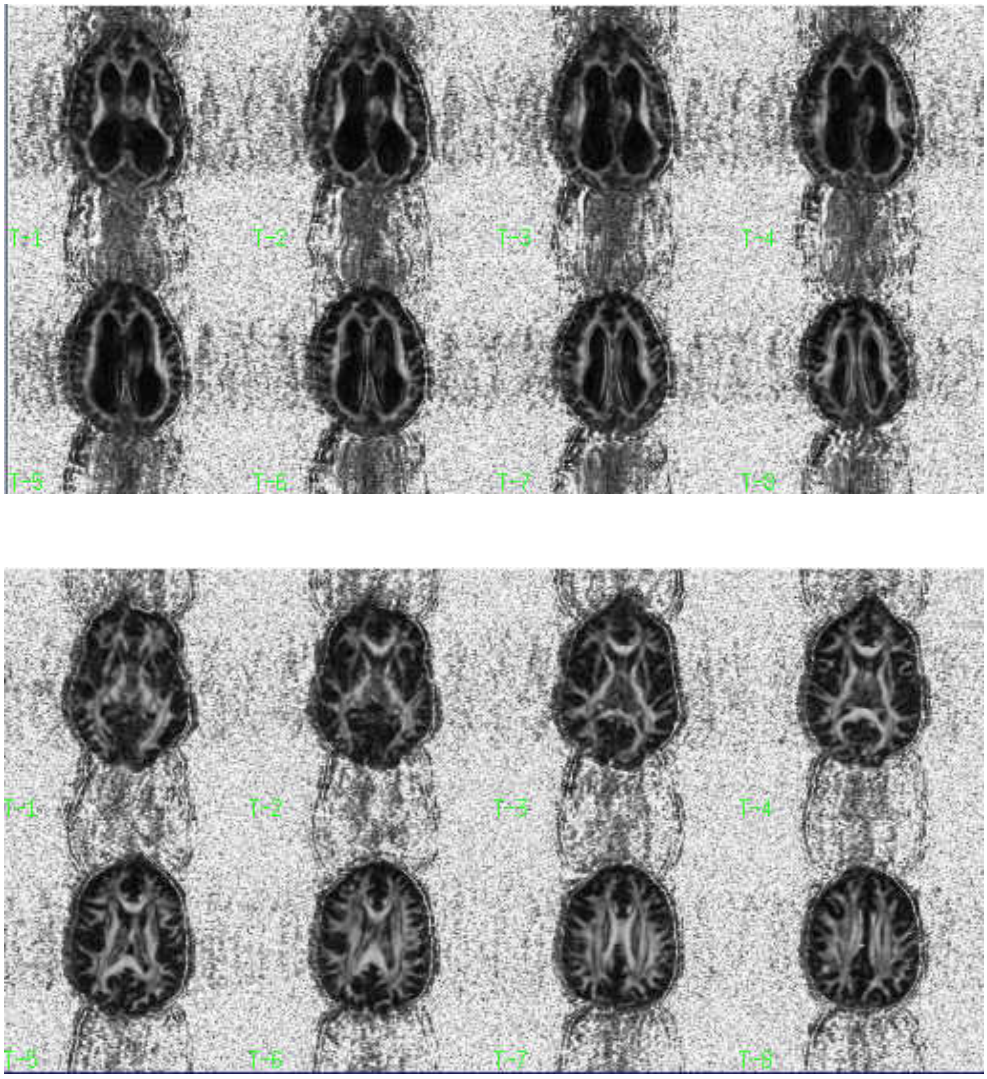

Figure 6.1a: Maps of fractional anisotropy of an NPH patient (top) and a normal volunteer (bottom).

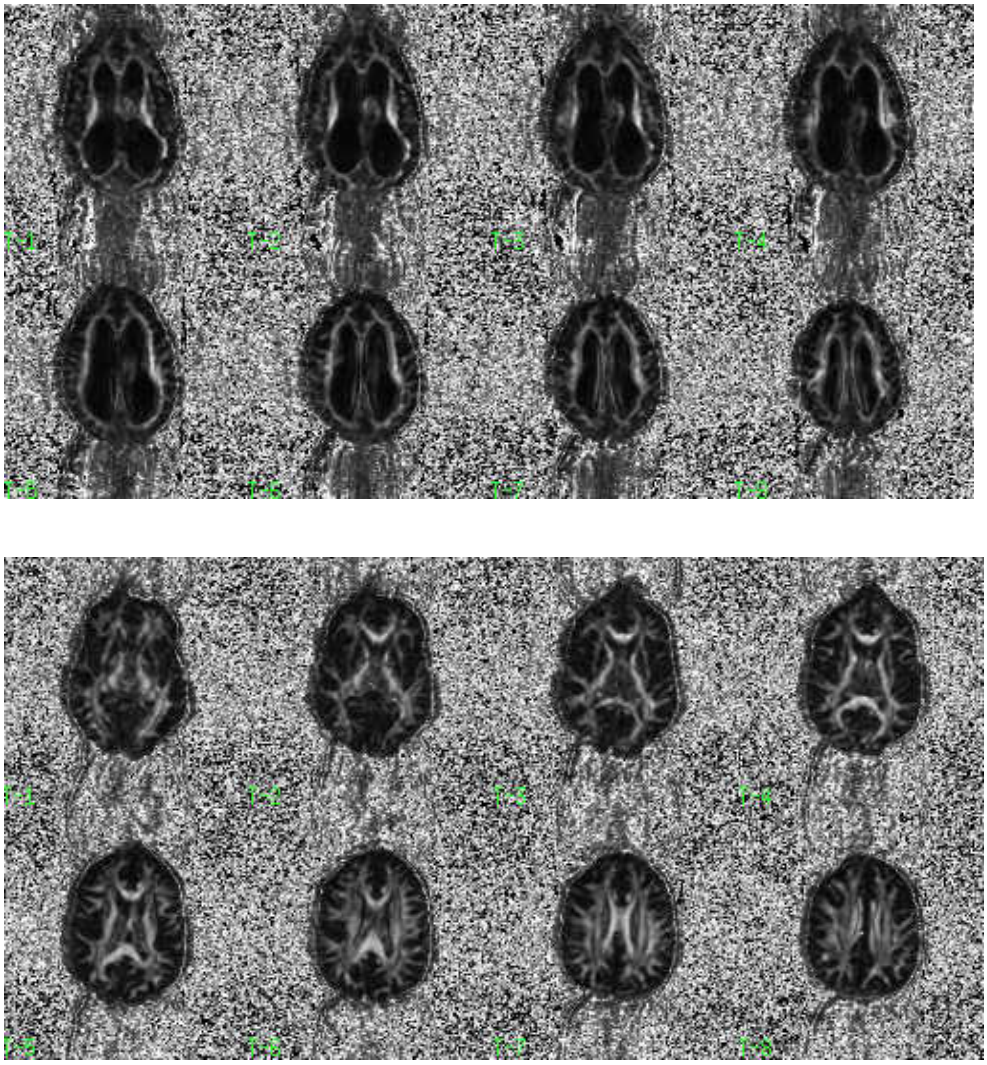

Figure 6.1b: Maps of regional anisotropy of an NPH patient (top) and a normal volunteer (bottom).

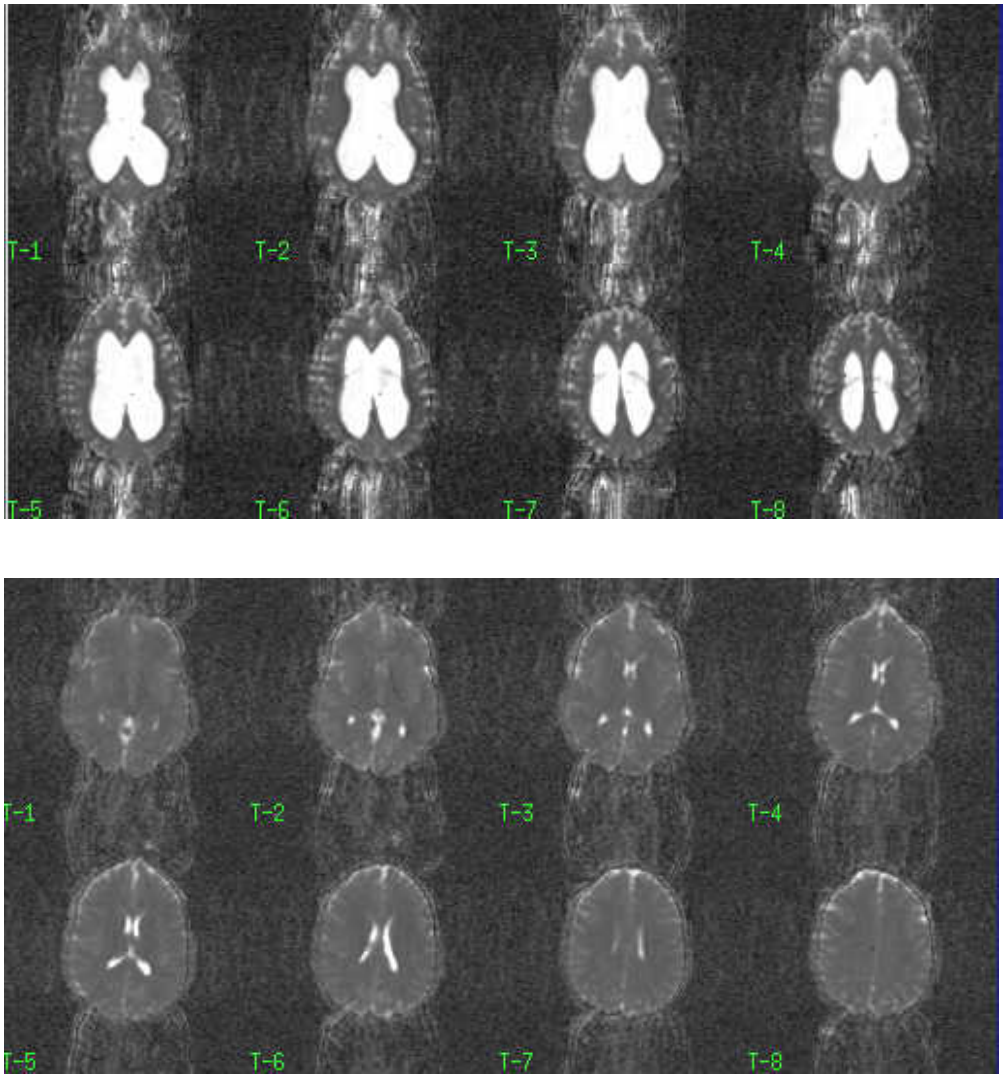

Figure 6.1c: Maps of trace of an NPH patient (top) and a normal volunteer (bottom).

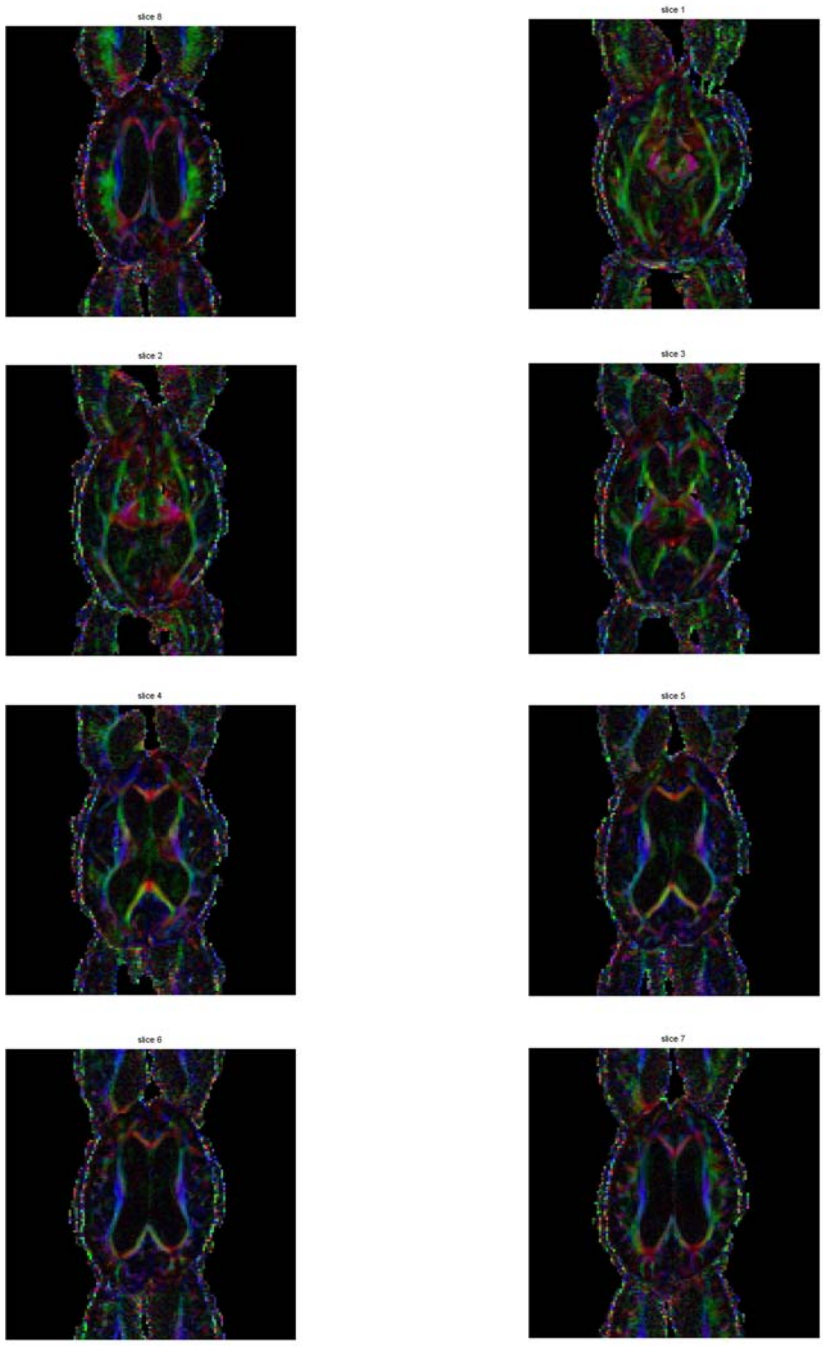

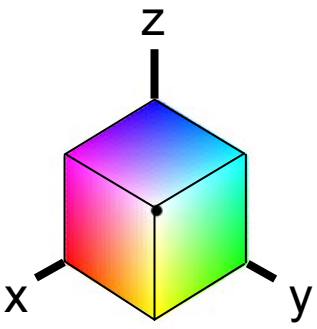

Figure 6.2a: Colour Maps NPH Patient.

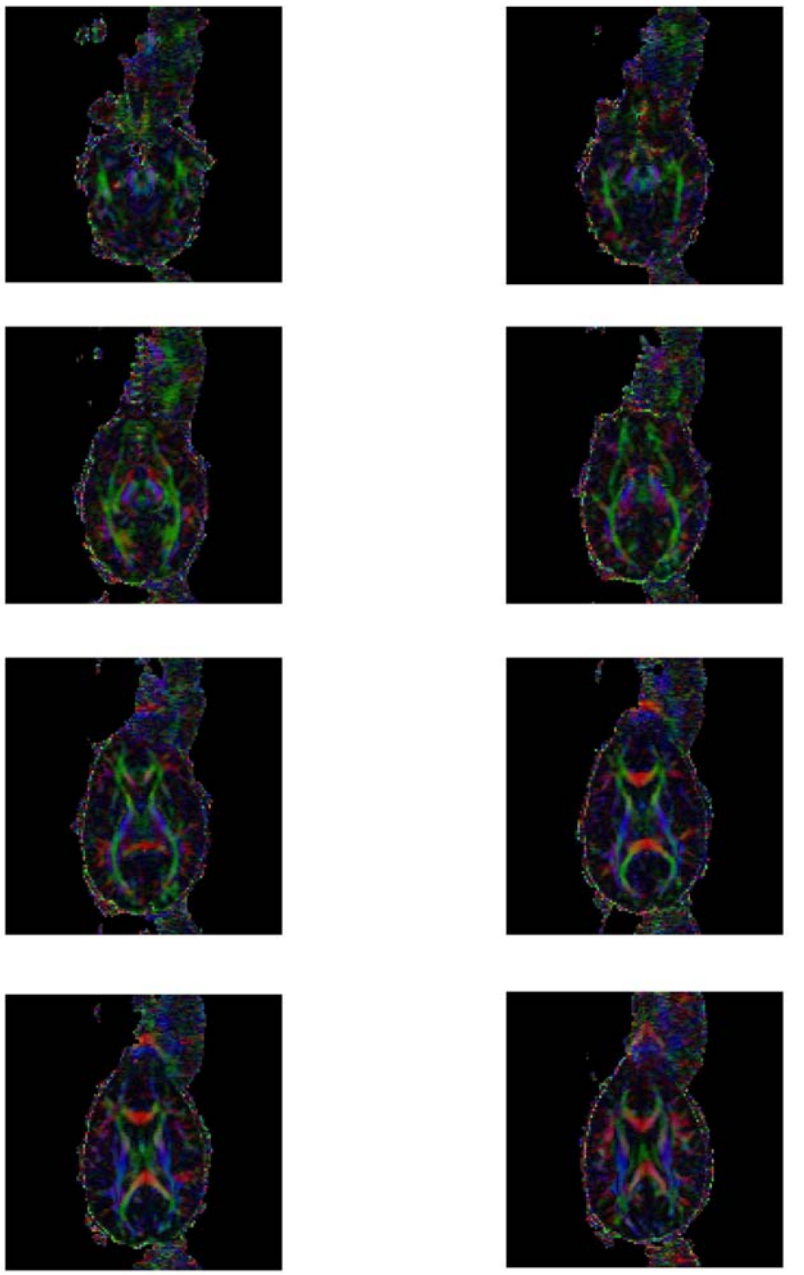

Figure 6.2b: Colour Maps Control.

Of the cerebral peduncle, internal capsule and corona radiata, the trace was significantly elevated in the internal capsule and corona radiata in patients with NPH. The FA and RA were also significantly higher in the corona radiata of NPH patients compared to controls but there were no differences in the other two regions.

There were no significant differences in trace, FA or RA for the frontal or occipital cortical/subcortical ROIs between controls and NPH patients. Trace was significantly increased and anisotropy (FA and RA) significantly decreased in the frontal deep white matter ROIs of NPH patients. Anisotropy was also significantly decreased in the occipital deep white matter ROIs of patients with NPH but trace was no different to the control group. The most striking differences were those noted in the frontal and occipital periventricular regions were the trace was significantly increased for both. Interestingly anisotropy was decreased significantly only in the occipital periventricular white matter of NPH patients. No significant difference between controls and NPH patients could be demonstrated for the frontal periventricular white matter anisotropy indices.

No significant difference in either trace or anisotropic indices was demonstrated for parietal cortex, temporo-parietal cortex, temporal white matter stem, temporo-parietal white matter or parietal white matter ROIs. There was a small but significant elevation in trace for the insular cortex but not the parieto-opercular white matter of NPH patients. There were no differences in either FA or RA.

In all regions of the corpus callosum examined the trace was significantly increased and both RA and FA were decreased. These regions exhibited the most striking differences of any region of the brain examined.

There were no significant differences in any of the invariants for the putamen. The trace was significantly increased in the caudate head but there were no significant differences observed for the anisotropic indices. Of the thalamic ROIs, the medial and lateral thalamic ROIs demonstrated significantly higher trace values for NPH patients compared to controls. No such difference was observed in the pulvinar and no significant difference was observed in either FA or RA in any of the thalamic ROIs.

There was no significant difference in the trace for the CSF of the lateral ventricles between the two groups. However a significant difference in both RA and FA was noted.

Trace							
	NPH	**Control**	**NPH**	**NPH**	**Control**	**Control**	
	n	n	Mean	SD	Mean	SD	P
Cerebral Peduncle	3	6	1.75	0.30	1.86	0.27	0.905
Internal Capsule	9	6	1.92	0.18	1.74	0.23	**0.036**
Corona Radiata	9	6	2.04	0.13	1.81	0.13	**0.008**
Frontal periventricular WM	9	6	2.89	0.58	2.08	0.39	**0.005**
Frontal WM	9	6	2.12	0.22	1.93	0.07	**0.050**
Frontal Cortex	9	6	2.45	0.28	2.33	0.10	0.529
Occipital periventricular WM	9	6	3.31	0.68	2.30	0.17	**0.000**
Occipital WM	9	6	2.09	0.19	1.99	0.06	0.388
Occipital Cortex	9	6	2.32	0.23	2.15	0.13	0.145
Temporal WM	4	4	1.94	0.33	1.89	0.20	0.486
Temporo-parietal WM	9	6	2.10	0.27	1.93	0.20	0.145
Temporo-parietal Cortex	9	6	2.27	0.39	2.20	0.18	0.689
Parietal WM	9	6	1.84	0.16	1.86	0.11	0.607
Parietal Cortex	9	6	2.09	0.14	2.22	0.18	0.145
Parieto-opercular WM	9	6	2.10	0.16	2.13	0.21	0.955
Insular Cortex	9	6	2.52	0.21	2.28	0.14	**0.036**
Corpus Callosum Genu	9	6	2.81	0.66	2.01	0.16	**0.003**
Corpus Callosum Anterolateral	9	6	2.84	0.48	1.94	0.33	**0.003**
Corpus Callosum Splenium	9	6	2.69	0.81	2.06	0.13	**0.036**
Corpus Callosum Posterolateral	9	6	2.73	0.73	2.03	0.08	**0.003**
Thalamus Posterior	8	6	2.48	0.33	2.11	0.22	0.081
Thalamus Medial	8	6	2.34	0.29	2.03	0.08	**0.043**
Thalamus Lateral	9	6	2.60	1.12	1.93	0.08	**0.018**
Putamen	8	6	2.49	0.52	2.05	0.11	0.108
Head of Caudate	9	6	2.51	0.36	2.12	0.14	**0.008**
CSF	9	6	8.81	1.10	8.27	1.73	0.529

Table 6.2.a: Trace values for NPH patients and controls.

FA							
	NPH	**Control**	**NPH**	**NPH**	**Control**	**Control**	
	n	n					P
Cerebral Peduncle	3	6	0.841	0.038	0.836	0.023	0.905
Internal Capsule	9	6	0.796	0.045	0.795	0.054	0.776
Corona Radiata	9	6	0.766	0.040	0.714	0.027	**0.018**
Frontal periventricular WM	9	6	0.312	0.093	0.370	0.063	0.145
Frontal WM	9	6	0.457	0.061	0.539	0.048	**0.036**
Frontal Cortex	9	6	0.262	0.030	0.260	0.035	0.529
Occipital periventricular WM	9	6	0.330	0.060	0.546	0.074	**0.000**
Occipital WM	9	6	0.508	0.058	0.577	0.047	**0.050**
Occipital Cortex	9	6	0.279	0.030	0.281	0.027	0.955
Temporal WM	4	4	0.495	0.081	0.523	0.075	0.886
Temporo-parietal WM	9	6	0.617	0.072	0.681	0.027	0.113
Temporo-parietal Cortex	9	6	0.254	0.041	0.230	0.033	0.328
Parietal WM	9	6	0.610	0.060	0.641	0.036	0.328
Parietal Cortex	9	6	0.290	0.045	0.270	0.035	0.388
Parieto-opercular WM	9	6	0.396	0.064	0.460	0.070	0.145
Insular Cortex	9	6	0.229	0.050	0.237	0.051	0.776
Corpus Callosum Genu	9	6	0.635	0.080	0.802	0.078	**0.003**
Corpus Callosum Anterolateral	9	6	0.590	0.080	0.824	0.064	**0.000**
Corpus Callosum Splenium	9	6	0.622	0.155	0.822	0.034	**0.012**
Corpus Callosum Posterolateral	9	6	0.642	0.104	0.803	0.092	**0.008**
Thalamus Posterior	8	6	0.343	0.078	0.307	0.020	0.345
Thalamus Medial	8	6	0.361	0.051	0.307	0.044	0.059
Thalamus Lateral	9	6	0.352	0.064	0.356	0.040	0.864
Putamen	8	6	0.242	0.069	0.203	0.033	0.414
Head of Caudate	9	6	0.218	0.055	0.190	0.031	0.388
CSF	9	6	0.104	0.016	0.211	0.026	**0.000**

Table 6.2.b: Fractional Anisotropy (FA) values for NPH patients and controls.

RA							
	NPH	**Control**	**NPH**	**NPH**	**Control**	**Control**	
	n	n	Mean	SD	Mean	SD	P
Cerebral Peduncle	3	6	0.471	0.038	0.476	0.028	1.000
Internal Capsule	9	6	0.441	0.050	0.440	0.063	0.724
Corona Radiata	9	6	0.412	0.036	0.362	0.022	**0.013**
Frontal periventricular WM	9	6	0.136	0.043	0.161	0.029	0.157
Frontal WM	9	6	0.205	0.033	0.250	0.029	**0.034**
Frontal Cortex	9	6	0.111	0.014	0.109	0.016	0.556
Occipital periventricular WM	9	6	0.144	0.028	0.255	0.043	**0.001**
Occipital WM	9	6	0.235	0.033	0.274	0.028	**0.045**
Occipital Cortex	9	6	0.115	0.017	0.119	0.012	0.724
Temporal WM	4	4	0.229	0.047	0.241	0.041	0.773
Temporo-parietal WM	9	6	0.299	0.047	0.341	0.020	0.068
Temporo-parietal Cortex	9	6	0.111	0.021	0.097	0.015	0.195
Parietal WM	9	6	0.299	0.041	0.317	0.024	0.517
Parietal Cortex	9	6	0.120	0.018	0.114	0.015	0.556
Parieto-opercular WM	9	6	0.175	0.032	0.208	0.036	0.112
Insular Cortex	9	6	0.100	0.027	0.100	0.022	0.953
Corpus Callosum Genu	9	6	0.324	0.057	0.450	0.077	**0.005**
Corpus Callosum Anterolateral	9	6	0.285	0.050	0.494	0.080	**0.001**
Corpus Callosum Splenium	9	6	0.321	0.128	0.470	0.033	**0.013**
Corpus Callosum Posterolateral	9	6	0.328	0.082	0.461	0.056	**0.007**
Thalamus Posterior	8	6	0.150	0.036	0.131	0.009	0.195
Thalamus Medial	8	6	0.156	0.024	0.131	0.020	0.053
Thalamus Lateral	9	6	0.152	0.030	0.154	0.019	1.000
Putamen	8	6	0.102	0.032	0.085	0.014	0.439
Head of Caudate	9	6	0.092	0.025	0.079	0.013	0.377
CSF	9	6	0.043	0.007	0.088	0.011	**0.001**

Table 6.2.c: Relative Anisotropy (RA) values for NPH patients and controls.

Figure 6.3a: Regional trace values for NPH patients (red) and controls (yellow)

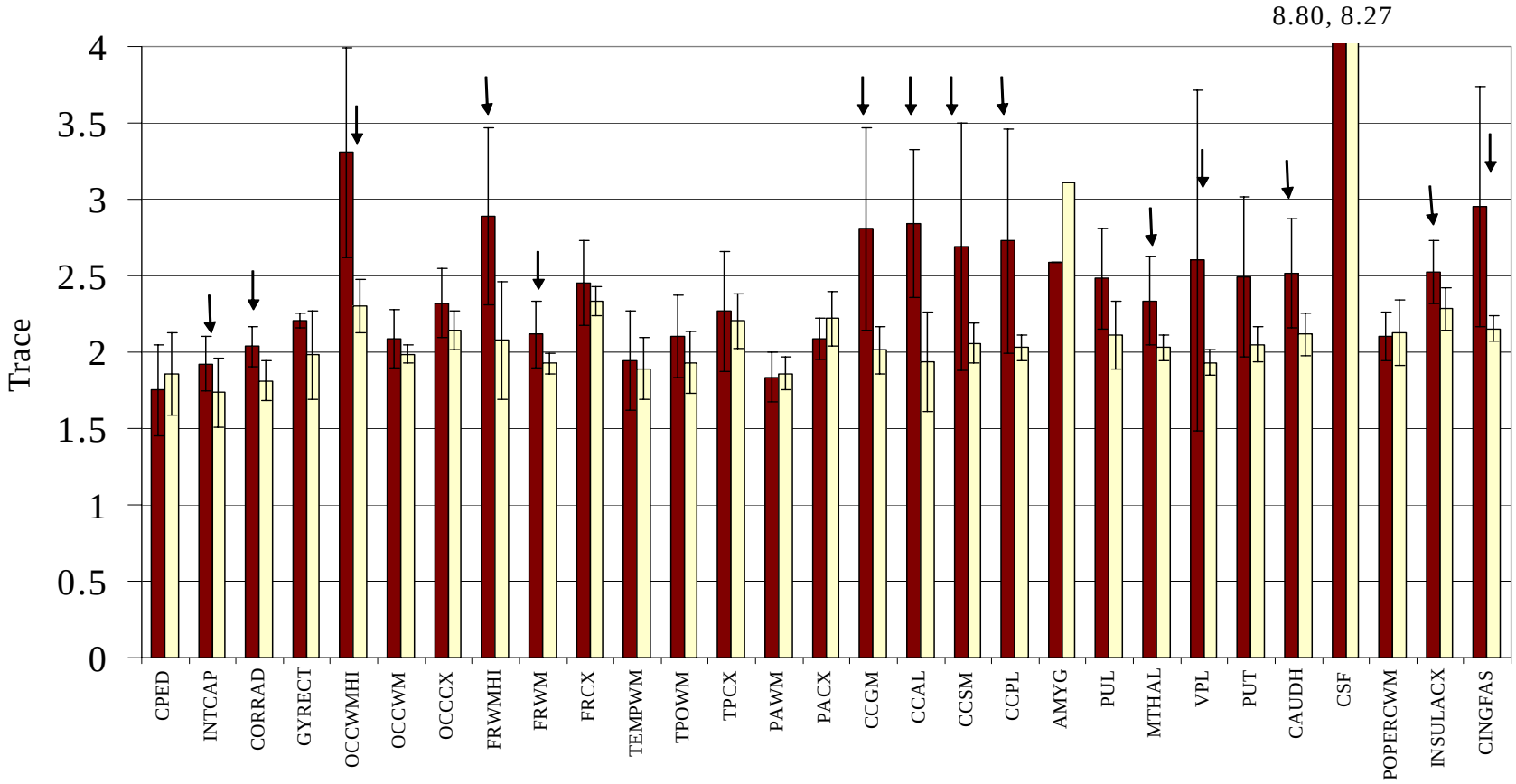

Abbreviations: CP =cerebral peduncle, IC=internal capsule, CR=corona radiata, FPWM=frontal periventricular white matter, FDWM=frontal deep white matter, FCx=front OPWM=occipital periventricular white matter, ODWM=occipital deep white matter, OCx=occipital cortex, TWM=temporal white matter, TPWM=temporoparietal whit TPCx=temporoparietal cortex, PWM=parietal white matter, PCx=parietal cortex, POWM=parieto-occipital white matter, InCx=Insular cortex, CCG=corpus callosum CCAL=corpus callosum anterolateral, CCS=corpus callosum splenium, CCPL=corpus callosum posterolateral, Thal P=thalamus pulvinar, Thal M= thalamus medial, Thal L= lateral, Put=Putamen, Caud-H=caudate - head, CSF=cerebrospinal fluid.

Figure 6.3b: Regional mean values of FA for NPH patients (red) and controls (yellow)

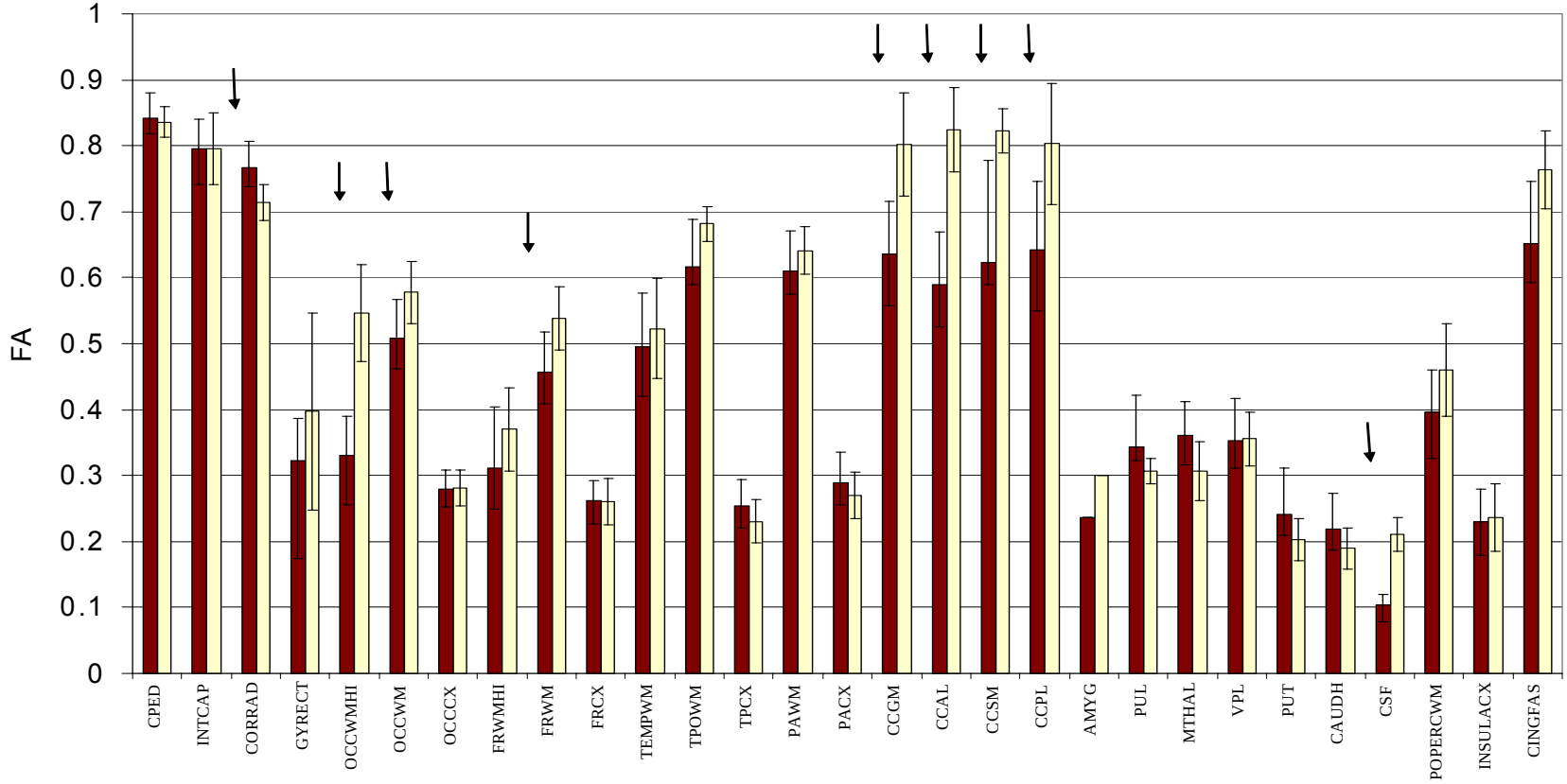

Abbreviations: CP =cerebral peduncle, IC=internal capsule, CR=corona radiata, FPWM=frontal periventricular white matter, FDWM=frontal deep white matter, FCx=front OPWM=occipital periventricular white matter, ODWM=occipital deep white matter, OCx=occipital cortex, TWM=temporal white matter, TPWM=temporoparietal whit TPCx=temporoparietal cortex, PWM=parietal white matter, PCx=parietal cortex, POWM=parieto-occipital white matter, InCx=Insular cortex, CCG=corpus callosum CCAL=corpus callosum anterolateral, CCS=corpus callosum splenium, CCPL=corpus callosum posterolateral, Thal P=thalamus pulvinar, Thal M= thalamus medial, Thal L= lateral, Put=Putamen, Caud-H=caudate - head, CSF=cerebrospinal fluid.

Figure 6.3c: Regional mean values of RA for NPH patients (red) and controls (yellow)

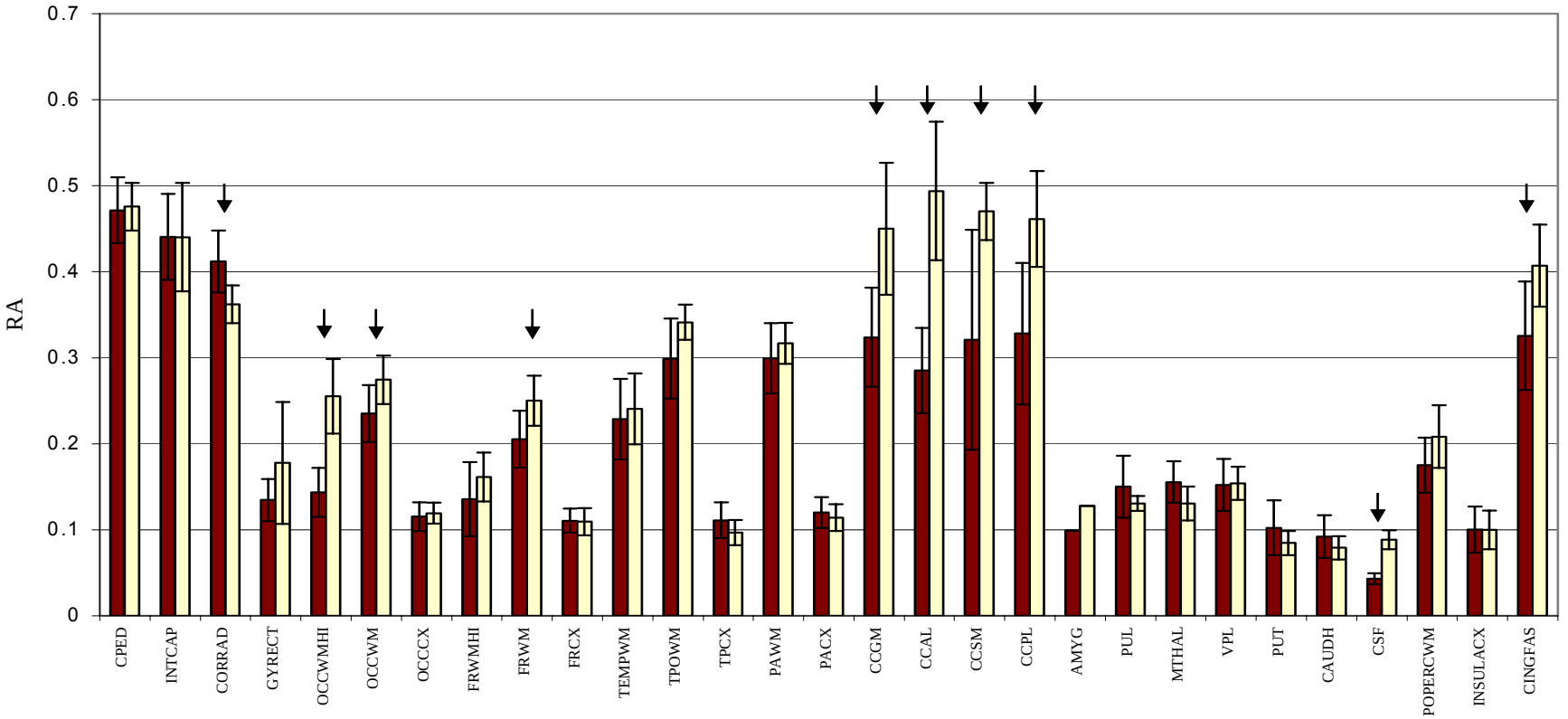

Abbreviations: CP =cerebral peduncle, IC=internal capsule, CR=corona radiata, FPWM=frontal periventricular white matter, FDWM=frontal deep white matter, FCx=front OPWM=occipital periventricular white matter, ODWM=occipital deep white matter, OCx=occipital cortex, TWM=temporal white matter, TPWM=temporoparietal whit TPCx=temporoparietal cortex, PWM=parietal white matter, PCx=parietal cortex, POWM=parieto-occipital white matter, InCx=Insular cortex, CCG=corpus callosum CCAL=corpus callosum anterolateral, CCS=corpus callosum splenium, CCPL=corpus callosum posterolateral, Thal P=thalamus pulvinar, Thal M= thalamus medial, Thal L= lateral, Put=Putamen, Caud-H=caudate - head, CSF=cerebrospinal fluid.

6.3.2 Global Analysis

The measured regional differences in trace and anisotropic indices are reflected in the global analysis of the distribution of these invariants. A histogram comparing the distribution of trace in NPH and control groups is shown in Figure 6.4 a. The control group exhibited a narrow range of distribution for the trace with the trace value of the vast majority of voxels falling within a narrow range. By comparison, the NPH patient group demonstrated a somewhat different distribution. The trace of the majority of voxels still fell within this range although the proportion was lower. The histogram of the NPH group had a longer tail at the upper end with a greater proportion of voxels falling into this upper end of the trace value range.

The histograms showing the distribution of the proportion of voxels with values of FA and RA are shown in Figures 6.4 b & c. The results for FA and RA were similar with the NPH group exhibiting an overall loss in the proportion of voxels with high anisotropic indices. There was a slightly higher proportion of voxels in the NPH group with very low anisotropic indices while the proportion of voxels with higher RA and FA was lower in the NPH group. Thus there appeared to be a shift in the distribution of voxels from higher to lower values in the NPH group compared to controls.

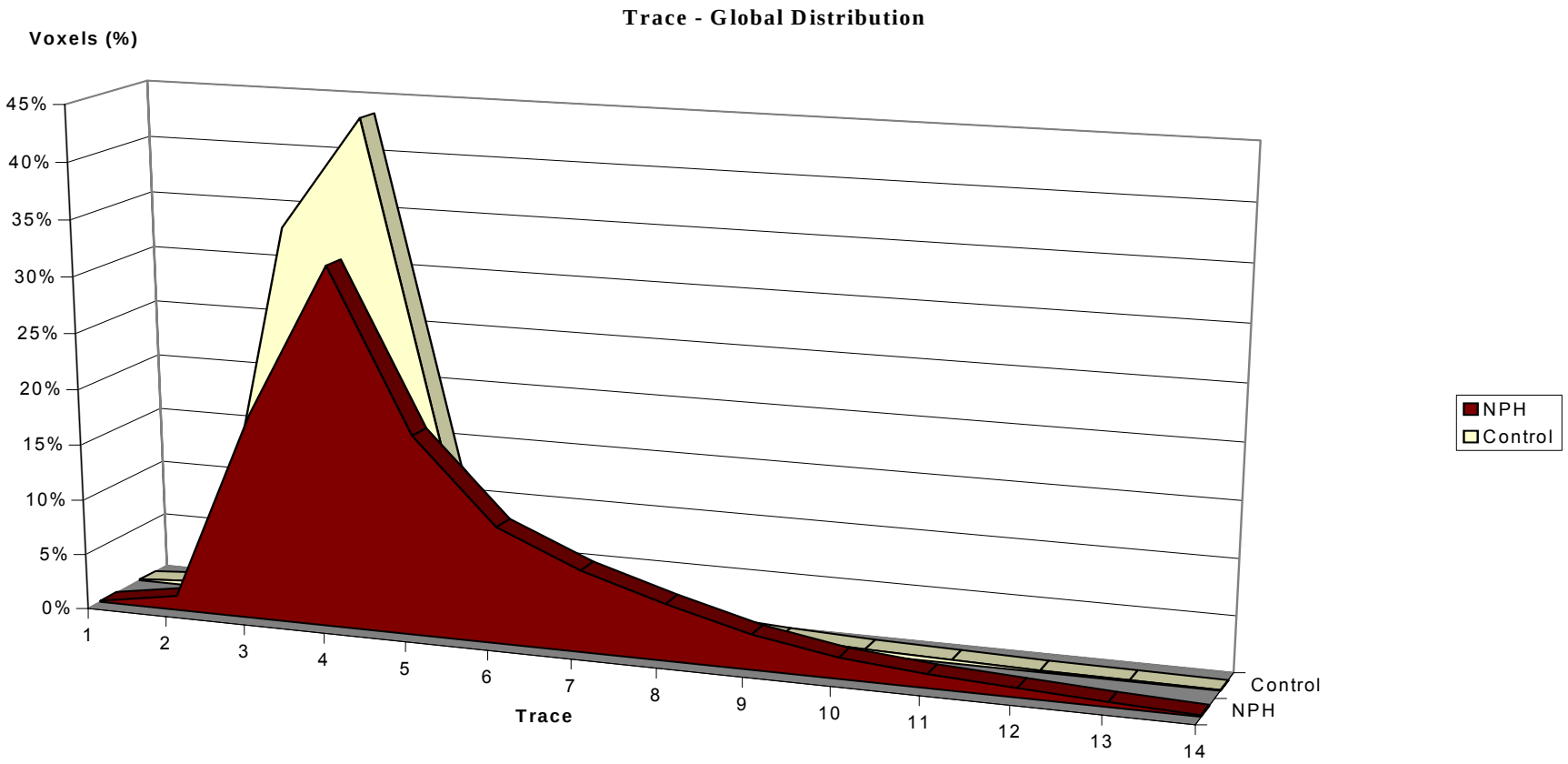

Figure 6.4a: Histogram showing the proportional distribution of voxels according to trace values

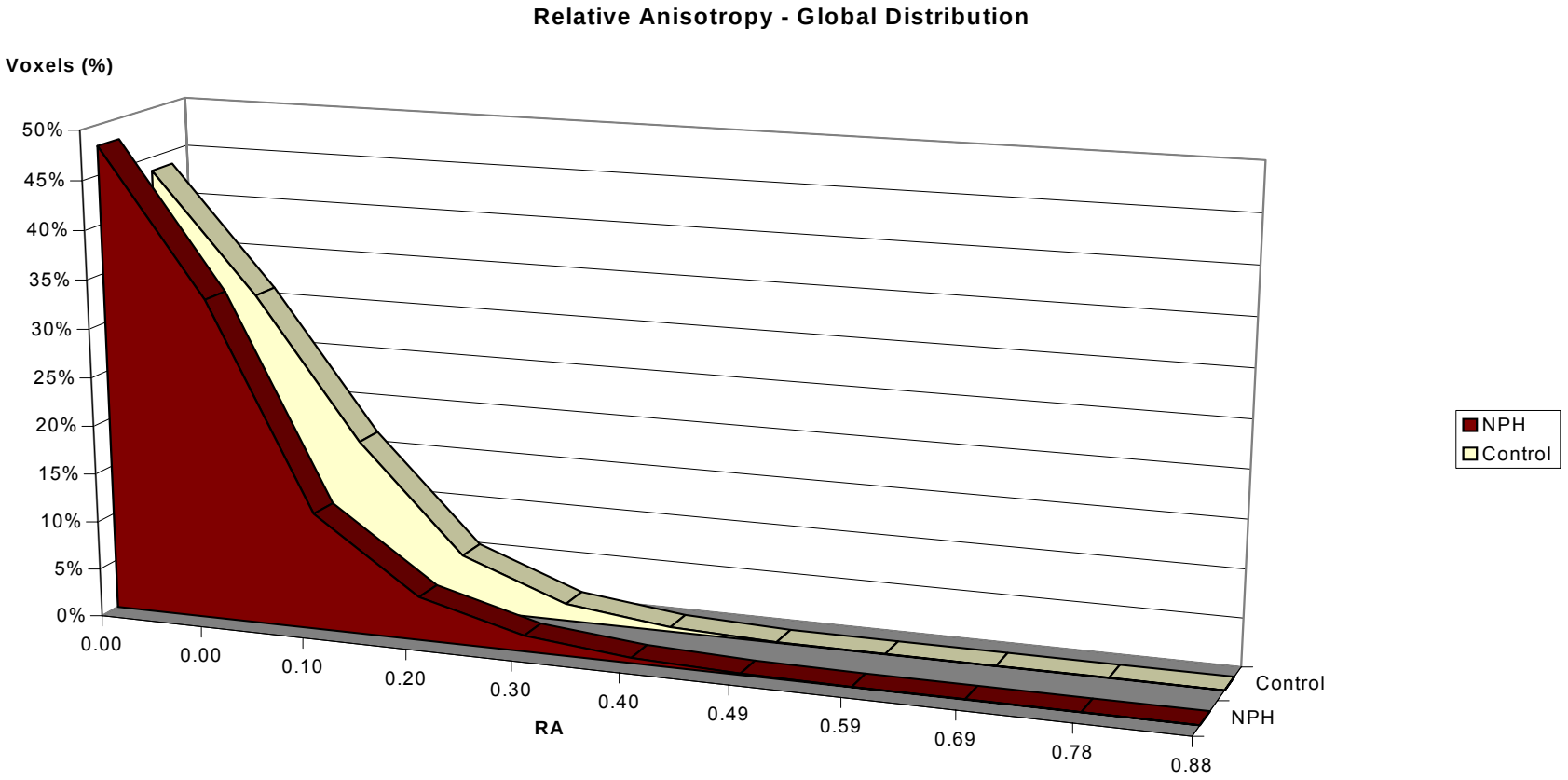

Figure 6.4b: Histogram showing the proportional distribution of voxels according to RA values

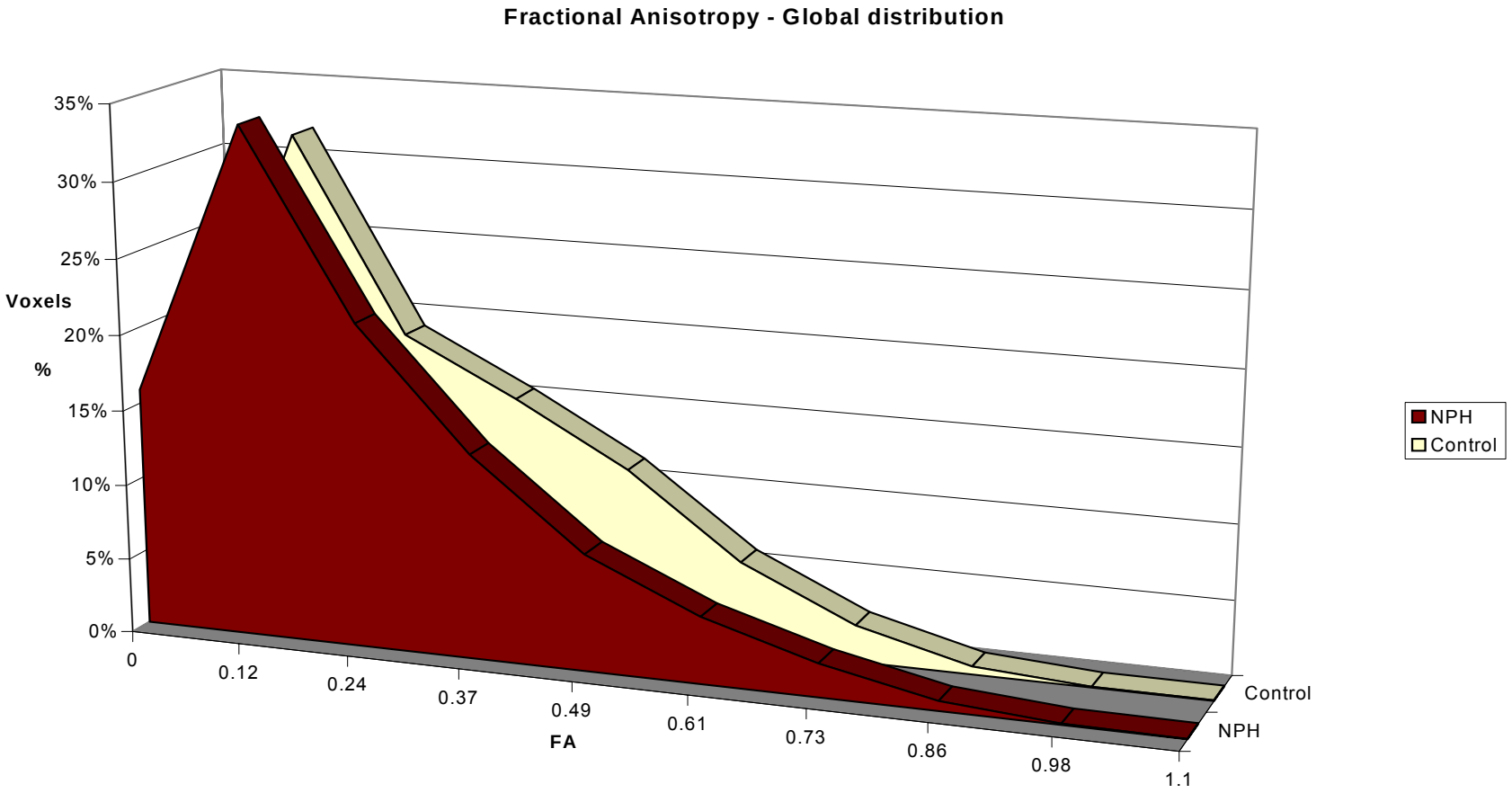

Figure 6.4c: Histogram showing the proportional distribution of voxels according to FA values

6.4 Discussion

This study is the first to apply to diffusion tensor MR imaging to the study of NPH. Significant changes in anisotropy and trace were recorded. Anisotropic diffusion in human white matter was first demonstrated by Chenevert (Chenevert *et al.*, 1990) and has been consistently confirmed since (Pierpaoli *et al.*, 1996; Shimony *et al.*, 1999). The exact source of anisotropy is still subject to debate however the myelin appears to contribute to anisotropy (Vorisek and Sykova, 1997) although it is not necessary (Beaulieu, 1994). Most information regarding changes in anisotropic diffusion has been generated from the stroke literature. Loss of white matter integrity is associated with loss of anisotropy. White matter anisotropy also falls early in cerebral ischaemia (Sorensen *et al.*, 1999a; Sorensen *et al.*, 1999b; Zelaya *et al.*, 1999) and persists as the lesion evolves. Similar findings have been demonstrated in white matter plaque associated with multiple sclerosis (Werring *et al.*, 1999; Bammer *et al.*, 2000). In our study there was loss of anisotropy in NPH patients in several white matter regions. This was most striking in the corpus callosum but also seen in the occipital and frontal white matter. This probably reflects demyelination or axonal loss. In terms of anisotropy, only one region demonstrated an increase – the corona radiata. This is suggestive of compression of white matter tracts coursing around the ventricles secondary to ventricular enlargement. By contrast the parietal and temporal white matter was relatively spared. As expected there were no increases in anisotropy in gray matter regions as these regions are normally mostly isotropic.

In health trace is relatively uniform throughout the brain, however increases in trace were found in a number of regions of NPH patients. While trace falls with acute ischemia (Moseley *et al.*, 1990), it is known to be increased in vasogenic oedema,

chronic ischemia and both acute (Werring *et al.*, 1999) and chronic (Bammer *et al.*, 2000) white matter plaques of multiple sclerosis. Regions that demonstrated an increase in trace were the periventricular regions with the most striking increases being in the frontal and occipital periventricular white matter. ROIs located more distant to the ventricles such as the cortical ROIs and putamen did not demonstrate significant increases in trace.

The histograms representing the distribution of the proportion of voxels as a function of trace and the anisotropic indices reflect the regional analysis. The increase in the proportion of voxels with increased trace is indicative of the increased trace in regions such as the frontal and occipital periventricular white matter and the corpus callosum. Likewise, the reduction in the proportion of voxels with high RA and FA and the corresponding increase in the proportion of voxels with low anisotropic indices, is likely to reflect the loss of anisotropy in white matter regions such as the corpus callosum, the frontal and occipital white matter.

Overall, the results suggest several pathophysiological processes. The increase in trace of the corona radiata is suggestive that there is compression of these white matter fibres as they course around the ventricles. There does not appear to be significant structural loss in these fibres tracts below the level of the body of the lateral ventricles as the internal capsule and cerebral peduncles do not demonstrate a decrease in anisotropy. By contrast, loss of anisotropy does appear to occur in the white matter regions in the frontal and occipital lobes as well as in the corpus callosum. This may represent loss of structure; however, the large increase in trace may also contribute to this decrease. The increase in trace in periventricular regions,

not only at the frontal and occipital horns, suggests that there is significant transependymal passage of CSF. This transependymal egress of CSF may contribute to the changes in CBF that have been observed in periventricular deep gray matter nuclei in previous chapters.

While there is still some debate on the source of the diffusion signal in diffusion tensor MR imaging and the relative contribution of certain structures to the anisotropic effects seen in diffusion tensor images, the correspondence between white matter integrity and anisotropy is not disputed. With this in consideration, the results are consistent with the results of studies of the histopathological findings in patients with NPH (Chapter 1). These demonstrate that the cortex is relatively spared in NPH and that most of the pathological changes are located in the periventricular and deep white matter regions. The most characteristic findings are those of demyelination, oedema and spongiosis. Axons may be decreased in number with some swelling and fragmentation whilst more peripheral arcuate fibres are often spared. In addition, microvascular disease of the deep and periventricular white matter as well as the deep gray nuclei is common in NPH.

The results are also consistent with imaging characteristics of NPH. Periventricular lucencies (PVLs) are often seen in the periventricular white matter of the frontal and occipital horns on CT scanning with corresponding hyperintensities on routine T2 MR imaging. These PVLs may be due to a number of processes. The most common is that of periventricular oedema and may be due to egress of CSF from the lateral ventricles into the parenchyma of these regions. However PVLs may represent areas of gliosis. The high trace values of frontal and occipital periventrcular white matter in NPH

patients may reflect either oedema or gliosis and do not appear to clarify this issue. A very interesting finding was the lack of a statistically significant reduction in either FA or RA in the frontal periventricular white matter despite the dramatic increase in trace.

There was clearly a significant difference in the age of the control and patient groups. The relationship between age and changes in DTI characteristics have been examined (Sullivan & Pfefferbaum, 2003). Fractional anisotropy does appear to decrease with age in some regions, particularly the genu of the corpus callosum (Sullivan *et al.*, 2000). Abe *et al.* (2002) found that FA was reduced only in this region. ADC and trace have been shown to increase by 3% per decade after 40 years of age in one study (Chen *et al.* 2002). However, when white matter and grey matter were analysed separately this increase was not apparent (Helenius *et al.* 2002). While the results of this study are influenced by factors associated with normal ageing the location and degree of the changes observed are distinct from those of ageing alone. Further study and comparison with age-matched controls will clarify the issue.

Other studies using diffusion weighted MR imaging of patients with Alzheimer's disease and of patients with vascular dementia have found that mean diffusion is increased and anisotropy reduced throughout the white matter (Hanyu *et al.*, 1998, 1999a &1999b) In addition it appears that the temporal white matter stem was preferentially effected in patients with Alzheimer's disease. The lack of difference between controls and patients with NPH in this study suggests that diffusion tensor MR imaging may be useful in the differential diagnosis of the conditions, a possibility worthy of further study.

Finally, a significantly higher value of anisotropy in the CSF of controls compared to NPH patients is an interesting finding. CSF obviously has no structure and should therefore have no anisotropy. The small anisotropic measurement in the CSF of patients with normal sized ventricles may be a reflection of CSF motion. Bulk coherent motion should not cause signal attenuation in diffusion tensor MR imaging. However incoherent second order motion due to arterial pulsation within the lateral ventricles may cause signal attenuation. If this is preferentially in one direction it may be reflected in the anisotropic indices and may account for the small amount of anisotropy of CSF measured in this study.

6.5 Conclusions

Diffusion tensor MR imaging is a non invasive method which is sensitive to pathological changes particularly those involving white matter. Such changes are demonstrable in the white matter of NPH patients using diffusion tensor MR imaging. Loss of white matter integrity in the corpus callosum as well as frontal and occipital white matter is reflected in by a significant reduction in both FA and RA. In addition the trace is increased in the frontal and occipital periventrcular white matter regions and is consistent with the oedema of periventricular lucencies. Further study of patients with NPH and correlation with shunt outcome is warranted. In addition, correlation of clinical changes after CSF shunting and diffusion tensor MR imaging post-CSF shunting may assist in clarifying pathological mechanisms of NPH.

Chapter Seven

General Discussion and Conclusions

7.1 Introduction

The aim of this thesis is to investigate the pathophysiology of NPH through the application of modern techniques that focus on the role of the brain parenchyma and its interaction with CSF dynamics. By increasing understanding of the pathophysiology of NPH, improvements in patient selection, treatment and outcome should be made.

In this chapter, the techniques applied in the previous studies and their development shall be considered. The results of the studies will then be summarized and a model of NPH will be formulated. The implications for patient management of the concepts developed will be assessed. Consideration will then be given to future studies.

7.2 Methodological Techniques and Developments

The techniques that form the core of this thesis are the computerised CSF infusion study, ^{15}O-labelled water PET for CBF measurement and diffusion tensor MR imaging.

The computerised CSF infusion study is a well-recognised technique for investigating CSF dynamics. In this thesis it was extended to gain information regarding some viscoelastic properties of the brain parenchyma by measuring the elastance co-efficient. It was also used to demonstrate the interaction of the brain parenchyma and

CSF dynamics through the time-constant tau. This is a novel extension of the technique that deserves further development.

CBF was measured in patients with NPH using ^{15}O-labelled water PET. While this in itself is not a substantial development, its the combination of accurate MR co-registration is, and has allowed a more robust assessment of regional CBF in NPH than previously.

This technology was combined with the computerised CSF infusion study allowing us to manipulate intracranial pressure (ICP) while simultaneously measuring CBF. By measuring mean arterial pressure and thus cerebral perfusion pressure, the technique allowed us to examine cerebral pressure autoregulation. Such a direct examination of pressure autoregulation has not been reported in humans.

Three-dimensional FE analysis simulation of stress distributions and brain displacement during CSF infusion, allowed us to validate the technique and correlate the results with the observed changes in CBF.

Diffusion tensor imaging (DTI) was used to enable an examination of changes in cerebral microstructure that occur in NPH. This technique at Addenbrooke's Hospital underwent substantial development for this project in terms of post-processing. This meant the creation of methods to calculate the components of the diffusion tensor and display the information which were developed in collaboration with other investigators.

7.3 Major findings

A short series of cases with what was termed ‘low-pressure hydrocephalus’ was presented. These patients initially failed to respond to CSF shunting but made dramatic improvement after a period of low or even sub-zero CSF pressure drainage. This study established the issues to be considered in the remainder of the thesis, that is, the role of the brain parenchyma and its interaction with CSF disturbances.

The clinical features, CSF infusion study results and outcome after CSF shunting of patients with NPH managed at Addenbrooke’s Hospital, Cambridge, UK were presented in chapter 3. The study confirmed the importance of R_{csf} in the management of NPH as this parameter correlated with clinical symptoms. However, the need to actually measure the parameters was demonstrated by the result that clinical features were not a predictor of R_{csf}. Patients with features typical of NPH, that is, prominent gait disturbance and absence of focal neurology, had a higher R_{csf} than those with atypical features. Moreover, those patients without a history of hypertension or cerebrovascular accident had a higher R_{csf} than those with a positive history for these factors. However the presence of these vasculopathies did not preclude response to CSF shunting.

CBF was found to be reduced for the whole cerebrum as well as in the cerebellum when compared to normal healthy volunteers. Regionally, CBF was not significantly reduced in the frontal, occipital, temporal or parietal white matter. In contrast, CBF was significantly reduced in the thalamus, head of caudate and putamen. In patients with only idiopathic NPH, low thalamic CBF correlated with a poor NPH score and a

low CBF in the putamen correlated with a poor level of function indicated by the Stein-Langfitt score.

With increases in CSF pressure most patients demonstrated reductions in both global and regional CBF. Those with high-normal R_{csf} had less pronounced changes in the CSF pressure and some of these patients exhibited no change in CBF or even a small increase. Overall, with increased CSF pressure, CBF was reduced significantly in the cerebrum, cerebellum, white matter regions as well as deep grey matter regions with the exception of the putamen. These results indicate that cerebral pressure autoregulation might be disturbed in patients with NPH. However, measurement of the MAP allowed CPP to be calculated. With this information, indices of static pressure autoregulation were examined. In most patients, but not all, pressure autoregulation at appeared intact, although the range in values was large. In terms of outcome after shunting, no statistical conclusions were reached. However, patients with both intact and disordered autoregulation, according to these parameters, responded to CSF shunting.

With DTI, it was demonstrated that NPH patients had a lower proportion of voxels with high FA and RA values. This indicates a reduction in the proportion of anisotropic regions. In contrast, the proportion of voxels with higher trace values was greater in patients with NPH.

Regionally, the most striking changes were seen in the corpus callosum where significant reductions in anisotropy were measured. In the frontal region, anisotropy was reduced in the white matter but not in the periventricular region. Anisotropy was

reduced in both of occipital white matter regions. No such changes were observed in the parietal or temporal white matter. In contrast, in corona radiata, there was an increase in the anisotropic indices.

Trace was increased in a number of regions. It was most markedly increased in the periventricular white matter surrounding the frontal and occipital horns. Other periventricular regions demonstrating an increase in trace were the corpus callosum. It was increased in deep gray matter nuclei adjacent to the ventricles such as the thalamus and head of caudate but not the putamen. Increased trace was also observed in the corona radiata and internal capsule. With the exception of the insular cortex, other cortical regions as well as the parietal and temporal regions showed no significant changes in trace.

Features predictive of a positive response to CSF shunting were not identified in the studies of this thesis. To some extent this is due to the fact that in several studies, the number of patients who actually underwent CSF shunting and who were available for follow-up was relatively small and did not allow for statistical comparisons to be made.

7.4 Synthesis of Results

In terms of CSF circulation, the extent to which it is disordered can be characterised by the measurement of R_{csf}. However as noted in chapter 3, the R_{csf} of an individual cannot be predicted by the clinical features. The corollary of this is that patients with very similar clinical features may have very different CSF circulation parameters. Furthermore, while R_{csf}, is predictive of shunt outcome, a lower value does not

necessarily preclude shunt response. These findings suggest that NPH cannot be considered as a CSF circulation disorder alone.

As noted in Chapter 2, some patients with CSF pressures below the normal range may demonstrate ventricular dilation. The finding that drainage of CSF at sub-zero pressures may result in normalization of ventricular size is suggestive that alterations in the viscoelastic properties of the brain parenchyma may initiate or, at least, maintain the hydrocephalic state.

The time-constant tau, which reflects the product of R_{csf} and cerebral compliance, was positively correlated with clinical parameters in 'typical' idiopathic NPH patients although R_{csf} and compliance alone were not. This illustrates the interaction between pathologies of brain parenchyma and CSF circulation. It is likely that patients with clinically typical idiopathic NPH consist of a spectrum of hydrocephalic patients in which patients have various combinations of CSF circulation disorders and parenchymal pathology. This would be consistent with the finding that patients with 'typical' idiopathic NPH without prominent vasculopathies have a higher mean R_{csf} than those that do have such vascular disease. The latter group may well consist of patients in which the parenchyma is the predominant factor in maintaining their hydrocephalus.

Alteration of the viscoelastic properties of the brain parenchyma may be caused by cerebrovascular disease. The finding that CBF was globally reduced in patients with NPH supports this hypothesis. The issue of cause or effect is commonly debated. The association with risk factors for cerebrovascular disease such as hypertension and

diabetes does suggest that cerebrovascular disease may be a primary phenomenon in NPH. This process may result in a softening of the parenchyma. However, there may be a vicious circle as ventricular dilation may actually increase the physical distortion of vessels in the periventricular region. Interestingly, the periventricular structures along the body the ventricle, that is, the head of caudate and thalamus, are the structures under most compressive stress during ventricular enlargement. It was these structures that demonstrated the most prominent reduction of regional CBF.

The finding that the thalamus and basal ganglia demonstrated particular reductions in CBF and that the reduction in thalamic CBF correlated with the clinical features suggests that these structures may have a role in the pathophysiology of the gait disorder of NPH. This is in contrast to current consensus that the gait is primarily frontal in origin. However, the role of the thalamus and basal ganglia in maintaining gait is well known. More importantly, the afferent and efferent connections of the basal ganglia or thalamus with the frontal cortex via frontostriatal projections may underlie the frontal nature of the deficits seen in patients with NPH.

Pressure autoregulation of CBF is important for protecting the brain against fluctuations in CPP. Although changes in CBF with changes in CSF pressure were observed in patients with NPH on a global and regional basis, analysis of static autoregulation using accepted indices demonstrated a wide range of autoregulatory capacity. While the majority were autoregulating according to these parameters, those patients who demonstrated poor pressure autoregulation might be more prone to develop parenchymal damage. In these patients, NPH might be more parenchymal in aetiology. However concepts of cerebral autoregulation are probably naïve as

demonstrated using a three-dimensional FE analysis model of stress distribution during changes in CSF pressure.

While the change from normal ventricular geometry to ventriculomegaly was not modelled in this thesis, previous studies of such changes have confirmed that these regions are those that undergo maximum pressure during ventricular dilation. (Péna *et al.*, 1999 & 2002a) It may be postulated that the clinical changes observed in NPH are a consequence of ventricular dilation and the effects of such changes on the basal ganglia and thalamus. Alternatively, vascular changes in these regions, supplied by lenticulostriate vessels, being particularly prone to hypertensive vascular changes, may institute an alteration in the viscoelastic properties of the brain with a subsequent reduction in its ability to resist the prevailing pressure of the CSF.

Finally, DTI revealed that globally there is a relative decrease in anisotropic regions within the brain. This probably reflects loss of microstructural integrity secondary to demyelination and axonal loss. However, the distribution of anisotropic changes is heterogeneous. While the corpus callosum and frontal and occipital white matter regions demonstrate loss of anisotropy, there was an increase in anisotropy in white matter regions lateral to the ventricles such as the corona radiata. This supports the role of compression in the regions lateral to the bodies of the lateral ventricles; a possible mechanism of gait disturbance (Yakovlev, 1947). Furthermore, the trace was increased in periventricular regions. This included the periventricular white matter surrounding the frontal and occipital horns as well as the deep gray matter nuclei; the thalamus and head of caudate. These results suggest that there is a significant transependymal seepage of CSF in patients with NPH. This may be aetiologically

related to the reduction in CBF observed in these structures in the CBF studies. Alternatively, the increase in trace may be due to microstructural changes as a result of cerebrovascular disease

7.5 Implications for Management of NPH

The implications of these results is that there may well be a population of idiopathic NPH patients with mild CSF circulation disturbance and a more pronounced alteration in the viscoelastic properties of the parenchyma. Between the two extremes may exist a spectrum of patients with varying components of parenchymal and CSF circulation pathology. Indeed, the only way in which the paradox of ventricular enlargement with normal CSF pressure, in the adult, can be resolved if is both the parenchyma and the CSF circulation are considered together.

Generally, the aim of CSF shunting in patients with NPH is to reduce the R_{csf} to a normal value. However, even a normal CSF pressure and R_{csf} may be too high for a brain in which the viscoelastic properties have been altered to render it more compliant than normal. In view of the results, hydrodynamically, the aim of CSF shunting should be to reduce CSF pressure and R_{csf} to values that are appropriate for the viscoelastic properties of the brain of that particular patient. Achievement of this aim should be reflected in the reduction of ventricular size and, hopefully, clinical improvement. This means that the valve characteristics of shunts should be tailored to the individual patient. Patients in whom R_{csf} is very high may benefit from a valve with a relatively normal resistance value. However, a patient with a marginally elevated R_{csf} but a significant parenchymal pathology may need a valve that will allow CSF pressure to reach very low levels.

Although elastance, compliance and pressure-volume indices of the brain may be estimated using the computerised CSF infusion studies and similar methods, further methods to examine the viscoelastic properties of the brain need to be established. It must be appreciated that NPH consists of a collection of patients with heterogeneous pathologies but a common characteristic clinical syndrome. In view of this, perhaps the quest for a predictive test in NPH is a naïve and characterization of all components of the disorder in an individual patient requires consideration.

7.6 Future Studies

The studies presented in this thesis have given origin to a number of further projects. CSF infusion studies are a routine part of clinical practice at both Addenbrooke's Hospital and Royal Prince Alfred Hospital. Further analysis of this data continues. Studies of changes in CBF with changes in CSF pressure on a voxel-by-voxel basis have begun. This is being combined with FE analysis in order to correlate the changes in CBF with various values of physical stress within these voxels. In order to perform this accurately a number of technical limitations have to be overcome. Solutions are currently being sought. Further development of the MR tractography using the DTI data is in progress.

In terms of outcome, the key in predicting the results of CSF shunting is in being able to define the brain parenchymal properties and in being able to differentiate between different pathologies. Studies aimed at answering issue need large numbers of well-defined patients. Development of DTI with increased numbers of patients will also be helpful, especially in relation to degrees of compression of structures such as the

corona radiata, as shown in this thesis. Further possibilities for examining the role of the parenchyma are being investigated and include the use of MR elastography.

Current approaches to predicting of CSF shunt response involve single parameters or 'tests'. More sophisticated approaches aimed at developing a better understanding of the pathophysiology of the condition overall and in individual patients are likely to be more successful. In addition, studies must give more emphasis to the valve type used in different patients when shunt response is being assessed.

7.7 Conclusions

In regard to pathophysiology, NPH is a clinical condition which consists of two inter-related components. It is a CSF circulation disorder but it is also a disorder of brain parenchyma. The properties of the brain parenchyma are altered in terms of its physical or viscoelastic properties. There is loss of microstructural integrity in some white matter regions and there is probably transependymal passage of CSF in periventricular regions. Ventricular enlargement compromises the corticospinal tracts. The brain parenchyma is also altered functionally as demonstrated by changes in CBF and, in some patients, loss of autoregulatory capacity. The ability of the brain to resist both physical stress and physiological stress are reduced. Refinement of the diagnosis and treatment of NPH depends on consideration of the pathophysiology of the CSF circulation and brain parenchyma as well as their interaction.

NPH remains important as a potentially reversible cause of dementia and gait disturbance, especially in the elderly. With an ageing population and increased recognition of the condition, it is likely to form an increasing proportion of

neurosurgical practice. The clinician's ability to manage patients with this condition is aided by the ability to investigate CSF dynamics using techniques such as CSF infusion studies. Improvements, knowledge of the condition and in the quality of care are most likely to come from the further investigation of the contribution of the parenchyma to the pathogenesis of NPH. Continued application and refinement of the techniques presented here, along with the development of new techniques is currently in progress in order address the issues raised in this thesis.

References

Abe O, Aoki S, Hayashi N, Yamada H, Kunimatsu A, Mori, H, Yoshikawa T, Okubo T, Ohtomo K. (2002) Normal aging in the central nervous system: quantitative MR diffusion-tensor analysis. *Neurobiol Aging.* 23(3) 433-441.

Adams RD (1966) Further observations on normal pressure hydrocephalus. *Proc R Soc Med* 59:1135-1140.

Adams RD (1975) Recent observations on normal pressure hydrocephalus. *Schweiz Arch Neurol Neurochir Psychiatr* 116:7-15.

Adams RD, Fisher CM, Hakim S, Ojemann RG, Sweet WH (1965) Symptomatic occult hydrocephalus with "normal" cerebrospinal fluid pressure. A treatable syndrome. *N Engl J Med* 273:117-126.

Akai K, Uchigasaki S, Tanaka U, Komatsu A (1987) Normal pressure hydrocephalus. Neuropathological study. *Acta Pathol Jpn* 37:97-110.

Albeck M, Skak C, Nielsen P, Olsen K, Borgesen S, Gjerris F (1998) Age-dependency of resistance to cerebrospinal fluid outflow. *J Neurosurg* 89:275-278.

Albeck MJ, Borgesen SE, Gjerris F, Schmidt JF, Sorensen PS (1991) Intracranial pressure and cerebrospinal fluid outflow conductance in healthy subjects. *J Neurosurg* 74:597-600.

Avezaat C, Eijndhoven J (1984) Cerebrospinal fluid pulse pressure and craniospinal dynamics. A theoretical, clinical and experimental study (thesis). The Hague.

Ball C, Sackett D, Phillips B, Haynes B, Straus S (1999) Levels of Evidence and Grades of Recommendations. In: NHS Research & Development: Centre for Evidence Based Medicine, Oxford UK.

Ball MJ (1976) Neurofibrillary tangles in the dementia of "normal pressure" hydrocephalus. *Can J Neurol Sci* 3:227-235.

Bammer R, Augustin M, Strasser-Fuchs S, Seifert T, Kapeller P, Stollberger R, Ebner F, Hartung HP, Fazekas F (2000) Magnetic resonance diffusion tensor imaging for characterizing diffuse and focal white matter abnormalities in multiple sclerosis. *Magn Reson Med* 44:583-591.

Bannister CM (1972) A report of eight patients with low pressure hydrocephalus treated by C.S.F. diversion with disappointing results. *Acta Neurochir (Wien)* 27:11-15.

Basser PJ (1995) Inferring microstructural features and the physiological state of tissues from diffusion-weighted images. *NMR Biomed* 8:333-344.

Behrman S, Cast I, O'Gorman P (1971) Two types of curves for transfer of RIHSA from cerebrospinal fluid to plasma in patients with normal pressure hydrocephalus. *J Neurosurg* 35:677-680.

Blomsterwall E, Bilting M, Stephensen H, Wikkelso C. (1995) Gait abnormality is not the only motor disturbance in normal pressure hydrocephalus. *Scand J Rehab Med* 24: 205-209.

Blomsterwall E, Svantesson U, Carlsson U, Tullberg M, Wikkelso C. (2000) Postural disturbance in patients with normal pressure hydrocephalus. *Acta Neurol Scand* 102:284-291.

Boon AJ, Tans JT, Delwel EJ, Egeler-Peerdeman SM, Hanlo PW, Wurzer HA, Avezaat CJ, de Jong DA, Gooskens RH, Hermans J (1997) Dutch normal-pressure hydrocephalus study: prediction of outcome after CSF shunting by resistance to outflow of cerebrospinal fluid. *J Neurosurg* 87:687-693.

Boon AJ, Tans JT, Delwel EJ, Egeler-Peerdeman SM, Hanlo PW, Wurzer HA, Avezaat CJ, de Jong DA, Gooskens RH, Hermans J (1998a) Dutch Normal-Pressure Hydrocephalus Study: randomized comparison of low- and medium-pressure shunts. *J Neurosurg* 88:490-495.

Boon AJ, Tans JT, Delwel EJ, Egeler-Peerdeman SM, Hanlo PW, Wurzer HA, Hermans J (1999) Dutch Normal-Pressure Hydrocephalus Study: the role of cerebrovascular disease. *J Neurosurg* 90:221-226.

Boon AJ, Tans JT, Delwel EJ, Egeler-Peerdeman SM, Hanlo PW, Wurzer HA, Hermans J (2000) The Dutch normal-pressure hydrocephalus study. How to select patients for CSF shunting? An analysis of four diagnostic criteria. *Surg Neurol* 53:201-207.

Boon AJ, Tans JT, Delwel EJ, Egeler-Peerdeman SM, Hanlo PW, Wurzer JA, Avezaat CJ, de Jong DA, Gooskens RH, Hermans J (1998b) Does CSF outflow resistance predict the response to CSF shunting in patients with normal pressure hydrocephalus? *Acta Neurochir Suppl (Wien)* 71:331-333.

Borgesen SE (1984) Conductance to outflow of CSF in normal pressure hydrocephalus. *Acta Neurochir (Wien)* 71:1-45.

Borgesen SE, Gjerris F (1982) The predictive value of conductance to outflow of CSF in normal pressure hydrocephalus. *Brain* 105:65-86.

Borgesen SE, Gjerris F, Sorensen SC (1979) Intracranial pressure and conductance to outflow of cerebrospinal fluid in normal-pressure hydrocephalus. *J Neurosurg* 50:489-493.

Bradley WG, Jr., Whittemore AR, Watanabe AS, Davis SJ, Teresi LM, Homyak M (1991) Association of deep white matter infarction with chronic communicating hydrocephalus: implications regarding the possible origin of

normal- pressure hydrocephalus [see comments]. *AJNR Am J Neuroradiol* 12:31-39.

Brooks DJ, Beaney RP, Powell M, Leenders KL, Crockard HA, Thomas DG, Marshall J, Jones T (1986) Studies on cerebral oxygen metabolism, blood flow, and blood volume, in patients with hydrocephalus before and after surgical decompression, using positron emission tomography. *Brain* 109:613-628.

Casmiro M, D'Alessandro R, Cacciatore FM, Daidone R, Calbucci F, Lugaresi E (1989) Risk factors for the syndrome of ventricular enlargement with gait apraxia (idiopathic normal pressure hydrocephalus): a case-control study. *J Neurol Neurosurg Psychiatry* 52:847-852.

Chang C, Kuwana N, Ito S, Ikegami T (2000) Impairment of cerebrovascular reactivity to acetazolamide in patients with normal pressure hydrocephalus. *Nucl Med Commun* 21:139-141.

Chen IH, Huang CI, Liu HC, Chen KK (1994) Effectiveness of CSF shunting in patients with normal pressure hydrocephalus predicted by temporary, controlled-resistance, continuous lumbar drainage: a pilot study. *J Neurol Neurosurg Psychiatry* 57:1430-1432.

Chen ZG, Li TQ, Hindmarsh T. (2002) Diffusion tensor trace mapping in normal adult brain using single-shot EPI technique: a methodological study of the aging brain. *Acta Radiol* 42: 447-458.

Chenevert TL, Brunberg JA, Pipe JG (1990) Anisotropic diffusion in human white matter: demonstration with MR techniques in vivo. *Radiology* 177:401-405.

Coles J, Minhas P, Fryer T, Smielewski P, Aigirhio F, Donovan T, Downey S, Williams G, Chatfield D, Matthews J, Gupta A, Carpenter T, Clark J, Pickard

J, Menon D (2002) Effect of hyperventilation on cerebral blood flow in traumatic head injury: clinical relevance and monitoring correlates. *Critical Care Medicine* 30:1950-1959.

Condon B, Patterson J, Wyper D, Hadley D, Grant R, Teasdale G, Rowan J (1986) Use of magnetic resonance imaging to measure intracranial cerebrospinal fluid volume. *Lancet* 1:1355-1357.

Corkill RG, Cadoux-Hudson TA (1999) Normal pressure hydrocephalus: developments in determining surgical prognosis. *Curr Opin Neurol* 12:671-677.

Crockard HA, Hanlon K, Duda EE, Mullan JF (1977) Hydrocephalus as a cause of dementia: evaluation by computerised tomography and intracranial pressure monitoring. *J Neurol Neurosurg Psychiatry* 40:736-740.

Czosnyka M, Batorski L, Laniewski P, Maksymowicz W, Koszewski W, Zaworski W (1990) A computer system for the identification of the cerebrospinal compensatory model. *Acta Neurochir (Wien)* 105:112-116.

Czosnyka M, Czosnyka Z, Whitfield P, Dovovan T, Pickard J (2001) Age dependence of cerebrospinal pressure-volume compensation in patients with hydrocephalus. *J Neurosurg* 94:482-486.

Czosnyka M, Whitehouse H, Smielewski P, Simac S, Pickard JD (1996) Testing of cerebrospinal compensatory reserve in shunted and non- shunted patients: a guide to interpretation based on an observational study. *J Neurol Neurosurg Psychiatry* 60:549-558.

Czosnyka Z, Czosnyka M, Copeman J, Smielewski P, Whitehouse H, Pickard JD (2000) Autoregulation in normal pressure hydrocephalus. In: ICP 2000 (Czosnyka M, ed). Cambridge, UK.

Czosnyka Z, Czosnyka M, Copeman J, Smielewski S, Piechnik S, Whitehouse H, Pickard JD (1999) Autoregulation of cerebral blood flow in patients with suspected normal pressure hydrocephalus. *J Cereb Blood Flow Metab* 19:S635.

de Leeuw F-E, de Groot J, E A, Oudkerk M, Ramos L, Heijboer R, Hofman A, Jolles J, van Gijn J, Breteler M (2001) Prevalence of cerebral white matter lesions in elderly people: a population based magnetic resonance imaging study. The Rotterdam Scan Study. *J Neurol Neurosurg Psychiatry* 70:9-14.

Deckel A, Weiner R, Szigeti D, V C, Vento J (2000) Altered patterns of regional cerebral blood flow in patients with Huntington's disease: a SPECT study during rest and cognitive or motor activation. *J Nucl Med* 41:773-780.

Del Bigio MR (1993) Neuropathological changes caused by hydrocephalus. *Acta Neuropathol (Berl)* 85:573-585.

Del Bigio MR, Bruni JE (1988) Changes in periventricular vasculature of rabbit brain following induction of hydrocephalus and after CSF shunting [published erratum appears in *J Neurosurg* 1988 Dec;69(6):963]. *J Neurosurg* 69:115-120.

Del Bigio MR, Cardoso ER, Halliday WC (1997) Neuropathological changes in chronic adult hydrocephalus: cortical biopsies and autopsy findings. *Can J Neurol Sci* 24:121-126.

DeLand FH, James AE, Jr., Ladd DJ, Konigsmark BW (1972) Normal pressure hydrocephalus: a histologic study. *Am J Clin Pathol* 58:58-63.

Di Chiro G (1973) Cisternography: from early tribulations to a useful diagnostic procedure. *Johns Hopkins Med J* 133:1-15.

Di Rocco C, Di Trapani G, Maira G, Bentivoglio M, Macchi G, Rossi GF (1977) Anatomo-clinical correlations in normotensive hydrocephalus. Reports on three cases. *J Neurol Sci* 33:437-452.

DiRocco C, McLone D, Shimoji T, Raimondi A (1975) Continuous intraventricular cerebrospinal fluid pressure recording in hydrocephalic children during wakefulness and sleep. *J Neurosurg* 42:683-689.

Drayer B, Rosenbaum A, Higman H (1977) Cerebrospinal fluid imaging using serial metrizamide CT cisternography. *Neuroradiol* 13:7-17.

Earnest MP, Fahn S, Karp JH, Rowland LP (1974) Normal pressure hydrocephalus and hypertensive cerebrovascular disease. *Arch Neurol* 31:262-266.

Ekstedt J (1978) CSF hydrodynamic studies in man. *J Neurol Neurosurg Psychiatry* 41:345-353.

Fisher CM (1978) Communicating hydrocephalus [letter]. *Lancet* 1:37.

Fisher CM (1980) Hydrocephalus in walking problems of the elderly. *Trans Am Neurol Assoc* 105:29-33.

Fisher CM (1982) Hydrocephalus as a cause of disturbances of gait in the elderly. *Neurology* 32:1358-1363.

Forslo H, Forssman B, Jarpe S, Radberg C (1972) Risa cisternography in possible hydrocephalus. Diagnostic and therapeutic experiences. *Acta Radiol [Diagn] (Stockh)* 13:531-545.

Frackowiak R, Pozzilli C, Legg N, du Boulay G, Marshall J, Lenzi G, Jones T (1981) Regional cerebral oxygen supply and utilisation in dementia: A clinical and physiological study with oxygen-15 and positron tomography. *Brain* 104:753-778.

Fried A, Shapiro K (1986) Subtle deterioration in shunted childhood hydrocephalus. A biomechanical and clinical profile. *J Neurosurg* 65:211-216.

Gado M, Coleman R, Lee K, Mikhael M, Alderson P, Archet C (1976) Correlation between computerized transaxial tomography and radionucleotide cisternography in dementia. *Neurology* 26:555-560.

Galvez S, Cartier L (1984) Computed tomography findings in 15 cases of Creutzfeldt-Jakob disease with histological verification. *J Neurol Neurosurg Psychiatry* 47:1244-1246.

Galvez S, Ferrer S, Cartier L, Palma A (1980) Subacute spongiform encephalopathy (Creutzfeldt-Jakob disease) associated with normal-pressure hydrocephalus Anatomoclinical report of one case. *Acta Neurochir (Wien)* 51:227-232.

Geschwind N (1968) The mechanism of normal pressure hydrocephalus. *J Neurol Sci* 7:481-493.

Gilles F, Davidson R (1971) Communicating hydrocephalus associated with deficient dysplastic parasagittal arachnoid granulations. *J Neurosurg* 35:421-426.

Gjerris F, Bech-Azeddine R (2001) Comment in: Hebb & Cusimano, Idiopathic Normal Pressure Hydrocephalus: a systematic review of diagnosis and outcome. *Neurosurgery* 49:1185-1186.

Gjerris F, Borgesen SE (1992) Current concepts of measurement of cerebrospinal fluid absorption and biomechanics of hydrocephalus. *Adv Tech Stand Neurosurg* 19:145-177.

Gjerris F, Borgesen SE, Sorensen PS, Boesen F, Schmidt K, Harmsen A, Lester J (1987) Resistance to cerebrospinal fluid outflow and intracranial pressure in patients with hydrocephalus after subarachnoid haemorrhage. *Acta Neurochir (Wien)* 88:79-86.

Gjerris F, Brogesen SE (1992) Pathophysiology of CSF circulation. In: Neurosurgery. The scientific basis of clinical practice. (Crockard A, Hayward A, Hoff JT, eds), pp 146-174. Oxford: Blackwell Scientific.

Godersky JC, Graff-Radford NR, Yuh WT (1990) Magnetic resonance imaging of patients with normal pressure hydrocephalus. *Adv Neurol* 52:554.

Golub G, Van Loan C (1996) Matrix Computations, 3rd Edition. Baltimore: The Johns Hopkins University Press.

Graff-Radford NR, Godersky JC (1986) Normal-pressure hydrocephalus. Onset of gait abnormality before dementia predicts good surgical outcome. *Arch Neurol* 43:940-942.

Graff-Radford NR, Godersky JC, Jones MP (1989) Variables predicting surgical outcome in symptomatic hydrocephalus in the elderly. *Neurology* 39:1601-1604.

Graff-Radford NR, Rezai K, Godersky JC, Eslinger P, Damasio H, Kirchner PT (1987) Regional cerebral blood flow in normal pressure hydrocephalus. *J Neurol Neurosurg Psychiatry* 50:1589-1596.

Granado JM, Diaz F, Alday R (1991) Evaluation of brain SPECT in the diagnosis and prognosis of the normal pressure hydrocephalus syndrome. *Acta Neurochir (Wien)* 112:88-91.

Greenberg JO, Shenkin HA, Adam R (1977) Idiopathic normal pressure hydrocephalus-- a report of 73 patients. *J Neurol Neurosurg Psychiatry* 40:336-341.

Greitz T (1969) Cerebral blood flow in occult hydrocephalus studied with angiography and the xenon 133 clearance method. *Acta Radiol [Diagn] (Stockh)* 8:376-384.

Greitz T, Grepe A (1971) Encephalography in the diagnosis of convexity block hydrocephalus. *Acta Radiologica (Diagnosis) (Stockhom)* 11:232-242.

Greitz TV, Grepe AO, Kalmer MS, Lopez J (1969) Pre- and postoperative evaluation of cerebral blood flow in low- pressure hydrocephalus. *J Neurosurg* 31:644-651.

Grubb RL, Jr., Raichle ME, Gado MH, Eichling JO, Hughes CP (1977) Cerebral blood flow, oxygen utilization, and blood volume in dementia. *Neurology* 27:905-910.

Gustafson L, Hagberg B (1978) Recovery of hydrocephalic dementia after shunt operation. *J Neurol Neurosurg Psychiatry* 41:940-947.

Gutierrez Y, Friede R, Kaliney W (1975) Agenesis of the arachnoid granulations and its relationship to communicating hydrocephalus. *J Neurosurg* 43:553-558.

Haidri NH, Modi SM (1977) Normal pressure hydrocephalus and hypertensive cerebrovascular disease. *Dis Nerv Syst* 38:918-921.

Hakim S (1971) Biomechanics of hydrocephalus. *Acta Neurol Latinoam* 1:169-194.

Hakim S, Adams RD (1965) The special clinical problem of symptomatic hydrocephalus with normal cerebrospinal fluid pressure. Observations in cerebrospinal fluid hydrodynamics. *J Neurol Sci* 2:307-327.

Hakim S, Venegas JG, Burton JD (1976) The physics of the cranial cavity, hydrocephalus and normal pressure hydrocephalus: mechanical interpretation and mathematical model. *Surg Neurol* 5:187-210.

Hanyu H, Asano T, Sakurai H, Imon Y, Iwamoto T, Takasaki M, Shindo H, Abe K (1999a) Diffusion-weighted and magnetization transfer imaging of the corpus callosum in Alzheimer's disease. *J Neurol Sci* 167:37-44.

Hanyu H, Imon Y, Sakurai H, Iwamoto T, Takasaki M, Shindo H, Kakizaki D, Abe K (1999b) Regional differences in diffusion abnormality in cerebral white matter lesions in patients with vascular dementia of the Binswanger type and Alzheimer's disease. *Eur J Neurol* 6:195-203.

Hanyu H, Sakurai H, Iwamoto T, Takasaki M, Shindo H, Abe K (1998) Diffusion-weighted MR imaging of the hippocampus and temporal white matter in Alzheimer's disease. *J Neurol Sci* 156:195-200.

Hartmann A, Alberti E (1977) Differentiation of communicating hydrocephalus and presenile dementia by continuous recording of cerebrospinal fluid pressure. *J Neurol Neurosurg Psychiatry* 40:630-640.

Hartmann A, Alberti E, Lange D (1977) Effects of CSF drainage on CBF and CBV in subarachnoid haemorrhage and communicating hydrocephalus. *Acta Neurol Scand* 56:336-337.

Hasselbalch S, Oberg G, Sorensen S, Andersen A, Waldemar G, Schmidt J, Fenger K (1992) Reduced regional cerebral blood flow in Huntington's disease studied by SPECT. *J Neurol Neurosurg Psychiatry* 55:1018-1023.

Hayashi M, Kobayashi H, Kawano H, Yamamoto S, Maeda T (1984) Cerebral blood flow and ICP patterns in patients with communicating hydrocephalus after aneurysm rupture. *J Neurosurg* 61:30-36.

Hayden P, Shurtleff D, Foltz E (1970) Ventricular fluid pressure recordingsin hydrocephalic patients. *Arch Neurol* 23:147-154.

Hebb A, Cusimano M (2001) Idiopathic normal pressure hydrocephalus: A systematic review of diagnosis and outcome. *Neurosurgery* 49:1166-1186.

Helenius J, Soinne L, Perkio J, Salonen O, Kangasmaki A, Kaste M, Carano RA, Aronen HJ, Tatlisumak T. (2002) Diffusion-weighted MR imaging in normal human brains in various age groups. *Am J Neuroradiol* 23: 194-199.

Hindmarsh T, Greitz T (1977) Hydrocephalus, atrophy and their differential diagnosis - CSF dynamics investigated by computer cisternography. In: Computerised axial tomography in clinical practice. (DuBoulay G, Moseley I, eds), pp 205-211. Berlin: Springer-Verlag.

Hochwald G, Lux W, Sahar A, Ransohoff J (1972) Experimental hydrocephalus. Changes in cerebrospinal fluid dynamics as a function of time. *Arch Neurol* 26:120-129.

Holodny AI, George AE, de Leon MJ, Golomb J, Kalnin AJ, Cooper PR (1998) Focal dilation and paradoxical collapse of cortical fissures and sulci in patients with normal-pressure hydrocephalus. *J Neurosurg* 89:742-747.

Iddon JL, Pickard JD, Cross JJ, Griffiths PD, Czosnyka M, Sahakian BJ (1999) Specific patterns of cognitive impairment in patients with idiopathic normal pressure hydrocephalus and Alzheimer's disease: a pilot study. *J Neurol Neurosurg Psychiatry* 67:723-732.

Illingworth RD, Logue V, Symon L, Uemura K (1971) The ventriculocaval shunt in the treatment of adult hydrocephalus. Results and complications in 101 patients. *J Neurosurg* 35:681-685.

James A, Strecker E, Sperber E, Flor W, Merz T, Burns B (1974a) An alternative pathway of cerebrospinal fluid absorption in communicating hydrocephalus. *Radiology* 111:143-146.

James AE, Jr., Sperber E, Strecker EP, Digel C, Novak G, Bush M (1974b) Use of serial cisternograms to document dynamic changes in the development of

communicating hydrocephalus: a clinical and experimental study. *Acta Neurol Scand* 50:153-170.

Kikuchi A, Takeda A, Kimpara T, Nakagawa M, Kawashima R, Sugiura M, al e (2001) Hypoperfusion in the supplementary motor area, dorsolateral prefrontal cortex and insular cortex in Parkinson's disease. *J Neurol Sci* 193:29-36.

Kimura M, Tanaka A, Yoshinaga S (1992) Significance of periventricular hemodynamics in normal pressure hydrocephalus. *Neurosurgery* 30:701-704; discussion 704-705.

Kinahan P, Rodgers J (1989) Analytic 3D image reconstruction using all detected events. *IEEE Transactions on Nuclear Science* 36:964-968.

Klinge P, Fischer J, Brinker T, Heissler HE, Burchert W, Berding G, Knapp WH, Samii M (1998) PET and CBF studies of chronic hydrocephalus: a contribution to surgical indication and prognosis. *J Neuroimaging* 8:205-209.

Klinge PM, Berding G, Brinker T, Knapp WH, Samii M (1999) A positron emission tomography study of cerebrovascular reserve before and after shunt surgery in patients with idiopathic chronic hydrocephalus. *J Neurosurg* 91:605-609.

Koto A, Rosenberg G, Zingesser LH, Horoupian D, Katzman R (1977) Syndrome of normal pressure hydrocephalus: possible relation to hypertensive and arteriosclerotic vasculopathy. *J Neurol Neurosurg Psychiatry* 40:73-79.

Krauss JK, Regel JP, Vach W, Droste DW, Borremans JJ, Mergner T (1996) Vascular risk factors and arteriosclerotic disease in idiopathic normal- pressure hydrocephalus of the elderly. *Stroke* 27:24-29.

Kristensen B, Malm J, Fagerland M, Hietala SO, Johansson B, Ekstedt J, Karlsson T (1996) Regional cerebral blood flow, white matter abnormalities, and

cerebrospinal fluid hydrodynamics in patients with idiopathic adult hydrocephalus syndrome. *J Neurol Neurosurg Psychiatry* 60:282-288.

Kushner M, Younkin D, Weinberger J, Hurtig H, Goldberg H, Reivich M (1984) Cerebral hemodynamics in the diagnosis of normal pressure hydrocephalus. *Neurology* 34:96-99.

Kyriacou SK, Mohamed A, Miller K, Neff S. (2002) Brain mechanisms for neurosurgery: modeling issues. *Biomech Model Mechanobiol*. 1(2): 151-64.

Larsson A, Bergh AC, Bilting M, Arlig A, Jacobsson L, Stephensen H, Wikkelso C. (1994) Regional cerebral blood flow in normal pressure hydrocephalus: diagnostic and prognostic aspects. *Eur J Nucl Med* 21:118-123.

Larsson A, Jensen C, Bilting M, Ekholm S, Stephensen H, Wikkelso C. (1992) Does the shunt opening pressure influence the effect of shunt surgery in normal pressure hydrocephalus? *Acta Neurochir* 117:15-22.

Larsson A, Wikkelso C, Bilting M, Stephensen H (1991) Clinical parameters in 74 consecutive patients shunt operated for normal pressure hydrocephalus. *Acta Neurol Scand* 84:475-482.

Lee EJ, Hung YC, Chang CH, Pai MC, Chen HH (1998) Cerebral blood flow velocity and vasomotor reactivity before and after CSF shunting surgery in patients with normal pressure hydrocephalus. *Acta Neurochir (Wien)* 140:599-604; discussion 604-595.

LeMay M, New PF (1970) Radiological diagnosis of occult normal-pressure hydrocephalus. *Radiology* 96:347-358.

Levine DN (2000) Ventricular size in pseudotumor cerebri and the theory of impaired CSF absorption. *J Neurol Sci* 177:85-94.

Lorenzo AV, Bresnan MJ, Barlow CF (1974) Cerebrospinal fluid absorption deficit in normal pressure hydrocephalus. *Arch Neurol* 30:387-393.

Lundar T, Nornes H (1990) Determination of ventricular fluid outflow resistance in patients with ventriculomegaly. *J Neurol Neurosurg Psychiatry* 53:896-898.

Lying-Tunell U, Lindblad BS, Malmlund HO, Persson B (1977) Cerebral blood flow and metabolic rate of oxygen, glucose, lactate, pyruvate, ketone bodies and amino acids in patients with normal pressure hydrocephalus before and after CSF shunting and in normal subjects. *Acta Neurol Scand Suppl* 64:338-339.

Lying-Tunell U, Lindblad BS, Malmlund HO, Persson B (1981) Cerebral blood flow and metabolic rate of oxygen, glucose, lactate, pyruvate, ketone bodies and amino acids. *Acta Neurol Scand* 63:337-350.

Maeder P, de Tribolet N (1995) Xenon CT measurement of cerebral blood flow in hydrocephalus. *Childs Nerv Syst* 11:388-391.

Mamo HL, Meric PC, Ponsin JC, Rey AC, Luft AG, Seylaz JA (1987) Cerebral blood flow in normal pressure hydrocephalus. *Stroke* 18:1074-1080.

Marmarou A, Shulman K, Rosende R (1978) A non-linear analysis of CSF system and intracranial pressure dynamics. *J Neurosurg* 48:332-344.

Mathew NT, Hartmann A, Meyer JS (1977) The use of regional cerebral blood flow measured with the gamma camera in neurological diagnosis. *Int J Neurol* 11:194-205.

Mathew NT, Meyer JS, Hartmann A, Ott EO (1975) Abnormal cerebrospinal fluid-blood flow dynamics. Implications in diagnosis, treatment, and prognosis in normal pressure hydrocephalus. *Arch Neurol* 32:657-664.

Matsuda M, Nakasu S, Nakazawa T, Handa J (1990) Cerebral hemodynamics in patients with normal pressure hydrocephalus: correlation between cerebral circulation time and dementia. *Surg Neurol* 34:396-401.

Matsuda M, Shino A, Kitano H, Inubushi T, Handa J (1999) Cerebral blood flow and N-acetylaspartate in patients with normal pressure hydrocephalus. *J Cereb Blood Flow Metab* 19:22.

Meixensberger J, Brawanski A, Ullrich OW, Gunreben G (1989) Cerebral blood flow in low pressure hydrocephalus. *Psychiatry Res* 29:307-308.

Meltzer C, Cantwell M, Greer P, Ben-Eliezer D, Smith G, Frank G, Kaye W, Houck P, Price J (2000) Does cerebral blood flow decline in healthy aging? A PET study with partial-volume correction. *J Nucl Med* 41:1842-1848.

Meyer JS, Kitagawa Y, Tanahashi N, Tachibana H, Kandula P, Cech DA, Clifton GL, Rose JE (1985a) Evaluation of treatment of normal-pressure hydrocephalus. *J Neurosurg* 62:513-521.

Meyer JS, Kitagawa Y, Tanahashi N, Tachibana H, Kandula P, Cech DA, Rose JE, Grossman RG (1985b) Pathogenesis of normal-pressure hydrocephalus--preliminary observations. *Surg Neurol* 23:121-133.

Meyer JS, Tachibana H, Hardenberg JP, Dowell RE, Jr., Kitagawa Y, Mortel KF (1984) Normal pressure hydrocephalus. Influences on cerebral hemodynamic and cerebrospinal fluid pressure--chemical autoregulation. *Surg Neurol* 21:195-203.

Miga MI, Paulsen KD, Hoopes PJ, Kennedy FE, Hartov A, Roberts DW. (2000). In vivo modeling of interstitial pressure in the brain under surgical load using finite elements. *J Biomech Eng* 122(4): 354-63.

Moretti JL, Sergent A, Louarn F, Rancurel G, le Percq M, Flavigny R, Degos JD, Caron JP, le Poncin Lafitte M, Bardy A, *et al.* (1988) Cortical perfusion assessment with 123I-isopropyl amphetamine (123I- IAMP) in normal pressure hydrocephalus (NPH). *Eur J Nucl Med* 14:73-79.

Moseley ME, Cohen Y, Mintorovitch J, Chileuitt L, Shimizu H, Kucharczyk J, Wendland MF, Weinstein PR (1990) Early detection of regional cerebral ischemia in cats: comparison of diffusion- and T2-weighted MRI and spectroscopy. *Magn Reson Med* 14:330-346.

Nakano H, Bandoh K, Miyaoka M, Sato K (1996) Evaluation of hydrocephalic periventricular radiolucency by dynamic computed tomography and xenon-computed tomography. *Neurosurgery* 39:758-762; discussion 762-753.

Newton H, Pickard JD, Weller RO (1989) Normal pressure hydrocephalus and cerebrovascular disease: findings of postmortem [letter]. *J Neurol Neurosurg Psychiatry* 52:804.

Ojemann RG, Fisher CM, Adams RD, Sweet WH, New PF (1969) Further experience with the syndrome of "normal" pressure hydrocephalus. *J Neurosurg* 31:279-294.

Ostertag CB, Mundinger F (1978) Diagnosis of normal-pressure hydrocephalus using CT with CSF enhancement. *Neuroradiol* 16:216-219.

Owen A, Doyon J, Dagher A, Sadikot A, Evans A (1998) Abnormal basal ganglia outflow in Parkinson's disease identified with PET. Implications for higher cortical functions. *Brain* 121:949-965.

Owler B, Jacobson E, Johnston I (2001) Low Pressure Hydrocephalus Syndrome. Report of 5 cases. *Br J Neurosurg* 14:353-359.

Owler B, Pickard J (2001) Normal pressure hydrocephalus and cerebral blood flow: a review. *Acta Neurol Scand* 104:325-342.

Panerai RB (1998) Assessment of cerebral pressure autoregulation in humans--a review of measurement methods. *Physiol Meas* 19:305-338.

Pang D, Altschuler E (1994) Low-pressure hydrocephalic state and viscoelastic alterations in the brain. *Neurosurgery* 35:643-655; discussion 655-646.

Péna A, Bolton M, Whitehouse H, Pickard J (1999) Effects of brain ventricular shape on periventricular biomechanics: a finite-element analysis. *Neurosurgery* 45:107-118.

Péna A, Harris N, Bolton M, Czosnyka M, Pickard J (2002a) Communicating hydrocephalus: the biomechanics of progressive ventricular enlargement revisited. *Acta Neurochir Suppl*. 81:59-63.

Péna, A., Owler B.K,. Fryer, T.D., Minhas, P., Czosnyka, M., Crawford, P.J., Pickard, J.D. (2002b) A case study of hemispatial neglect using finite element analysis and positron emission tomography. *J Neuroimag*. 12(4):360-7.

Penar PL, Lakin WD, Yu J (1995) Normal pressure hydrocephalus: an analysis of aetiology and response to CSF shunting based on mathematical modelling. *Neurol Res* 17:83-88.

Penfield W, Elvidge A (1932) Hydrocephalus and the atrophy of cerebral compression. In: Cytology and cellular pathology of the nervous system. (Penfield W, ed), pp 1201-1217. New York: P. S. Hoebner.

Pickard JD, Teasdale G, Matherson M, al e (1980) Intraventricular pressure waves - the best predictive test for CSF shunting in normal pressure hydrocephalus. In: Intracranial Pressure IV (Shulman K, Marmarou A, Miller JD, Becker DP, Hochwold GM, Brock M, eds), pp 498-500. Berlin: Springer-Verlag.

Pierpaoli C, Jezzard P, Basser PJ, Barnett A, Di Chiro G (1996) Diffusion tensor MR imaging of the human brain. *Radiology* 201:637-648.

Poca MA, Mataro M, Sahuquillo J, Catalan R, Ibanez J, Galard R (2001) Shunt related changes in somatostatin, neuropeptide Y, and corticotropin releasing factor concentrations in patients with normal pressure hydrocephalus. *J Neurol Neurosurg Psychiatry* 70:298-304.

Raabe A, Czosnyka M, Piper I, Seifert V (1999) Monitoring of intracranial compliance: correction for a change in body position. *Acta Neurochir (Wien)* 141:31-36; discussion 35-36.

Raftopoulos C, Deleval J, Chaskis C, Leonard A, Cantraine F, Desmyttere F, Clarysse S, Brotchi J (1994) Cognitive recovery in idiopathic normal pressure hydrocephalus: a prospective study. *Neurosurgery* 35:397-404; discussion 404-395.

Reilly, P. (2001) In normal pressure hydrocephalus, intracranial pressure monitoring is the only useful test. *J Clin Neurosci* 8:66-67.

Reynolds NJ, Hellman R, Tikofsky R, Prost R, Mark L, Elejalde B. (2002) Single photon emission computerized tomography (SPECT) in detecting neurodegeneration in Huntington's disease. *Nucl Med Commun* 23:13-18.

Russell DS (1949) Observations on the pathology of hydrocephalus. *Medical Research Council (GB): Special Report* 265:1-138.

Salmon JH, Timperman AL (1971a) Cerebral blood flow in posttraumatic encephalopathy. The effect of ventriculoatrial shunt. *Neurology* 21:33-42.

Salmon JH, Timperman AL (1971b) Effect of intracranial hypotension on cerebral blood flow. *J Neurol Neurosurg Psychiatry* 34:687-692.

Schmidt JF, Albeck M, Gjerris F (1990a) The effect of nimodipine on ICP and CBF in patients with normal- pressure hydrocephalus. *Acta Neurochir (Wien)* 102:11-13.

Schmidt JF, Andersen AR, Paulson OB, Gjerris F (1990b) Angiotensin converting enzyme inhibition, CBF autoregulation, and ICP in patients with normal-pressure hydrocephalus. *Acta Neurochir (Wien)* 106:9-12.

Shenkin HA, Greenberg J, Bouzarth WF, Gutterman P, Morales JO (1973) Ventricular CSF shunting for relief of senile symptoms. *JAMA* 225:1486-1489.

Shenkin HA, Greenberg JO, Grossman CB (1975) Ventricular size after CSF shunting for idiopathic normal pressure hydrocephalus. *J Neurol Neurosurg Psychiatry* 38:833-837.

Shih WJ, Tasdemiroglu E (1995) Reversible hypoperfusion of the cerebral cortex in normal-pressure hydrocephalus on technetium-99m-HMPAO brain SPECT images after shunt operation. *J Nucl Med* 36:470-473.

Shimoda M, Oda S, Shibata M, Masuko A, Sato O (1994) Change in regional cerebral blood flow following glycerol administration predicts clinical result from CSF shunting in normal pressure hydrocephalus. *Acta Neurochir (Wien)* 129:171-176.

Shimony JS, McKinstry RC, Akbudak E, Aronovitz JA, Snyder AZ, Lori NF, Cull TS, Conturo TE (1999) Quantitative diffusion-tensor anisotropy brain MR imaging: normative human data and anatomic analysis. *Radiology* 212:770-784.

Shukla D, Singh BM, Strobos RJ (1980) Hypertensive cerebrovascular disease and normal pressure hydrocephalus. *Neurology* 30:998-1000.

Sorensen AG, Copen WA, Ostergaard L, Buonanno FS, Gonzalez RG, Rordorf G, Rosen BR, Schwamm LH, Weisskoff RM, Koroshetz WJ (1999a) Hyperacute stroke: simultaneous measurement of relative cerebral blood volume, relative cerebral blood flow, and mean tissue transit time. *Radiology* 210:519-527.

Sorensen AG, Wu O, Copen WA, Davis TL, Gonzalez RG, Koroshetz WJ, Reese TG, Rosen BR, Wedeen VJ, Weisskoff RM (1999b) Human acute cerebral ischemia: detection of changes in water diffusion anisotropy by using MR imaging. *Radiology* 212:785-792.Stein SC, Langfitt TW (1974) Normal-pressure hydrocephalus. Predicting the results of cerebrospinal fluid CSF shunting. *J Neurosurg* 41:463-470.

Steinbok P, Thompson G (1976) Complications of ventriculo-vascular shunts: Computer analysis of aetiological factors. *Surgical Neurology* 5:31-35.

Stejskal E, Tanner J (1965) Spin diffusion measurements: spin echoes in the presence of a time dependent field gradient. *J Chem Phys* 42:288-292.

Stephensen H, Tisell M, Wikkelso C. (2002) There is no transmantle pressure gradient in communicating or noncommunicating hydrocephalus. *Neurosurgery* 50: 763-771.

Stolze H, Kuhtz-Buschbeck JP, Drucke H, Johnk K, Diercks C, Palmie S, Mehdorn HM, Illert M, Deuschl G (2000) Gait analysis in idiopathic normal pressure hydrocephalus--which parameters respond to the CSF tap test? *Clin Neurophysiol* 111:1678-1686.

Stolze H, Kuhtz-Buschbeck JP, Drucke H, Johnk K, Illert M, Deuschl G (2001a) Comparative analysis of the gait disorder of normal pressure hydrocephalus and Parkinson's disease. *J Neurol Neurosurg Psychiatry* 70:289-297.

Stolze H, Kuhtz-Buschbeck JP, Drucke H, Johnk K, Illert M, Deuschl G (2001b) Comparative analysis of the gait disorder of normal pressure hydrocephalus and Parkinson's disease. *J Neurol Neurosurg Psychiatry* 70:289-297.

Stump D, Sires B, Toole J, McHenry LJ, McWorter J (1983) Regional cerebral blood flow, auto-regulations and normal pressure hydrocephalus. *Neurology* 33:182.

Sullivan EV, Adalsteinsson E, Hedehus M, Ju C, Moseley M, Lim KO, Pfefferbaum A. (2002) Equivalent disruption of regional white matter microstructure in ageing healthy men and women. *Neuroreport.* 12(1): 99-104.

Sullivan EV, Pfefferbaum A. (2003) Diffusion tensor imaging in normal aging and neuropsychiatric disorders. *Eur J Radiol* 45: 244-255.

Symon L, Dorsch N, Stephens R (1972) Pressure waves in so-called low pressure hydrocephalus. *Lancet* 2:1291-1293.

Tamaki N, Kusunoki T, Wakabayashi T, Matsumoto S (1984) Cerebral hemodynamics in normal-pressure hydrocephalus. Evaluation by 133Xe inhalation method and dynamic CT study. *J Neurosurg* 61:510-514.

Tamura E (1985) PVL type cerebral atrophy in the elderly with disturbed CSF flow, with specific reference to the gait characteristics, disturbed CSF flow and pathological changes in arachnoid granulations. *J Nihon Univ Med Ass* 44:821-842.

Tanaka A, Kimura M, Nakayama Y, Yoshinaga S, Tomonaga M (1997) Cerebral blood flow and autoregulation in normal pressure hydrocephalus. *Neurosurgery* 40:1161-1165; discussion 1165-1167.

Tans JD, Poortvliet DC. (1989) Does compliance predict ventricular reduction after shunting for normal pressure hydrocephalus. *Neurol Res* 11:136–138.

Tarkowski E, Tullberg M, Fredman P, Wikkelso C. (2003) Normal pressure hydrocephalus triggers intrathecal production of TNF - alpha. *Neurobiol Aging*. 24(5) 707-714.

Tedeschi E, Hasselbalch SG, Waldemar G, Juhler M, Hogh P, Holm S, Garde L, Knudsen LL, Klinken L, Gjerris F, *et al.* (1995) Heterogeneous cerebral glucose metabolism in normal pressure hydrocephalus. *J Neurol Neurosurg Psychiatry* 59:608-615.

Tisell M, Edsbagge M, Stephensen H, Czosnyka M, Wikkelso C. (2002) Elastance correlates with outcome after endoscopic third ventriculostomy in adults with hydrocephalus caused by primary aqueduct stenosis. *Neurosurgery* 50: 70-77.

Tullberg M (2001) White matter pathology in normal pressure hydrocephalus and subcortical arteriosclerotic encephalopathy. Institute of Clinical Neuroscience, Goteborg: Goteborg University.

Tullberg M, Hultin L, Ekholm S, Mansson JE, Fredman P, Wikkelso C. (2002) White matter changes in normal pressure hydrocephalus and Binswanger disease: specificity, predictive value and correlations to axonal degeneration and demyelination. *Acta Neurol Scand* 105:417-426.

Tullberg M, Jensen C, Ekholm S, Wikkelso C. (2001) Normal pressure hydrocephalus: vascular white matter changes on MR images must not exclude patients from shunt surgery. *ARNR: Am J Neuroradiol* 22:1665-1673.

Tullberg M, Mansson JE, Fredman P, Lekman A, Blennow K, Ekman R, Rosengren LE, Tisell M, Wikkelso C (2000) CSF sulfatide distinguishes between normal pressure hydrocephalus and subcortical arteriosclerotic encephalopathy. *J Neurol Neurosurg Psychiatry* 69:74-81.

Tullberg M, Rosengren L, Blomsterwall E, Karlsson JE, Wikkelso C (1998) CSF neurofilament and glial fibrillary acidic protein in normal pressure hydrocephalus. *Neurology* 50:1122-1127.

Udvarhelyi GB, Wood JH, James AE, Jr., Bartelt D (1975) Results and complications in 55 shunted patients with normal pressure hydrocephalus. *Surg Neurol* 3:271-275.

Vanneste J, Augustijn P, Dirven C, Tan WF, Goedhart ZD (1992) CSF shunting normal-pressure hydrocephalus: do the benefits outweigh the risks? A multicenter study and literature review. *Neurology* 42:54-59.

Vanneste J, Augustijn P, Tan WF, Dirven C (1993) CSF shunting normal pressure hydrocephalus: the predictive value of combined clinical and CT data. *J Neurol Neurosurg Psychiatry* 56:251-256.

Vorisek I, Sykova E (1997) Evolution of anisotropic diffusion in the developing rat corpus callosum. *J Neurophysiol* 78:912-919.

Vorstrup S, Christensen J, Gjerris F, Sorensen PS, Thomsen AM, Paulson OB (1987) Cerebral blood flow in patients with normal-pressure hydrocephalus before and after CSF shunting. *J Neurosurg* 66:379-387.

Waldemar G, Schmidt JF, Delecluse F, Andersen AR, Gjerris F, Paulson OB (1993) High resolution SPECT with [99mTc]-d,l-HMPAO in normal pressure hydrocephalus before and after shunt operation. *J Neurol Neurosurg Psychiatry* 56:655-664.

Werring DJ, Clark CA, Barker GJ, Thompson AJ, Miller DH (1999) Diffusion tensor imaging of lesions and normal-appearing white matter in multiple sclerosis. *Neurology* 52:1626-1632.

Wikkelso C, Andersson H, Blomstrand C, Lindqvist G, Svendsen P (1986) Normal pressure hydrocephalus. Predictive value of the cerebrospinal fluid tap-test. *Acta Neurol Scand* 73:566-573.

Wikkelso C, Blomsterwall E, Frisen L. (2003) Subjective visual vertical and Rhomberg's test in hydrocephalus. *J Neurol* 250:741-745.

Wikkelso C, Blomstrand C (1982) Cerebrospinal fluid proteins and cells in normal-pressure hydrocephalus. *J Neurol* 228:171-180.

Wikkelso C, Ekman R, Westergren I, Johansson B (1991) Neuropeptides in cerebrospinal fluid in normal-pressure hydrocephalus and dementia. *Eur Neurol* 31:88-93.

Wikkelso C, Fahrenkrug J, Blomstrand C, Johansson BB (1985) Dementia of different etiologies: vasoactive intestinal polypeptide in CSF. *Neurology* 35:592-595.

Wolfson L, Leenders K, Brown L, Jones T (1985) Alterations of regional cerebral blood flow and oxygen metabolism in Parkinson's disease. *Neurology* 35:1399-1405.

Yakovlev P (1947) Paraplegias of hydrocephalus. *Am J Ment Def* 51:561-576.

Yamada F, Fukuda S, Samejima H, Yoshii N, Kudo T (1978) Significance of pathognomonic features of normal-pressure hydrocephalus on computerized tomography. *Neuroradiol* 16:212-213.

Zelaya F, Flood N, Chalk JB, Wang D, Doddrell DM, Strugnell W, Benson M, Ostergaard L, Semple J, Eagle S (1999) An evaluation of the time dependence of the anisotropy of the water diffusion tensor in acute human ischemia. *Magn Reson Imaging* 17:331-348.

List of Appendices

Appendix A

Normal pressure hydrocephalus and cerebral blood flow: a review

Appendix B

Basis of Diffusion Tensor MR Imaging and Analysis

Appendix A

Cerebral Blood Flow and Normal Pressure Hydrocephalus. A Review

Owler B. K. and Pickard J.D. (2001) Cerebral Blood Flow and Normal Pressure Hydrocephalus. A Review. *Acta Neurologica Scandanavica* 104: 325-342.

Appendix B

Basis of Diffusion Tensor MR Imaging and Analysis

Diffusion and its Measurement using NMR

Diffusion is a normal physical process exhibited in biological systems. The ability to measure diffusion *in vivo* has been provided by relatively new MR imaging techniques that do not interfere with the process itself, that is, diffusion weighted (DWI) and diffusion tensor imaging (DTI). Images generated using these techniques allow information regarding both microstructure and physiology to be elucidated.

Diffusion may be defined as the random motion of a molecule in a fluid due to its intrinsic kinetic energy. Diffusion may occur along a concentration gradient (bulk diffusion) but also occurs in the absence of such a gradient. In the case of water this is known as the 'self-diffusion' of water. The thermal energy of water molecules is transferred to kinetic energy such that water molecules are in constant random (Brownian) motion. Collisions and other interactions between molecules mean that each molecule is constantly being deflected and rotated so that the position and orientation of each molecule changes in a random way. After a series of random movements, the distance r from the starting point will vary with time t and the diffusion coefficient D. The diffusion coefficient can be incorporated into a conditional probability relationship. The probability may be denoted by $P(r_2, r_1, t)$ is the conditional Gaussian probability of finding a particular molecule at a distance r_1 between positions r_2 and $r_2 + dr_2$ after a time t. For three-dimensional free diffusion the distribution is given by:

$$P(r_2, r_1, t) = \frac{1}{\sqrt{(4\pi Dt)^3}} \exp\left(\frac{-(r_1 - r_2)^2}{4Dt}\right)$$

The quantification of the diffusion coefficient using NMR is dependent on Gaussian nature of this distribution.

When the RF pulse is applied to a voxel of water molecules, the hydrogen nuclei (or spins) are tipped from the state of longitudinal magnetization to the transverse state. The spins precess with a frequency proportional to the local field strength. Each spin precesses around its local field with a given phase and creates a small signal. In the case of a spin moving through a non-uniform magnetic field the magnetization after a time t depends on the history of magnetic fields felt by the spin. The field at the spin could vary for two reasons: 1) as the water molecule tumbles, the orientation of the spin relative to another nearby magnetic moment changes, creating a change in the magnetic field, or 2) the spin diffuses into another region where the field is different. The first effect is the basis for T2 relaxation, and the second is more directly related to displacements caused by diffusion.

If an individual spin is considered, the variation with time of the magnetic field at the spin may be approximated by imagining that the molecular motions (tumbling and displacement) take place in small jumps. The spin may be pictured as "sitting" in a constant field B, for a short time Δt and then jumping to a new field B_2 and remaining in that field for the same time Δt. In each instant Δt the spin precesses at a rate set by the current value of B and acquires a phase increment $\Delta\phi = \gamma tG$ where γ is the gyromagnetic ratio for the proton. The final phase value after a time t is the sum of

these phase increments. But because each phase increment is proportional to the current value of B, the final phase ϕ is the same as it would have been if the spin felt only the average field B_{av} for the total time t.

$$\phi = \gamma \int_0^t B.dt = \gamma t B_{av}$$

In diffusion NMR imaging, a gradient pulse is applied that encodes the spins in each voxel with a spatially varying resonant frequency. For static spins there would be characteristic phase dispersion which could be easily re-phased. However, if the spins are diffusing within that voxel, the phase dispersion become more complicated and incoherent with time as the spins randomly translate with varying velocities along the direction of the applied gradient. At the end of the elapsed time t there is a distribution of phase values for the signals from different spins because each spin has experienced a different B_{av}. The standard deviation σ_ϕ of the final phase values is thus age field felt by a nucleus:

$$\sigma_\phi^2 = (\gamma t)^2 = \sigma_B^2$$

The standard deviation σ_ϕ of the phase distribution $p(\phi)$ can be thought of as a measure of the width of the distribution. Thus the effect of diffusion is to increase the variance of the intra-voxel phase dispersion although the average phase remains zero. The result of this increase in phase dispersion is signal attenuation. This is due to destructive interference from the phase dispersed spins within that voxel. Thus when σ_ϕ is large, the net signal is strongly attenuated when the individual signals are added.

A basic diffusion sensitive sequence is that of the Stejskal & Tanner (1965) experiment which is that of a simple bipolar pulsed gradient. An initial 90 degree radio-frequency (RF) pulse creates coherent transverse magnetisation. Application of a gradient G along induces a phase shift in spins which is dependent on the position of those spins along the direction of the gradient. The phase shifts are reversed by the 180 degree RF pulse. If spins do not diffuse during this time then this RF pulse would re-phase the spins after the second gradient pulse resulting in an echo at TE. However, due to diffusion since the time of the first RF pulse, the 180 RF pulse does not result in re-phasing of all spins. Instead there is phase dispersion and the subsequent echo is weaker, that is, the signal is attenuated.

For an ensemble of spins, the signal attenuation is a function of phase dispersion and the conditional probability expression $P(r_2, r_1, t)$ (Le Bihan, 1995) Signal attenuation is thus related to the diffusion coefficient. It is important to appreciate also that this is quite different from bulk coherent motion in which the overall phase signal will shift but the NMR signal will not be attenuated. The Stejskal-Tanner equation (Stejskal and Tanner, 1965) describes the relationship between these factors assuming the Gaussian form of the probability term.

$$\ln\left(\frac{S(G,\Delta,\delta)}{S(0)}\right) = -\gamma^2 G^2 \delta^2 \left(\Delta - \frac{\delta}{3}\right) D$$

where $S(G,\Delta,\delta)$ and $S(0)$ are the signals of the diffusion and non-diffusion sensitive gradients. The gradient amplitude G, time interval between gradients Δ and the gradient duration δ can be expressed as a b-value (time/length^2). The equation becomes:

$$S(b) = S(0)\exp(-bD)$$

The validity of this expression is limited to homogenous materials with isotropic diffusion properties which is not the case in biological materials. It also neglects the effects of the imaging gradients.

To obtain a map of the diffusion coefficient, images may be acquired using a range of b-values and fitting a curve based on the above equation on a pixel-by-pixel basis. In the simplest case, measurement of D requires measurement of attenuation for two different b values. However, it is often desirable to have more data points to increase the precision and allow investigation of more complex systems in which the signal decay may not be a single exponential. In chapter 6 the measurement of D for each direction was obtained using 5 different b-values equally spaced between b_{min} = 318 s/mm^2 to b_{max} = 1541s/mm^2 as well as b(0) thus yielding 6 points to which the attenuation curve could be fitted.

Diffusion in Biological Tissue

In biological tissues diffusion is more complex. Structures such as cell membranes, myelin sheaths and even large proteins restrict the diffusion of water. The complexity of diffusion in a biological system can only be approximated using diffusion theory and NMR imaging. A consequence of restricted diffusion in biological systems is that the alteration in attenuation as a result of diffusion in different regions can be used to gain information regarding the microstructures and physiology of various regions. The alteration in NMR signal due to restricted diffusion is less than that in free diffusion. This is because the average field felt by the restricted molecule is less varied than that felt by the free molecule.

Water in biological tissues is compartmentalised, for example, between intra- and extracellular compartments. In addition, within the intracellular compartment, water is further compartmentalised between cytoplasm and organelles. Water is continuously being exchanged between the various compartments. If the exchange between the compartments is fast then the diffusion attenuation curve will approximate a single exponential. If the exchange is slow, the signal attenuation curve will be that of a multi-exponential. The reality is likely to be intermediate between the two situations. In addition it must be realised that the molecular environment within various compartments is likely to differ such that intracellular T_2 is expected to be significantly smaller than in the intracellular compartment. Generally the multi-exponential behaviour is not observed and a single exponential is usually fitted. To acknowledge these differences between theoretical and observed measurements of diffusion a volume average apparent diffusion coefficient (ADC) is normally measured.

When the possibility of diffusion is equal in all directions this may be termed isotropic diffusion. This is the case in a freely diffusible medium. However when diffusion is restricted, it is usually more restricted in one direction than another. The possibility of diffusion not being equal in all directions is termed anisotropic diffusion. Such anisotropic diffusion is classically seen in several tissues such as the cerebral white matter where diffusion is greater parallel to, rather than perpendicular to, white matter fibres. There are many implications of such anisotropy. Most importantly it allows us to acquire information about the microstructural integrity of various tissues. However in order to do this properly, measurement of diffusion in

multiple directions is required, that is, diffusion must be considered as a tensor rather than scalar *(vide infra).*

Diffusion Weighted Imaging (DWI)

Diffusion weighted imaging relies on the addition of diffusion sensitive gradients as described above. In DWI these gradients are generally applied in one, two or three directions. An ADC value is provided for each of the directions imaged. In tissues with anisotropic diffusion, if diffusion is measured in one direction only then the resulting ADC will be almost totally dependent on the orientation of the axis along which diffusion is measured in relation to the orientation of the tissue (or fibres) (Chenevert *et al.*, 1990). Measuring diffusion in three orthogonal directions does not completely overcome this problem. The measurements only apply to the laboratory frame of reference and are therefore dependent on 1) the number and directions of diffusion measurements, and 2) the orientation of the tissue with respect to the magnet and diffusion gradients.

Diffusion Tensor Imaging (DTI)

Full characterisation of diffusion to avoid the problems outlined above depends on acquiring the components of the diffusion tensor. This is possible through echo-planar imaging (EPI) which is very suited to diffusion imaging with very short acquisition times.

The diffusion tensor $\underline{D}$ is a Cartesian tensor with nine components and can be written in the form of a matrix D_{ij}.

$$D_{ij} = \begin{bmatrix} D_{xx} & D_{xy} & D_{xz} \\ D_{xy} & D_{yy} & D_{yz} \\ D_{xz} & D_{xy} & D_{zz} \end{bmatrix}$$

The mathematical formalism of the diffusion tensor can also be applied to signal attenuation in NMR.

$$\ln \frac{S(b)}{S(0)} = \sum_{i=1}^{3} \sum_{j=1}^{3} b_{ij} D_{ij}$$

where b_{ij} (b-matrix) represents the matrix of b-values and their applied directions. It also incorporates the effects of interactions between the imaging and diffusion sensitising gradients which must be taken into account when calculating the tensor from the diffusion values.

Thus the general description of three-dimensional diffusion depends on the diffusion tensor $\underline{D}$. An important property of the tensor is that it is symmetric (i.e., $D_{ij} = D_{ji}$,), so that there are only six different components. This theoretically reduces the experimental time necessary to determine the tensor $\underline{D}$. The components of $\underline{D}$ can be estimated experimentally using seven measurements: six for each of the unique components of D_{ij} and one for b(0). In order to increase the accuracy of diffusion tensor calculation diffusion gradients may be applied in more directions. In chapter 6 diffusion gradients were applied in 12 directions for each b-value.

The shape of the acquired tensor will vary with diffusion. For isotropic materials the tensor will describe a sphere. Any anisotropy contained in the tensor will describe an ellipsoid. Thus the diffusion tensor can be visualised as a diffusion ellipsoid (Figure A.C.1). The surface of this three-dimensional structure corresponds to a constant

translational displacement probability for a given diffusion time. The diffusion ellipsoid has been used a method visualising the tensor for each voxel in DTI analysis but is often impractical. There are also the difficulties of visualising a three dimensional object in two dimensions. These problems and the methods used to overcome them are described below and in the subsequent chapters.

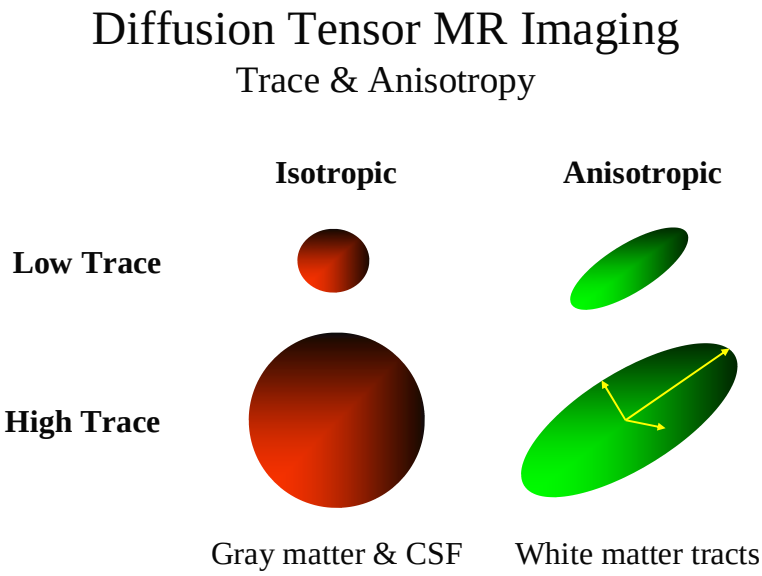

Figure A.C.1: Illustration of the concept of the diffusion ellipsoid. If diffusion is isotropic it defines a sphere, the size of which is determined by the amount of diffusion (trace). If diffusion is anisotropic then an ellipsoid is defined, the size of which is also determined by the amount of diffusion (trace).

The principal axes $(\varepsilon_1, \varepsilon_2, \varepsilon_3)$ of the ellipsoid are those of the mean effective diffusive displacements along the principal axes of the tensor. These principal axes will not normally correspond to the arbitrary coordinate system (x,y,z) used to measure the

diffusion tensor. However, the principal axes and diffusivities can be calculated by diagonalising the tensor and computing the eigenvectors and eigenvalues. For the diagonalised tensor

$$\underline{D} = D_{av}E = E\Lambda \text{ where } E(\varepsilon_1, \varepsilon_2, \varepsilon_3) \text{ and } \Lambda = \begin{bmatrix} \lambda_1 & 0 & 0 \\ 0 & \lambda_2 & 0 \\ 0 & 0 & \lambda_3 \end{bmatrix}$$

The eigenvalues themselves are valuable in that they estimate the size and shape of the tensor. If the three eigenvalues are equal, the diffusion tensor is spherical and diffusion is isotropic. Unequal eigenvalues indicate anisotropy and their relative values may correspond to certain paradigms of anisotropy. For instance, if $\lambda_1 >> \lambda_2 = \lambda_3$ then the tensor is 'cigar' shaped. Alternatively, if $\lambda_1 << \lambda_2 = \lambda_3$, then the diffusion ellipsoid will be 'disc' shaped.

From the diagonalised tensor, scalar invariant measures may be derived. The value of these invariants is that they are unchanged with rotation or translation of the tensor relative to an arbitrary frame of reference. Thus they are particularly useful to describe apparent diffusion characteristics in MR imaging (*vide infra*).

Scalar Invariants of the Diffusion Tensor

Through algebraic transformation of the tensor matrix scalar invariant measures of diffusion may be derived. These scalar measurements do not vary with rotation or translation of the tensor. They describe both the size and the shape of the tensor and hence the amount of diffusion and any apparent direction-dependent restriction of diffusion. Invariants that have found application in the field of DTI analysis are the trace, the fractional anisotropy and the relative anisotropy.

The derivation of the trace is straight forward. It is simply the sum of the principal eigenvalues.

$$Trace(D) = \lambda_1 + \lambda_2 + \lambda_s$$

It is a measure of the 'amount' of diffusion and is related to the average diffusion by

$$D_{av} = \frac{Trace(D)}{3}$$

Derivation of the other invariants is somewhat more complex and is best appreciated with reference to principal space.

Principal Space & Derivation of the Anisotropy Indices

A tensor $\underline{D}$ may be represented by plotting its eigenvalues on a principal (Haigh-Westerguard) space diagram. Each eigenvalue is plotted along the principal axes as in Figure A.C.2. Thus a point $D(\lambda_1', \lambda_2', \lambda_3')$ is defined in principal space for the tensor $\underline{D}$. By joining this line to the origin, the tensor may be represented by a vector. In this principal space diagram, an isotropic line may also be defined along which the eigenvalues must be equal $\lambda_1 = \lambda_2 = \lambda_s$.

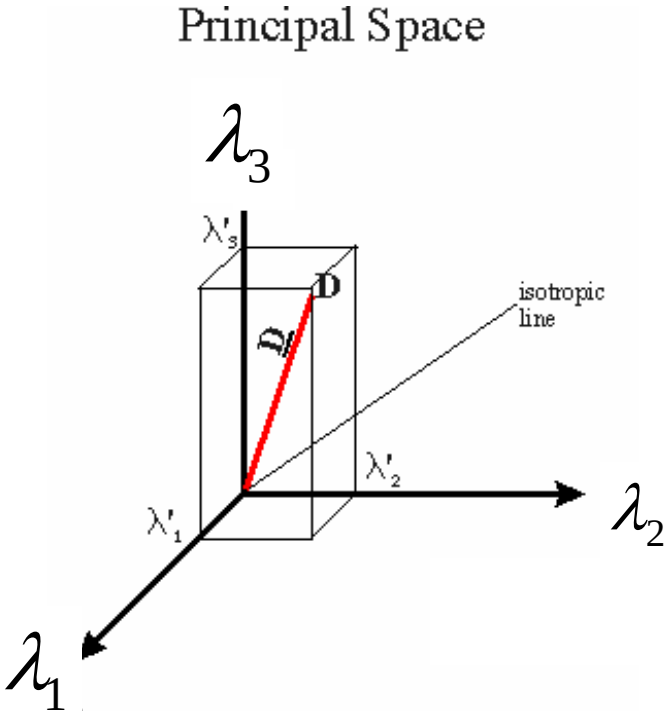

Figure A.C.2: The principal space diagram that may be used to plot the diffusion tensor (D). The axes define each of the eigenvalues.

The diffusion tensor $\underline{D}$ is composed of isotropic *p* and anisotropic (or deviatoric) parts *q*. The isotropic part of the tensor may be defined as the product of the average diffusion $\bar{\lambda}$ and the isotropic identity tensor $\underline{I}$

$$p = \bar{\lambda}\underline{I}$$

where:

$$\underline{I} = \begin{bmatrix} 1 & 0 & 0 \\ 0 & 1 & 0 \\ 0 & 0 & 1 \end{bmatrix} \text{ and } \bar{\lambda} = \frac{\lambda_1 + \lambda_2 + \lambda_3}{3}$$

The anisotropic component of the tensor is may be defined as:

$$q = \underline{D} - \bar{\lambda}\underline{I}$$

Therefore:

$$\underline{D} = \bar{\lambda}\underline{I} + \left(\underline{D} - \bar{\lambda}\underline{I}\right)$$

In the principal space diagram this can be demonstrated as in Figure A.C.3. The isotropic part is represented by a vector which lies on the isotropic line. The anisotropic part of the is represented by another vector perpendicular to the isotropic line such that the three vectors form a triangle

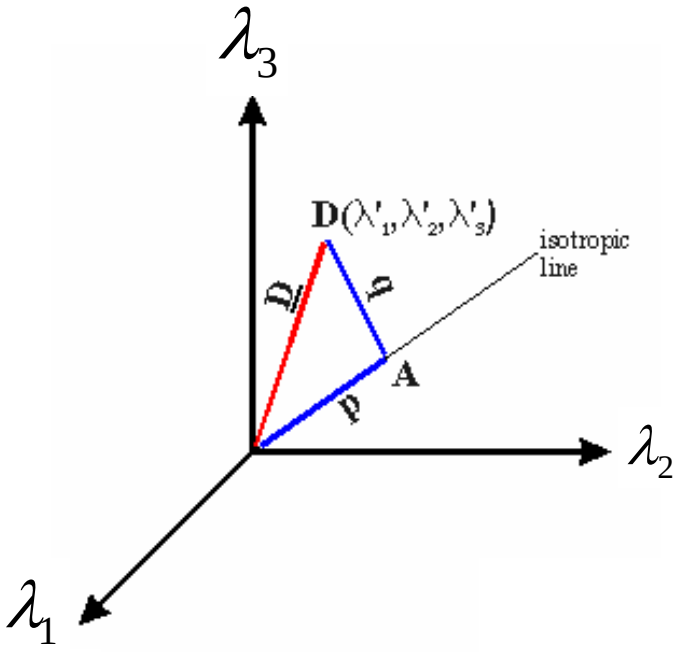

Figure A.C.3: When the diffusion tensor D has been plotted in principal space then the isotropic component *p*, and the anisotropic component *q* are represented in relation to the isotropic line.

The magnitude of a tensor is given by the square root of the (scalar) generalised tensor product or tensor dot product

$$\underline{D} = \sqrt{\underline{D} : \underline{D}}$$

$$\underline{D} : \underline{D} = \lambda_1^2 + \lambda_2^2 + \lambda_3^2$$

Thus for the isotropic part of the tensor

$$\sqrt{\bar{\lambda}\underline{I} : \bar{\lambda}\underline{I}} = \bar{\lambda}\sqrt{\underline{I} : \underline{I}}$$

For the isotropic identity tensor the eigenvalues are equal to 1. Thus:

$$p = \bar{\lambda}\sqrt{\underline{I} : \underline{I}} = \bar{\lambda}\sqrt{3}$$

The anisotropic part of the tensor can be defined as

$$q = \left(\lambda_1 - \bar{\lambda}\right) + \left(\lambda_2 - \bar{\lambda}\right) + \left(\lambda_3 - \bar{\lambda}\right)$$

thus

$$\sqrt{q^2} = \sqrt{\left(\lambda_1 - \bar{\lambda}\right)^2 + \left(\lambda_2 - \bar{\lambda}\right)^2 + \left(\lambda_3 - \bar{\lambda}\right)^2}$$

Relative anisotropy (RA) is defined as the ratio of anisotropic diffusion to isotropic diffusion. Thus, RA may be defined as:

$$RA = \frac{q}{p}$$

$$RA = \frac{\sqrt{\left(\lambda_1 - \bar{\lambda}\right)^2 + \left(\lambda_2 - \bar{\lambda}\right)^2 + \left(\lambda_3 - \bar{\lambda}\right)^2}}{\sqrt{3}\bar{\lambda}}$$

$$RA = \frac{1}{\sqrt{3}} \frac{\sqrt{\left(\lambda_1 - \bar{\lambda}\right)^2 + \left(\lambda_2 - \bar{\lambda}\right)^2 + \left(\lambda_3 - \bar{\lambda}\right)^2}}{\sqrt{\lambda_1^2 + \lambda_2^2 + \lambda_3^2}}$$

In defining fractional anisotropy the principal space diagram is most useful (Figure A.C.4). At a point A, that is, where the isotropic and anisotropic diffusion vectors meet, a plane is constructed perpendicular to the isotropic line. This plane is known as the π-plane or deviatoric plane. The anisotropic diffusion component of diffusion lies within this plane. The plane allows for comparison of the eigenvalues without compromising mathematical integrity. When comparing eigenvalues or tensors, it is their projection onto this plane which is most important rather than their actual values. The projection of these values onto the π-plane is best appreciated by rotating the axes

such that the isotropic line is viewed straight on and hence from this perspective it becomes a point (Figure A.C.5).

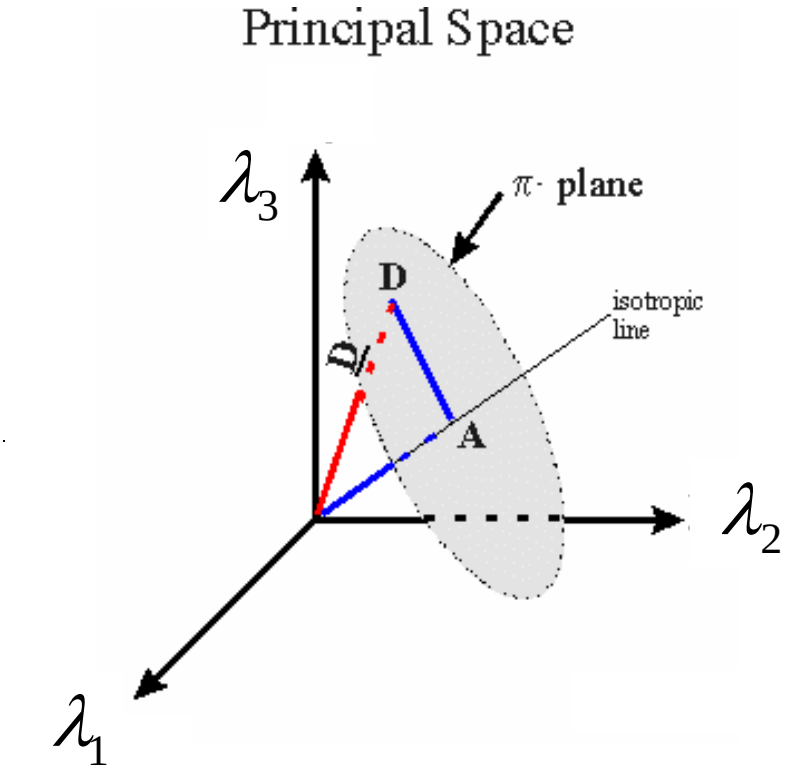

Figure A.C.4: The π-plane in the principal space diagram is perpendicular to the isotropic line.

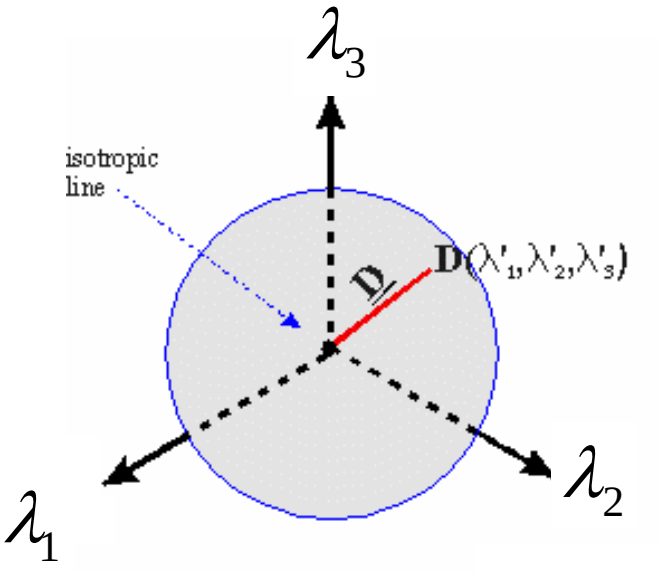

Figure A.C.5: The diffusion tensor can be represented by its projection into the π-plane.

As the axes and π-plane and the principal axes make $\cos^{-1}\sqrt{2/3}$ then the projected eigenvalues are $\sqrt{2/3}\lambda_1, \sqrt{2/3}\lambda_2, \sqrt{2/3}\lambda_3$ Hence the projection of $\underline{D}$ is also $\sqrt{2/3}\underline{D}$.

Fractional anisotropy (FA) is defined as the ratio of anisotropic diffusion to total diffusion.. Thus FA may be defined as:

$$FA = \frac{q}{\underline{D}}$$

$$FA = \frac{\sqrt{\left(\lambda_1 - \overline{\lambda}\right)^2 + \left(\lambda_2 - \overline{\lambda}\right)^2 + \left(\lambda_3 - \overline{\lambda}\right)^2}}{\sqrt{2/3}\sqrt{\lambda_1^2 + \lambda_2^2 + \lambda_3^2}}$$

$$FA = \sqrt{3/2}\frac{\sqrt{\left(\lambda_1 - \overline{\lambda}\right)^2 + \left(\lambda_2 - \overline{\lambda}\right)^2 + \left(\lambda_3 - \overline{\lambda}\right)^2}}{\sqrt{\lambda_1^2 + \lambda_2^2 + \lambda_3^2}}$$

Maps of these invariants can be calculated on the basis of the eigenvalues of each voxel to display information regarding regional diffusion and anisotropy. Measures of anisotropy and in particular the direction of the principal eigenvectors also serve as a basis from the technique of MR tractography. A disadvantage of the invariants is that information regarding the symmetry of the tensor is lost. In order to answer this question, the eigenvalues themselves must be considered.

References to Appendix B

Chenevert TL, Brunberg JA, Pipe JG (1990) Anisotropic diffusion in human white matter: demonstration with MR techniques in vivo. *Radiology* 177:401-405.

Le Bihan D (1995) Molecular diffusion, tissue microdynamics and microstructure. *NMR Biomed* 8:375-386.

Stejskal E, Tanner J (1965) Spin diffusion measurements: spin echoes in the presence of a time dependent field gradient. *J Chem Phys* 42:288-292.